

æ

æ

*This document is a chapter from the unpublished manuscript of a book: **Gravitational Radiation: A New Window onto the Universe** by Kip S. Thorne; draft of 16 September 1989 — copyright 1989 by Kip S. Thorne*

## 5 Propagation of Gravitational Waves

In this chapter we shall study the propagation of gravitational waves from their source to the earth. We begin in Sec. 5.A by writing down the propagation laws in their simplest form, that appropriate to the *geometric-optics approximation*. Then in Secs. 5.B, 5.C, and 5.D we derive those geometric-optics propagation laws in a careful manner, identifying along the way the various assumptions that must be made. Each assumption entails discarding physical effects that might be important in special but unusual situations.

For simplicity, our geometric-optics laws are specialized to propagation through vacuum; however, as part of our derivation of them, we obtain in Secs. 5.B and 5.C a propagation equation that describes the interaction of the waves with matter and with electromagnetic fields. In Secs. 5.E and 5.F we seek insight into that interaction by calculations with this propagation equation. Our calculations show that, although the coupling of waves to matter and electromagnetism is fascinating in principle, it is almost never significant in practice: In realistic astrophysical situations the vacuum approximation to wave propagation is excellent.

In Sec. 5.G we study a wide variety of vacuum propagation phenomena (scattering and parametric amplification by background curvature, tails of waves, gravitational focusing and diffraction, nonlinear wave-wave coupling, ...); we describe how to analyze these effects; and we discuss their relevance to wave propagation in the real universe. We conclude the chapter in Sec. 5.H with a brief discussion of two special, non-geometric-optics analyses of wave propagation: a set of exact solutions to the Einstein field equation, which describe propagating waves; and the theory of the asymptotic structure of the gravitational-wave field outside an isolated source in an asymptotically flat spacetime.

In order to understand this chapter and Chap. 6, the reader will need prior familiarity with general relativity at, e.g., the level of “track one” of MTW (Misner, Thorne, and Wheeler, 1973). Readers without such familiarity can move on to Chaps. 7–12, which should be understandable without mastery of Chaps. 5 and 6.

Our notation and mathematical conventions will be those of MTW. A key role will be played, in the mathematical formalism, by a split of the full, gravitational-wave-endowed spacetime into a background spacetime [obtained by averaging over several wavelengths of the waves, cf. Eqs. (4.4) above and (5.6) below], plus the waves. After the split has been made, the waves will be thought of as a field that propagates through the background spacetime. We shall use a vertical slash to denote covariant derivatives, i.e., gradients, in the background spacetime, so if  $S^\alpha$  (also denoted abstractly as  $\mathbf{S}$ ) is a vector field that lives in the background spacetime, then  $S^\alpha|_\mu$  (also denoted abstractly as  $\nabla\mathbf{S}$ ) is its gradient.

Similarly, we shall use a semicolon to denote covariant derivatives in the full, pre-split, wave-endowed spacetime, so if  $A^\alpha$  lives in the full spacetime, then  $A^\alpha_{;\mu}$  is its gradient.

### 5.A. Geometric-optics propagation laws

*Geometric optics* is a very general formalism for studying the propagation of any kind of wave through any kind of medium. This formalism is valid whenever the wave's reduced wavelength  $\bar{\lambda}$  is small compared to the radius of curvature of its wave fronts, and also small compared to all inhomogeneity scales of the medium through which it propagates.

For gravitational waves *in vacuum*, the geometric-optics propagation can be described as follows. (We shall derive this description in Secs. 5.B, 5.C, 5.D, and we shall show in Secs. 5.E and 5.F that it is also valid to high accuracy for gravitational waves propagating through astrophysically realistic matter.)

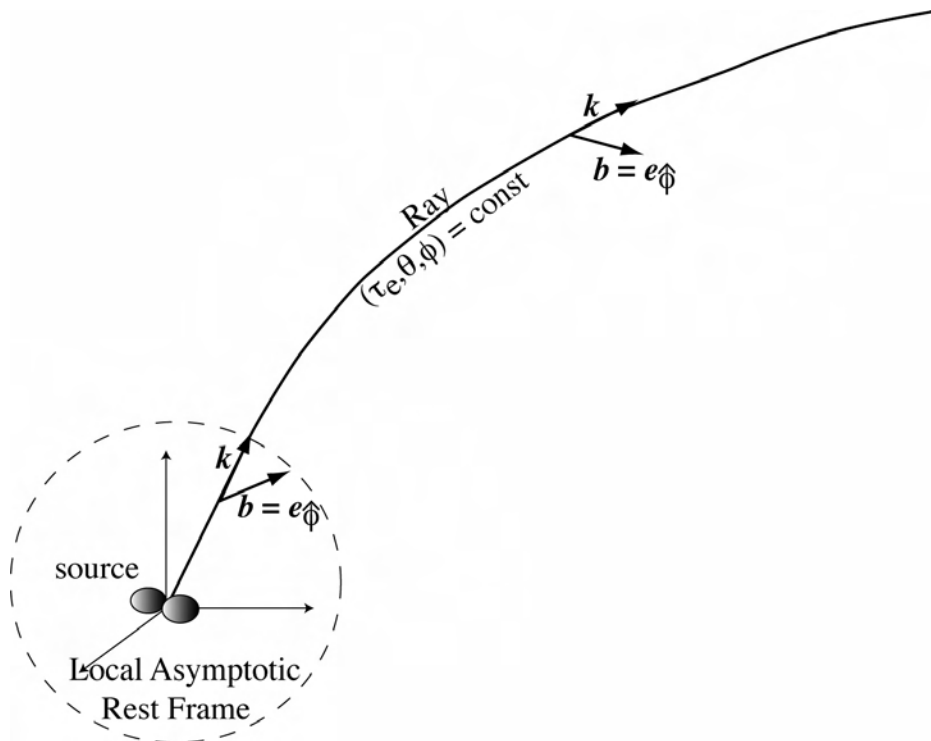


**Fig. 5.1** Geometric-optics construction for the propagation of gravitational waves from a source's local asymptotic rest frame (region inside dotted circle) out through the external universe (region outside dotted circle).

Consider, for concreteness, a source of gravitational waves somewhere far out in the universe. In the vicinity of the source but some wavelengths away from it (so as to avoid near-zone fields that will be discussed in Chap. 6), introduce a local Lorentz reference frame in which the source is at rest (the source's *local asymptotic rest frame*; Fig. 5.1). In that frame construct spherical polar coordinates  $(t, r, \theta, \phi)$  centered on the source and construct the associated orthonormal basis vectors  $\mathbf{e}_0, \mathbf{e}_r, \mathbf{e}_\theta, \mathbf{e}_\phi$ . The gravitational waves

propagate radially through this asymptotic rest frame, with their retarded time  $\tau_e$  and their wave vector  $\mathbf{k} = -\nabla\tau_e$  (introduced in Sec. 4.D) given by

$$\tau_e = t - r , \quad \mathbf{k} = \mathbf{e}_0 + \mathbf{e}_r . \quad (5.1a)$$

The gravitational-wave field  $h_{\alpha\beta}^{\text{GW}}$  associated with the asymptotic rest frame will have the form [Eq. (4.26)]

$$h_{\alpha\beta}^{\text{GW}} = h_+(a_\alpha a_\beta - b_\alpha b_\beta) + h_\times(a_\alpha b_\beta + b_\alpha a_\beta) , \quad (5.1b)$$

Here  $a_\alpha$  and  $b_\alpha$  are polarization vectors that are purely spatial in the source's asymptotic rest frame, have unit length, and are orthogonal to each other and to the waves' (radial) propagation direction. For example, we are free to choose them to be the unit vectors in the  $\theta$  and  $\phi$  directions

$$\mathbf{a} = \mathbf{e}_{\hat{\theta}} , \quad \mathbf{b} = \mathbf{e}_{\hat{\phi}} . \quad (5.1c)$$

Any other choice will be rotated relative to this choice by some angle  $\psi$  in the transverse plane, and correspondingly  $h_+$  and  $h_\times$  will be modified in the manner of expression (4.23). The propagation of the waves (5.1b) through the source's asymptotic rest frame and then on out through the entire universe is described by the following geometric-optics construction:

(i) The waves propagate along a family of null geodesics of the background spacetime, which are called the waves' *rays*. These rays are the specific solutions to the geodesic equation

$$k_{\alpha|\beta}k^\beta = 0 , \quad (5.2a)$$

which begin in the asymptotic rest frame with  $\mathbf{k} = \mathbf{e}_0 + \mathbf{e}_r$  and extend from there on out through the universe (Fig. 5.1). Each ray is labeled by the direction  $(\theta, \phi)$  in which it emerges from the source, and by the retarded time  $\tau_e$  at which it emerges. By this labeling,  $\tau_e$ ,  $\theta$ , and  $\phi$  are carried out through the universe on the rays. The tangent vector  $\mathbf{k}$  to the rays is given by

$$\mathbf{k} = -\nabla\tau_e , \quad (5.2b)$$

not just in the source's local asymptotic rest frame, but everywhere in the universe, as one can verify by checking that this  $\mathbf{k}$  satisfies the geodesic equation (5.2a). [Specifically,  $k_{\alpha|\beta}k^\beta = \tau_{e|\alpha\beta}\tau_e^{|\beta}$ , which, by commutation of the covariant derivatives of a scalar field, is equal to  $\tau_{e|\beta\alpha}\tau_e^{|\beta} = 1/2(\tau_{e|\beta}\tau_e^{|\beta})_{|\alpha}$ , which vanishes because  $\tau_{e|\beta}$  is null.] (ii) Next, parallel transport the polarization vectors  $a_\alpha$  and  $b_\alpha$  along the waves' rays out through the universe,

$$a_{\alpha|\beta}k^\beta = 0 , \quad b_{\alpha|\beta}k^\beta = 0 . \quad (5.2c)$$

(iii) Define all along each ray a *radius function*  $r$  in the following way: Consider the 2-dimensional bundle of rays, surrounding the ray of interest, which all have the same  $\tau_e$  as that ray but which have  $\theta$  in the range  $\Delta\theta$  and  $\phi$  in the range  $\Delta\phi$ , so they subtend, as seen from the source, a solid angle  $\Delta\Omega = \sin\theta\Delta\theta\Delta\phi$ . As one moves out along the ray of interest, the cross-sectional area  $\Delta A$  of this bundle (which is locally Lorentz-invariant; cf. Exercise 22.13 of MTW) changes, but by definition  $\Delta\Omega$  remains fixed. The radius function is defined to be

$$r \equiv (\Delta A/\Delta\Omega)^{1/2} . \quad (5.2d)$$

Of course, in the source's local asymptotic rest frame this is just equal to the distance to the source. However, far out in the universe it might be quite different from that distance. For example, gravitational lenses (to be discussed in Sec. 5.G.c below) can make the area of the bundle and thence also  $r$  switch over from increasing along a ray to decreasing. (iv) The (frame-invariant) gravitational-wave fields  $h_+$  and  $h_\times$  are carried outward along each ray unchanged, except for an overall alteration proportional to  $1/r$  (which is required to conserve the waves' energy as they propagate):

$$h_+ = \frac{Q_+(\tau_e, \theta, \phi)}{r}, \quad h_\times = \frac{Q_\times(\tau_e, \theta, \phi)}{r}. \quad (5.2e)$$

The functions  $Q_+$  and  $Q_\times$  can be evaluated in the source's local asymptotic rest frame using the theory of gravitational-wave generation (Chap. 6), and then can be carried out along the rays unchanged. (v) The polarization tensors  $e_{jk}^+$  and  $e_{jk}^\times$  associated with these fields, as measured in any proper reference frame anywhere in the universe, are

$$e_{jk}^+ = (a_j a_k - b_j b_k)^{\text{TT}}, \quad e_{jk}^\times = (a_j b_k + b_j a_k)^{\text{TT}}, \quad (5.2f)$$

where the superscripts TT denote the transverse-traceless projection of Eq. (4.50).

(vi) Correspondingly, the gravitational-wave field

$$h_{jk}^{\text{GW}} = h_+ e_{jk}^+ + h_\times e_{jk}^\times, \quad (5.2g)$$

as measured in that proper reference frame, is given by

$$h_{jk}^{\text{GW}} = (h_{jk})^{\text{TT}}, \quad (5.2h)$$

[Eq. (4.45)], where  $h_{jk}$  is the spatial part of the field

$$h_{\alpha\beta} \equiv h_+(a_\alpha a_\beta - b_\alpha b_\beta) + h_\times(a_\alpha b_\beta + b_\alpha a_\beta). \quad (5.2i)$$

As a simple example, consider the propagation of gravitational waves through a closed Friedman model for our universe. The background metric [obtained by averaging over the waves' short-wavelength ripples in the manner of Eq. (4.4a)] has the standard Friedman form [MTW, Eqs. (27.46) and (27.23)]

$$ds^2 = a^2[-d\eta^2 + d\chi^2 + \sin^2 \chi(d\theta^2 + \sin^2 \theta d\phi^2)], \quad (5.3)$$

where  $a = a(\eta)$  is the universe's "expansion factor". (Never mind that this spacetime is filled with matter rather than being vacuum; as we shall see in Sec. 5.E the presence of matter has no significant influence on the propagation.) Place the source of gravitational waves at the origin of the spatial coordinates,  $\chi = 0$ . Then the waves' rays are the radial null geodesics  $\chi = \eta - \eta_e$ , where  $\eta_e$  is the coordinate time at which the ray is emitted. Retarded time on each ray is the proper time of emission,  $\tau_e = \int_0^{\eta_e} a d\eta$ ; and the ray's radial function is  $r = a \sin \chi$ , which is the same radial function as appears in the expression for the optical brightness of a source of electromagnetic radiation [Eq. (29.28) of MTW].

Expressed in terms of the “deceleration parameter”  $q_o$  and “Hubble expansion rate”  $H_o$  of the universe, and the redshift  $z$  of the source as viewed optically from earth, this radial function is [Eq. (29.33) of MTW]

$$r = \frac{H_o^{-1}}{q_o^2(1+z)}[-q_o + 1 + q_o z + (q_o - 1)(2q_o + 1)^{1/2}]. \quad (5.4)$$

Note that, if the waves are emitted in an epoch when the universe’s expansion factor is  $a_e$  and are received at earth when it is  $a_o$ , then in terms of proper time  $t$  as measured in the earth’s local proper reference frame, the source’s retarded time is  $\tau_e = (a_e/a_o)t + \text{const.} = t/(1+z) + \text{const.}$ , where  $z = a_o/a_e$  is the source’s “cosmological redshift”. Correspondingly, the time dependence of the waveform as measured at earth is unchanged by the waves’ propagation, except for a frequency-independent redshift  $f_{\text{received}}/f_{\text{emitted}} = 1/(1+z)$  which is identically the same as for electromagnetic waves.

In fact, this similarity to electromagnetic waves is completely general: If one develops the geometric-optics formalism for electromagnetic wave propagation, one finds that the electromagnetic vector potential has the form

$$A_\alpha = A_1 a_\alpha + A_2 b_\alpha, \quad (5.5a)$$

where  $a_\alpha$  and  $b_\alpha$  are precisely the same polarization vectors as we used for gravitational waves; and that

$$A_1 = \frac{Q_1(\tau_e, \theta, \phi)}{r}, \quad A_2 = \frac{Q_2(\tau_e, \theta, \phi)}{r}, \quad (5.5b)$$

where  $\tau_e, \theta, \phi, r$  are precisely the same functions as we used above in the gravitational-wave formulas. (See, e.g., the treatment of monochromatic, electromagnetic geometric optics in Sec. 22.5 of MTW, translated into the notation of this book and with many frequencies superposed to give waveforms with arbitrary time dependences.) By comparing Eqs. (5.2e) and (5.5b) we infer that, in the geometric optics limit, the gravitational-wave fields  $h_+$  and  $h_\times$  experience precisely the same amplitude changes and redshift changes as do the components  $A_1$  and  $A_2$  of the electromagnetic vector potential.

## 5.B. Linear Perturbations of Curved Spacetime

As a foundation for deriving the above geometric-optics description of vacuum wave propagation (and also for discussing the effects discarded by geometric optics, the energy and momentum carried by gravitational waves, the generation of gravitational waves, and propagation through nonvacuum regions of spacetime), we shall develop in this section some mathematical formalism. This formalism will describe linearized perturbations of an arbitrary, nonvacuum spacetime geometry.

Whereas our description of gravitational waves thus far has focussed on the Riemann curvature tensor, our analysis here will focus on the metric  $g_{\alpha\beta}$  of spacetime. We shall write that metric as the sum of a *background* metric  $g_{\alpha\beta}^B$  and a perturbation  $h_{\alpha\beta}$ :

$$g_{\alpha\beta} = g_{\alpha\beta}^B + h_{\alpha\beta}. \quad (5.6a)$$

The precise way of making the split into background plus perturbation will depend on the situation. The background might be a smooth part, defined by averaging  $g_{\alpha\beta}$  over several wavelengths of gravitational radiation, and the perturbation then will be the remaining, rippled part; or the background might be a spherically symmetric part, and the perturbation the deviations from spherical symmetry; or the background might be the equilibrium spacetime for a rotating black hole, and the perturbation the deviations from that equilibrium. In order to be able to handle, with one formalism, all these situations and more, we shall here regard the split (5.6a) as a purely formal one: The *background* metric  $g_{\alpha\beta}^B$  is one solution to the Einstein field equation with one stress-energy tensor  $T_B^{\alpha\beta}$  as its source; the *full* metric  $g_{\alpha\beta}$  is another solution, with another stress-energy tensor  $T^{\alpha\beta}$ ; and the two solutions are nearly but not quite the same. Nearly identical coordinate systems are set up in the spacetimes of these two solutions, the coordinates are given the same names  $x^\mu$ , and events in the background spacetime and the full spacetime are regarded as “the same” if they have the same coordinate values. The perturbation  $h_{\alpha\beta}$  at location  $x^\mu$  is then the difference between the two functions  $g_{\alpha\beta}(x^\mu)$  and  $g_{\alpha\beta}^B(x^\mu)$ .

We shall regard the metric perturbation  $h_{\alpha\beta}$  as a symmetric tensor field that lives in the background spacetime, and correspondingly, we shall raise and lower indices on  $h_{\alpha\beta}$  using the background metric  $g_{\alpha\beta}^B$ . Because  $g^{\alpha\beta}$  is the inverse of  $g_{\alpha\beta}$  ( $g_{\alpha\beta}g^{\beta\gamma} = \delta_\alpha^\gamma$ ),  $g^{\alpha\beta}$  takes the form

$$g^{\alpha\beta} = g_B^{\alpha\beta} - h^{\alpha\beta}, \quad \text{where } h^{\alpha\beta} = g_B^{\alpha\mu} g_B^{\beta\nu} h_{\mu\nu}. \quad (5.6b)$$

Note the opposite signs in expressions (5.6a,b) for  $g_{\alpha\beta}$  and  $g^{\alpha\beta}$ , and note that there is no significance to whether the B (for background) is placed up or down.

The difference between the stress-energy tensor of the full spacetime and that of the background spacetime, at the same coordinate locations  $x^\mu$ , we shall write in the form

$$T^{\alpha\beta} = T_B^{\alpha\beta} + \mathcal{T}^{\alpha\beta} - h^{\mu(\alpha} T_B^{\beta)}_{\mu}. \quad (5.7a)$$

Here and henceforth the parentheses on indices denote symmetrization:

$$h^{\mu(\alpha} T_B^{\beta)}_{\mu} \equiv 1/2(h^{\mu\alpha} T_B^{\beta}_{\mu} + h^{\mu\beta} T_B^{\alpha}_{\mu}).$$

Equation (5.7a) serves as a definition of the stress-energy perturbation field  $\mathcal{T}^{\alpha\beta}$ . We choose this specific definition because it simplifies subsequent equations [e.g., Eqs. (5.33) and (5.34)]. We shall regard this  $\mathcal{T}^{\alpha\beta}$ , like  $h_{\alpha\beta}$ , as a linear field that resides in the background spacetime, with indices to be raised and lowered using  $g_{\alpha\beta}^B$ . By lowering indices on  $T^{\alpha\beta}$  with  $g_{\alpha\beta} = g_{\alpha\beta}^B + h_{\alpha\beta}$  and linearizing in  $\mathcal{T}^{\alpha\beta}$  and  $h_{\alpha\beta}$ , we obtain

$$T_{\alpha\beta} = T_{\alpha\beta}^B + \mathcal{T}_{\alpha\beta} + h^{\mu}{}_{(\alpha} T_{\beta)\mu}^B. \quad (5.7b)$$

Note the opposite signs on the last terms in expressions (5.7a) and (5.7b), completely analogous to the opposite signs in (5.6a) and (5.6b).

The evolution of  $\mathcal{T}^{\alpha\beta}$  will be governed by first-order perturbations of the law of energy-momentum conservation; and the evolution of  $h_{\alpha\beta}$ , by first-order perturbations of the

Einstein field equation. In discussing these evolution laws, we shall use a semicolon to denote a covariant derivative in the full spacetime, a vertical bar for a covariant derivative in the background spacetime, and a comma for an ordinary partial derivative with respect to our chosen coordinates. Correspondingly, the laws of energy-momentum conservation in the full and background spacetimes are

$$T^{\alpha\beta}{}_{;\beta} \equiv T^{\alpha\beta}{}_{,\beta} + \Gamma^{\alpha}{}_{\mu\beta} T^{\mu\beta} + \Gamma^{\beta}{}_{\mu\beta} T^{\alpha\mu} = 0; \quad (5.8a)$$

$$T_B^{\alpha\beta}{}_{|\beta} \equiv T_B^{\alpha\beta}{}_{,\beta} + \Gamma^{B\alpha}{}_{\mu\beta} T_B^{\mu\beta} + \Gamma^{B\beta}{}_{\mu\beta} T_B^{\alpha\mu} = 0; \quad (5.8b)$$

Here  $\Gamma^{\alpha}{}_{\beta\gamma}$  is the connection coefficient for the full spacetime, and  $\Gamma^{B\alpha}{}_{\beta\gamma}$  is that for the background spacetime:

$$\Gamma^{\alpha}{}_{\beta\gamma} = 1/2 g^{\alpha\mu} (g_{\mu\beta,\gamma} + g_{\mu\gamma,\beta} - g_{\beta\gamma,\mu}), \quad \Gamma^{B\alpha}{}_{\beta\gamma} = 1/2 g_B^{\alpha\mu} (g_{\mu\beta,\gamma}^B + g_{\mu\gamma,\beta}^B - g_{\beta\gamma,\mu}^B); \quad (5.9)$$

[see, e.g., Eqs. (8.24b,c) of MTW]. Their difference can be evaluated to linear order with the help of Eqs. (5.6). The result, expressed in terms of the background's covariant derivative of  $h_{\alpha\beta}$ , is

$$S^{\alpha}{}_{\beta\gamma} \equiv \Gamma^{\alpha}{}_{\beta\gamma} - \Gamma^{B\alpha}{}_{\beta\gamma} = 1/2 g_B^{\alpha\mu} (h_{\mu\beta|\gamma} + h_{\mu\gamma|\beta} - h_{\beta\gamma|\alpha}). \quad (5.10)$$

(For a sophisticated method of deriving this and the equations that follow, see Exercise 35.11 of MTW. However, sophistication is not needed; one can derive these equations by elementary algebra and index shuffling, plus a lot of sweat.)

It is a straightforward calculation to take the difference between the full and the background laws of energy-momentum conservation [Eqs. (5.8a,b)] and express it in terms of the perturbations of the stress-energy tensor and of the connection coefficients. The result, after also using Eq. (5.10), is the following *evolution equation for the stress-energy perturbation*:

$$\mathcal{T}^{\alpha\mu}{}_{|\mu} = 1/2 (h_{\mu\nu}{}^{|\alpha} - h^{\alpha}{}_{\mu|\nu}) T_B^{\mu\nu} + 1/2 (h_{\mu\nu}{}^{|\nu} - h^{\nu}{}_{\nu|\mu}) T_B^{\mu\alpha}. \quad (5.11)$$

This shows how gradients of the metric perturbations  $h_{\alpha\beta|\gamma}$  couple to the background stress-energy to generate stress-energy perturbations  $\mathcal{T}_{\alpha\beta}$ .

One application of this equation is to gravitational-wave detection: there  $h_{\alpha\beta}$  is the metric perturbation associated with the gravitational radiation,  $T_B^{\alpha\beta}$  is the stress-energy tensor of an unperturbed detector, and  $\mathcal{T}^{\alpha\beta}$  is the influence of the waves on the detector. When the detector involves a set of masses on which the waves act, and the coordinate system is a proper reference frame of  $g_{\alpha\beta}$  and also of  $g_{\alpha\beta}^B$ , in which the masses are nearly at rest, then the dominant spatial term (driving force) on the right-hand side of (5.11) is

$$1/2 h_{00}{}^{|j} T_B^{00} = -(R_{j0k0}^{\text{GW}} x^k) T_B^{00}$$

[cf. Eq. (4.39)]. This is the “per-unit-volume” version of the gravitational-wave force (4.12) of Chap. 4.

The Riemann curvature tensors of our two spacetimes can be expressed in terms of the connection coefficients and their derivatives by the standard formula [MTW, Eq. (8.44)]

$$R^\alpha{}_{\beta\gamma\delta} = \Gamma^\alpha{}_{\beta\delta,\gamma} - \Gamma^\alpha{}_{\beta\gamma,\delta} + \Gamma^\alpha{}_{\mu\gamma}\Gamma^\mu{}_{\beta\delta} - \Gamma^\alpha{}_{\mu\delta}\Gamma^\mu{}_{\beta\gamma}, \quad (5.12)$$

and the same formula for the background but with a superscript B on all quantities. By taking the difference between these two formulas and discarding terms nonlinear in the metric perturbation, we obtain

$$\begin{aligned} \delta R^\alpha{}_{\beta\gamma\delta} &\equiv R^\alpha{}_{\beta\gamma\delta} - R^{\text{B}\alpha}{}_{\beta\gamma\delta} = S^\alpha{}_{\beta\delta|\gamma} - S^\alpha{}_{\beta\gamma|\delta} \\ &= 1/2g_{\text{B}}^{\alpha\mu}(h_{\mu\beta|\delta\gamma} + h_{\mu\delta|\beta\gamma} - h_{\beta\delta|\mu\gamma} - h_{\mu\beta|\gamma\delta} - h_{\mu\gamma|\beta\delta} + h_{\beta\gamma|\mu\delta}). \end{aligned} \quad (5.13)$$

Since the Ricci curvature tensors are obtained by contracting on the first and third indices of the Riemann tensors, Eq. (5.13) yields immediately for the perturbation of the Ricci tensor

$$\delta R_{\beta\delta} \equiv R_{\beta\delta} - R_{\beta\delta}^{\text{B}} = 1/2(h_{\mu\beta|\delta}{}^\mu + h_{\mu\delta|\beta}{}^\mu - h_{\beta\delta|\mu}{}^\mu - h_{|\beta\delta}), \quad (5.14)$$

where the  $h$  with no subscripts denotes the contraction of  $h_{\mu\nu}$  (using, of course, the background metric:  $h \equiv h_{\mu\nu}g_{\text{B}}^{\mu\nu}$ ).

It is the Einstein tensor,  $G_{\mu\nu} \equiv R_{\mu\nu} - 1/2Rg_{\mu\nu}$  (where  $R \equiv R_{\alpha\beta}g^{\alpha\beta}$ ) that appears on the left-hand side of the Einstein field equation. The perturbation in the Einstein tensor is readily computed from Eq. (5.14) and the perturbation (5.6) in the metric. The result is most nicely expressed not in terms of the metric perturbation  $h_{\alpha\beta}$ , but rather in terms of the trace-reversed metric perturbation

$$\bar{h}_{\alpha\beta} \equiv h_{\alpha\beta} - 1/2hg_{\alpha\beta}^{\text{B}}. \quad (5.15)$$

The result is brought into the nicest form by commuting a pair of background covariant derivatives [at the price of introducing a term proportional to the background Riemann tensor; cf. Eqs. (16.6) of MTW]. The resulting, “nicest form” is

$$\begin{aligned} G_{\alpha\beta} - G_{\alpha\beta}^{\text{B}} &\equiv G_{\alpha\beta}^{(1)}(h) = -1/2(\bar{h}^\mu{}_{\alpha\beta|\mu} + g_{\alpha\beta}^{\text{B}}\bar{h}^{\mu\nu}{}_{|\mu\nu} - 2\bar{h}_{\mu(\alpha|\mu}{}^\beta) + 2R_{\mu\alpha\nu\beta}^{\text{B}}\bar{h}^{\mu\nu} \\ &\quad - 2R_{\mu(\alpha}^{\text{B}}\bar{h}_{\beta)}{}^\mu - R_{\mu\nu}^{\text{B}}\bar{h}^{\mu\nu}g_{\alpha\beta}^{\text{B}} + R^{\text{B}}\bar{h}_{\alpha\beta}). \end{aligned} \quad (5.16)$$

Here  $R^{\text{B}} \equiv R^{\text{B}\mu}{}_{\mu}$  is the background scalar curvature, and the parentheses on indices denote symmetrization. This is the nicest form of  $G_{\alpha\beta}^{(1)}$  because it simplifies so much when one specializes the *gauge*:

By “gauge” we mean “the choice of which points in the full spacetime correspond to which points in the background spacetime”. To change the gauge, we can hold fixed the coordinates in the background spacetime, but change those in the full spacetime by the following very small amount (i.e., the following “infinitesimal coordinate transformation”):

$$x_{\text{old}}^\alpha = x_{\text{new}}^\alpha - \xi^\alpha(x_{\text{new}}^\mu). \quad (5.17)$$



This gauge change produces the following change in the metric coefficients of the full spacetime:

$$g_{\alpha\beta}^{\text{new}}(x_{\text{new}}^{\mu}) = g_{\rho\sigma}^{\text{old}}(x_{\text{old}}^{\mu}) \frac{\partial x_{\text{old}}^{\sigma}}{\partial x_{\text{new}}^{\alpha}} \frac{\partial x_{\text{old}}^{\sigma}}{\partial x_{\text{new}}^{\beta}}. \quad (5.18)$$

By combining this with Eq. (5.17) and with Eq. (5.6) for both the old and the new gauges, we obtain the relationship between the new and the old metric perturbations

$$h_{\alpha\beta}^{\text{new}} = h_{\alpha\beta}^{\text{old}} - \xi_{\alpha|\beta} - \xi_{\beta|\alpha}. \quad (5.19)$$

Thus, the *generator of the gauge change*  $\xi_{\alpha}$ , viewed as a field living in the background spacetime, produces the change (5.19) in the metric perturbation. This is completely analogous to gauge changes in electromagnetism: The  $h_{\alpha\beta}$  here is the analog of the electromagnetic vector potential  $A_{\alpha}$ ; the generator of the gauge change  $\xi_{\alpha}$  is the analog of the electromagnetic gauge-change generator  $\psi$ ; and Eq. (5.19) is the analog of  $A_{\alpha}^{\text{new}} = A_{\alpha}^{\text{old}} - \psi_{,\alpha}$ . Moreover, just as the electromagnetic evolution equation for  $A_{\alpha}$  takes on an especially simple form when one specializes to the ‘‘Lorentz gauge’’ ( $A^{\alpha}{}_{|\alpha} = 0$ ), so also the Einstein-tensor perturbation and thence the Einstein equation take on especially simple forms when one specializes to the *gravitational Lorentz gauge*

$$\bar{h}^{\alpha\beta}{}_{|\beta} = 0. \quad (5.20)$$

If one is not initially in this Lorentz gauge, one can go there by the gauge change whose generator satisfies the wave-equation-with-source

$$\xi_{\alpha|\beta}{}^{\beta} = -R_{\alpha\beta}^{\text{B}}\xi^{\beta} + h_{\alpha\beta}^{\text{old}}{}_{|\beta}. \quad (5.21)$$

In Lorentz gauge the perturbation (5.16) of the Einstein tensor simplifies to

$$G_{\alpha\beta}^{(1)}(h) = -1/2(\bar{h}_{\alpha\beta|\mu}{}^{\mu} + 2R_{\mu\alpha\nu\beta}^{\text{B}}\bar{h}^{\mu\nu} - 2R_{\mu(\alpha}^{\text{B}}\bar{h}_{\beta)}{}^{\mu} - R_{\mu\nu}^{\text{B}}\bar{h}^{\mu\nu}g_{\alpha\beta}^{\text{B}} + R_{\text{B}}\bar{h}_{\alpha\beta}), \quad (5.22)$$

which involves only the wave operator plus the coupling of  $\bar{h}_{\alpha\beta}$  to background curvature.

The perturbed Einstein equation [with Newton’s gravitation constant  $G$  set to unity as we shall do throughout Chaps. 5 and 6, cf. Eqs. (4.3)] equates this  $G_{\alpha\beta}^{(1)}$  to  $8\pi$  times the stress-energy perturbation [Eq. (5.7b)]

$$G_{\alpha\beta}^{(1)}(h) = 8\pi(T_{\alpha\beta} - T_{\alpha\beta}^{\text{B}}) = 8\pi(\mathcal{T}_{\alpha\beta} + h^{\mu}{}_{(\alpha}T_{\beta)\mu}^{\text{B}}). \quad (5.23)$$

By combining Eqs. (5.22), (5.23), and the background Einstein equation  $G_{\text{B}}^{\alpha\beta} = 8\pi T_{\text{B}}^{\alpha\beta}$ , we obtain our final Lorentz-gauge form for the first-order, perturbed Einstein equation:

$$\bar{h}_{\alpha\beta|\mu}{}^{\mu} + 2R_{\mu\alpha\nu\beta}^{\text{B}}\bar{h}^{\mu\nu} = -16\pi(\mathcal{T}_{\alpha\beta} - 1/2\bar{h}_{\mu\nu}T_{\text{B}}^{\mu\nu}g_{\alpha\beta}^{\text{B}} - 1/2\bar{h}T_{\alpha\beta}^{\text{B}} + 1/4\bar{h}T_{\text{B}}g_{\alpha\beta}^{\text{B}}). \quad (5.24)$$

The equation of motion (5.11) for  $\mathcal{T}_{\alpha\beta}$ , which goes hand-in-hand with this wave equation, takes the following form when expressed in terms of  $\bar{h}_{\alpha\beta}$  rather than  $h_{\alpha\beta}$ , and when specialized to Lorentz gauge:

$$\mathcal{T}^{\alpha\mu}{}_{|\mu} = 1/2(\bar{h}_{\mu\nu}{}^{|\alpha} - \bar{h}^{\alpha}{}_{\mu|\nu})T_{\text{B}}^{\mu\nu} + 1/2\bar{h}_{|\mu}T_{\text{B}}^{\mu\alpha} - 1/4\bar{h}{}^{|\alpha}T_{\text{B}}. \quad (5.25)$$

In Eqs. (5.24) and (5.25),  $\bar{h}$  and  $T_B$  without indices denote the traces of  $\bar{h}_{\alpha\beta}$  and  $T_B^{\alpha\beta}$ :  $\bar{h} \equiv \bar{h}_{\alpha\beta} g_B^{\alpha\beta}$  and  $T_B \equiv T_B^{\alpha\beta} g_{\alpha\beta}^B$ .

Equations (5.24) and (5.25) describe the joint, coupled evolution of the gravitational perturbations  $\bar{h}_{\alpha\beta}$  and the stress-energy perturbations  $T_{\alpha\beta}$ . In the remainder of this chapter we shall use these coupled equations to study the propagation of gravitational waves in the presence of matter and electromagnetic fields. In Chap. 6 we shall use them to study the generation of gravitational waves by astrophysical sources.

### 5.C. Shortwave Formalism

Turn, now, from general formalism to a specific situation: the propagation of gravitational radiation with reduced wavelength  $\bar{\lambda}$  through a background spacetime with inhomogeneity scale  $\mathcal{L}$ . Assume, as in Chap. 4, that  $\bar{\lambda} \ll \mathcal{L}$  so the waves are well defined. Then the propagation is beautifully described using a *shortwave formalism* due to Isaacson (1968a,b). In this section we shall develop that formalism.

In our analysis we shall need, in addition to  $\bar{\lambda}$  and  $\mathcal{L}$ , a third lengthscale: the radius of curvature  $\mathcal{R}$  of the background spacetime. We define it to be the inverse square root of the largest components of the background Riemann tensor, evaluated in a proper reference frame

$$\mathcal{R} \equiv (\text{minimum value of } |R_{\alpha\beta\gamma\delta}^B|^{-1/2}) : \quad (5.26)$$

This lengthscale is depicted heuristically in Fig. 4.1 on page XX. We shall always define the inhomogeneity lengthscale  $\mathcal{L}$  to be no larger than the curvature lengthscale,

$$\mathcal{L} \lesssim \mathcal{R}, \quad (5.27)$$

because of a philosophical viewpoint that curvature itself is a form of inhomogeneity. (This also simplifies some of the conceptual issues that follow.)

We introduce into the full spacetime a coordinate system which, for the moment, we constrain in only one way: we demand that in it the metric coefficients  $g_{\alpha\beta}$ , like the physical curvature, vary on lengthscales  $\bar{\lambda}, \sim \mathcal{L}$ , and possibly  $\gg \mathcal{L}$ , but not on any lengthscales between  $\bar{\lambda}$  and  $\mathcal{L}$ .

Following Isaacson (1968a), we shall call such a coordinate system *steady*. We then define the background spacetime by the demand that there exist in it coordinates in which the background metric coefficients are the average over several wavelengths of the steady coordinates'  $g_{\alpha\beta}$ :

$$g_{\alpha\beta}^B(x^\mu) \equiv \langle g_{\alpha\beta}(x^\mu) \rangle. \quad (5.28)$$

The difference between  $g_{\alpha\beta}$  and  $g_{\alpha\beta}^B$  describes, of course, the gravitational radiation. In analyzing this radiation we shall be interested not only in linear effects, but also in nonlinear ones—for example, the energy and momentum carried by the waves. In preparation for discussing nonlinear effects, we shall write the difference between  $g_{\alpha\beta}$  and  $g_{\alpha\beta}^B$  not as a single field  $h_{\alpha\beta}$ , but rather as a power series:

$$g_{\alpha\beta} = g_{\alpha\beta}^B + \frac{h_{\alpha\beta}}{h\bar{\lambda}} + \frac{j_{\alpha\beta}}{h^2\bar{\lambda}^2} + \dots \quad (5.29)$$

Below each term we show the characteristic magnitude ( $1, h, h^2$ ) of the term, and also the lengthscale  $\lambda^-$  (or  $\mathcal{L}$ ) on which it varies. Note that  $j_{\alpha\beta}$  is a nonlinear correction to the propagating waves. This nonlinear correction is not yet precisely defined. We are free to shove pieces of it in and out of  $h_{\alpha\beta}$  in such a way as to make the computational formalism as simple as possible.

Similarly, we split up the covariant components of the stress-energy tensor in the following way:

$$T_{\alpha\beta} = T_{\alpha\beta}^{\text{B}} + \mathcal{T}_{\alpha\beta} + h^\mu{}_{(\alpha} T_{\beta)\mu}^{\text{B}} + j^\mu{}_{(\alpha} T_{\beta)\mu}^{\text{B}} + \dots \quad (5.30a)$$

[cf. Eq. (5.7b)]. Here, by definition,  $T_{\alpha\beta}^{\text{B}}$  is the average of  $T_{\alpha\beta}$  over several wavelengths

$$T_{\alpha\beta}^{\text{B}} \equiv \langle T_{\alpha\beta} \rangle ; \quad (5.30b)$$

and  $\mathcal{T}_{\alpha\beta} + h^\mu{}_{(\alpha} T_{\beta)\mu}^{\text{B}} + j^\mu{}_{(\alpha} T_{\beta)\mu}^{\text{B}} + \dots$  is the fluctuating part, which averages to zero. Our chosen form (5.30a) of  $T_{\alpha\beta}$  amounts to a definition of the stress-energy perturbation field  $\mathcal{T}_{\alpha\beta}$ . This specific definition is carefully chosen to make the fluctuating parts of the field equations [Eqs. (5.33) and (5.34) below] especially simple. We shall meet evidence of that simplicity in specific calculations with the formalism in Sec. 5.E.

In formulating the mathematics of our shortwave formalism, as in the linear perturbation theory of Sec. 5.C, we shall treat  $h_{\alpha\beta}$ ,  $j_{\alpha\beta}$ ,  $\mathcal{T}_{\alpha\beta}$ , and all other quantities except  $T_{\alpha\beta}$  and  $g_{\alpha\beta}$ , as fields that reside in the background spacetime. Correspondingly, we shall raise and lower their indices using the background metric  $g_{\alpha\beta}^{\text{B}}$ .

By a calculation analogous to that of the last section, but one which includes nonlinear terms as well as linear, one can derive a power-series expansion for the Einstein curvature tensor  $G_{\alpha\beta}$  of the full spacetime:

$$G_{\alpha\beta} = \lesssim \mathcal{R}^{-2}, \mathcal{L} + \frac{G_{\alpha\beta}^{\text{B}}}{\mathbf{h}^{-2}\lambda^-} + \frac{G_{\alpha\beta}^{(1)}(h)}{h\mathbf{h}^{-2}\lambda^-} + \frac{G_{\alpha\beta}^{(1)}(j)}{h\mathbf{h}^{-2}\lambda^-} + \dots \quad (5.31)$$

Here, as in Eq. (5.29), we write below each term its magnitude and the lengthscale on which it varies. The notation has the following meanings:  $G_{\alpha\beta}^{\text{B}}$  is the Einstein curvature tensor of the background spacetime, computed from the metric  $g_{\alpha\beta}^{\text{B}}$ ;  $G_{\alpha\beta}^{(1)}(h)$ , the piece that is linear in the radiation field  $h_{\alpha\beta}$ , is given by expression (5.16);  $G_{\alpha\beta}^{(1)}(j)$  is this same expression, but with  $h_{\alpha\beta}$  replaced by  $j_{\alpha\beta}$ ; and  $G_{\alpha\beta}^{(2)}(h)$  is the piece that is quadratic in  $h_{\alpha\beta}$  [derivable from MTW Eqs. (35.58)].

Following Isaacson (1968a,b), we split the Einstein field equation  $G_{\alpha\beta} = 8\pi T_{\alpha\beta}$ , through order  $h^2$ , into three parts: a part which varies on scales  $\mathcal{L}$  (obtained by averaging over a few wavelengths)

$$G_{\alpha\beta}^{\text{B}} = -\langle G_{\alpha\beta}^{(2)}(h) \rangle + 8\pi T_{\alpha\beta}^{\text{B}} ; \quad (5.32a)$$

a part whose individual terms have magnitude  $\mathbf{h}^{-2}$  or smaller, vary on scales  $\lambda^-$ , and average to zero on larger scales

$$G_{\alpha\beta}^{(1)}(h) = 8\pi(\mathcal{T}_{\alpha\beta} + h^\mu{}_{(\alpha} T_{\beta)\mu}^{\text{B}}) ; \quad (5.32b)$$

and a part whose terms have magnitude  $h\lambda^{-2}$  or smaller, vary on scales  $\lambda^-$  and average to zero on larger scales

$$G_{\alpha\beta}^{(1)}(j) = -G_{\alpha\beta}^{(2)}(h) + \langle G_{\alpha\beta}^{(2)}(h) \rangle + 8\pi j^\mu (T_{\beta\mu}^B)_{;\alpha} . \quad (5.32c)$$

This choice of how to split up the field equations determines the details of the split of the waves into  $h_{\alpha\beta} + j_{\alpha\beta}$ . Changing the split-up [pulling a piece of Eq. (5.32c) into Eq. (5.32b)] would shove a piece of  $j_{\alpha\beta}$  into  $h_{\alpha\beta}$ . Our specific choice of the split is guided by a desire to make the first-order equation (5.32b) identical to the linearized equation (5.23), so that when a weak wave enters a region of rapidly varying curvature  $\mathcal{L} \not\sim \mathcal{A}$  (e.g., when it impinges on a black hole), our first-order equation continues to be valid.

The first-order equation (5.32b) is a wave equation for the propagation of the first-order gravitational wave  $h_{\alpha\beta}$ . By specializing to Lorentz gauge, expressing the background Ricci tensor in terms of the background Einstein tensor, using Eq. (5.36) below for the background Einstein tensor, and discarding terms of the form  $\bar{h}_{\alpha\beta} T_{\gamma\delta}^{\text{GW}}$  because they are cubic in the wave amplitude  $h$  (one order smaller than the accuracy of our analysis), we bring Eq. (5.32b) into the standard linearized form (5.24):

$$\square \bar{h}_{\alpha\beta} \equiv \bar{h}_{\alpha\beta|\mu}{}^\mu = -2R_{\mu\alpha\nu\beta}^B \bar{h}^{\mu\nu} - 16\pi(\mathcal{T}_{\alpha\beta} - 1/2\bar{h}_{\mu\nu} T_B^{\mu\nu} g_{\alpha\beta}^B - 1/2\bar{h} T_{\alpha\beta}^B + 1/4\bar{h} T_B g_{\alpha\beta}^B) . \quad (5.33)$$

Much of the rest of this chapter will be devoted to a discussion of this wave equation and the physical effects associated with it.

In Lorentz gauge and in vacuum, Eq. (5.32c) takes on the form

$$\square \bar{j}_{\alpha\beta} = -2R_{\mu\alpha\nu\beta}^B \bar{j}^{\mu\nu} + 8\pi(\bar{j}_{\mu\nu} T_B^{\mu\nu} g_{\alpha\beta}^B + \bar{j} T_{\alpha\beta}^B - 1/2\bar{j} T_B g_{\alpha\beta}^B) + 2G_{\alpha\beta}^{(2)}(h) - 2\langle G_{\alpha\beta}^{(2)}(h) \rangle . \quad (5.34)$$

Here  $\bar{j}_{\alpha\beta} \equiv j_{\alpha\beta} - 1/2j_\mu{}^\mu g_{\alpha\beta}^B$ , and  $\bar{j} \equiv \bar{j}_\mu{}^\mu$ . The terms on the right-hand side involving  $G^{(2)}(h)$ , which are quadratic in  $h_{\alpha\beta}$ , act as a source for the nonlinear corrections  $j_{\alpha\beta}$  to  $h_{\alpha\beta}$ . Thus, this equation describes nonlinear wave-wave coupling (“3-wave coupling” in the standard jargon of nonlinear physics) analogous to that which occurs in plasma physics or for electromagnetic waves in a nonlinear medium. We shall discuss the effects of this wave-wave coupling in Sec. 5.G.e below.

Equation (5.32a) describes the waves’ nonlinear generation of background curvature. This equation, in fact, is the foundation for Isaacson’s (1968b) description of the energy and momentum carried by the waves: Isaacson defines the *gravitational-wave stress-energy tensor* by

$$T_{\alpha\beta}^{\text{GW}} \equiv -\frac{1}{8\pi} \langle G_{\alpha\beta}^{(2)}(h) \rangle , \quad (5.35)$$

and then notes that in terms of this tensor Eq. (5.32a) takes on the same form as the standard Einstein field equation

$$G_{\alpha\beta}^B = 8\pi(T_{\alpha\beta}^B + T_{\alpha\beta}^{\text{GW}}) . \quad (5.36)$$

Equation (5.36) shows that the gravitational-wave stress-energy tensor, like any nongravitational stress-energy tensor, generates spacetime curvature. Isaacson points out, moreover, that because  $G_{\alpha\beta}^B$ , like any Einstein tensor, automatically has vanishing divergence, the sum  $T_{\alpha\beta}^B + T_{\alpha\beta}^{\text{GW}}$  is guaranteed also to have vanishing divergence:

$$(T^B{}^{\alpha\beta} + T^{\text{GW}}{}^{\alpha\beta})_{|\beta} = 0. \quad (5.37)$$

In other words, when averaged over a few wavelengths, the sum of the gravitational-wave energy-momentum and the nongravitational energy-momentum is conserved. For example, when a gravitational-wave detector is driven into motion by a passing wave, the detector's energy (embodied in  $T^B{}^{\alpha\beta}$ ) goes up, and the wave's energy (embodied in  $T^{\text{GW}}{}^{\alpha\beta}$ ) goes down.

A straightforward but tedious calculation (Isaacson, 1968b; Eq. (35.70) of MTW and associated discussion) gives the following explicit expression for  $T_{\alpha\beta}^{\text{GW}}$  in an arbitrary gauge:

$$T_{\alpha\beta}^{\text{GW}} = \frac{1}{32\pi} \langle \bar{h}_{\mu\nu|\alpha} \bar{h}_{|\beta}^{\mu\nu} - 1/2 \bar{h}_{|\alpha} \bar{h}_{|\beta} - \bar{h}^{\mu\nu}{}_{|\nu} \bar{h}_{\mu\alpha|\beta} - \bar{h}^{\mu\nu}{}_{|\nu} \bar{h}_{\mu\beta|\alpha} \rangle. \quad (5.38)$$

Here  $\bar{h}_{\alpha\beta}$  is the trace-reversed, first-order metric perturbation [Eq. (5.15)]. Note that in Lorentz gauge the last two terms vanish; and in a nearly Lorentz frame and TT gauge, because  $\bar{h}_{00} = \bar{h}_{0j} = 0$  and  $\bar{h}_{jk} = h_{jk}^{\text{GW}}$  which is trace free, Eq. (5.38) reduces to

$$T_{\alpha\beta}^{\text{GW}} = \frac{1}{32\pi} \langle h_{jk,\alpha}^{\text{GW}} h_{jk,\beta}^{\text{GW}} \rangle. \quad (5.39)$$

Here there is an implied summation on  $j$  and  $k$ , which are Cartesian, spatial indices. When, moreover, the waves propagate in the  $z$ -direction of a nearly Lorentz frame so  $h_{xx}^{\text{GW}} = -h_{yy}^{\text{GW}} = h_+(t-z)$ ,  $h_{xy}^{\text{GW}} = h_{yx}^{\text{GW}} = h_\times(t-z)$ , this becomes the expression (4.33) that was discussed in Chap. 4.

Note that the magnitude of the gravitational-wave stress-energy tensor is  $T_{\alpha\beta}^{\text{GW}} \sim (h\lambda)^2$ ; cf. Eq. (4.34). Since this stress-energy is a source of background curvature through the averaged Einstein equation  $G_{\alpha\beta}^B = 8\pi(T_{\alpha\beta}^B + T_{\alpha\beta}^{\text{GW}})$  [Eq. (5.36)], it must be that  $G_{\alpha\beta}^B \gtrsim (h\lambda)^2$ . However, because  $G_{\alpha\beta}^B$  is constructed as a sum of components of the background Riemann tensor, the largest of which have magnitudes  $1/\mathcal{R}^2$ , it must be that  $G_{\alpha\beta}^B \lesssim 1/\mathcal{R}^2$ . From these relations and  $\mathcal{R} \gtrsim \mathcal{L}$  we infer that

$$h \lesssim \lambda/\mathcal{R} \lesssim \lambda/\mathcal{L}. \quad (5.40)$$

Since the very concept of a gravitational wave has meaning only when  $\lambda \ll \mathcal{L}$ , Eq. (5.40) tells us that *gravitational radiation always has a small dimensionless amplitude*,

$$h \ll 1. \quad (5.41)$$

Equation (5.37) is only one portion of the law of conservation of energy-momentum: the portion obtained by averaging  $T^{\alpha\beta}{}_{;\beta} = 0$  over a few wavelengths. The other portion, that which fluctuates on scales of order  $\lambda$  and averages to zero, has the linearized form (5.25):

$$\mathcal{T}^{\alpha\mu}{}_{|\mu} = 1/2(\bar{h}_{\mu\nu}{}^{|\alpha} - \bar{h}^{\alpha}{}_{\mu|\nu})T_B^{\mu\nu} + 1/2\bar{h}_{|\mu}T_B^{\mu\alpha} - 1/4\bar{h}^{|\alpha}T_B. \quad (5.42)$$

The right side is the force exerted by the waves on the matter or fields through which they propagate, and the left side is the response of the matter or fields to this gravitational force.

## 5.D. Geometric Optics

Turn, next, to the task of solving the wave equation (5.33) for the propagation of  $\bar{h}^{\alpha\beta}$  from its source to the earth. As we shall see in Secs. 5.E and 5.F, in the real astrophysical universe (except near the Planck time) the effects of matter and electromagnetic fields on the propagating waves are minuscule. This permits us to simplify our analysis by setting to zero, in the propagation equation (5.33), the nongravitational stress-energies  $\mathcal{T}_{\alpha\beta}$  and  $T_{\alpha\beta}^{\text{B}}$ —a procedure we shall call the *vacuum approximation* for wave propagation.

The wave equation (5.33) has already been simplified by specializing to Lorentz gauge; and we shall now simplify it further by an additional specialization of the gauge: It is not difficult to verify that the gauge will remain Lorentz ( $\bar{h}_{|\beta}^{\alpha\beta} = 0$  will continue to be satisfied) if the generator  $\xi_\alpha$  of the gauge change (5.19) satisfies the wave equation  $\square\xi_\alpha = 0$ . Note, further, that the trace of the propagation equation (5.33) guarantees (in vacuum) that  $\bar{h} = \bar{h}^\alpha{}_\alpha$  satisfies the wave equation  $\square\bar{h} = 0$ . Accordingly, if we choose  $\xi_\alpha$  to be a solution of the wave equation  $\square\xi_\alpha = 0$  such that  $\xi^\alpha{}_{|\alpha} = 1/2h^{\text{old}} = -1/2\bar{h}^{\text{old}}$ , then the gauge change (5.19) will remove the trace of  $h_{\alpha\beta}$ . We make this gauge change, thereby guaranteeing that

$$h = \bar{h} = 0, \quad \bar{h}_{\alpha\beta} = h_{\alpha\beta}. \quad (5.43)$$

This permits us to omit bars from  $h_{\alpha\beta}$  in what follows.

We expect the field  $h_{\alpha\beta}$  to be a rapidly varying function of the source's retarded time  $\tau_e$ , and a slowly varying function of all other spacetime coordinates. More specifically, it should vary in  $\tau_e$  on a lengthscale  $\lambda$  (the reduced wavelength of the waves); and all its other variations should have lengthscales no longer than

$$\mathcal{D} \equiv \text{minimum of } \mathcal{L} \text{ and radius of curvature of wave fronts.} \quad (5.44)$$

Accordingly, we shall seek a solution of the propagation equation which is accurate only to leading order in the small dimensionless parameter  $\lambda/\mathcal{D}$ —in other words, we shall solve for the propagation using the *vacuum, geometric-optics approximation*.

As a formal mathematical tool in the solution, we introduce a parameter  $\epsilon$  which tells us at a glance the relative orders of magnitude of various terms: If a specific term is of order  $(\lambda/\mathcal{D})^n$  relative to other terms with which it is compared, then we shall prepend to it a factor  $\epsilon^n$ . However, we shall take the numerical value of  $\epsilon$  to be one, thereby allowing ourselves to drop it when it ceases to be useful. In this spirit, we write the field  $h_{\alpha\beta}$  in the form (“geometric optics expansion”)

$$h_{\alpha\beta} = h_{\alpha\beta}^{[0]}(\tau_e/\epsilon, x^\mu) + \epsilon h_{\alpha\beta}^{[1]}(\tau_e/\epsilon, x^\mu) + \epsilon^2 h_{\alpha\beta}^{[2]}(\tau_e/\epsilon, x^\mu) + \dots \quad (5.45)$$

The term  $h_{\alpha\beta}^{[0]}$  is the geometric optics approximation to  $h_{\alpha\beta}$ , and  $h_{\alpha\beta}^{[1]}, h_{\alpha\beta}^{[2]}, \dots$  are “post-geometric-optics corrections”. It will be straightforward to read off our formalism the equations governing the corrections, but we will focus attention in the end only on the leading term,  $h_{\alpha\beta}^{[0]}$ . Each  $h_{\alpha\beta}^{[n]}$  varies in  $\tau_e$  on the scale  $\lambda$  and in its argument  $x^\mu$  on the scale  $\mathcal{D}$ ; i.e., it can be thought of as varying on scales of order unity in both  $\tau_e\lambda^{-1}$  and  $x^\mu/\mathcal{D}$ —which means that by comparison with  $x^\mu$ , the  $\tau_e$  in the functional form requires a factor

$\epsilon^{-1}$ . That is why we write the functional form as  $h_{\alpha\beta}^{[n]}(\tau_e/\epsilon, x^\mu)$ . Because of this functional form, we write the covariant derivative (gradient) of  $h_{\alpha\beta}^{[n]}$  as

$$h_{\alpha\beta|\mu}^{[n]} = -\epsilon^{-1}\dot{h}_{\alpha\beta}^{[n]}k_\mu + h_{\alpha\beta|\mu'}^{[n]}. \quad (5.46)$$

Here the dot denotes a derivative with respect to  $\tau_e$

$$\dot{h}_{\alpha\beta} \equiv \left( \frac{\partial h_{\alpha\beta}}{\partial \tau_e} \right)_{x^\mu}; \quad (5.47a)$$

$k_\mu$  is the negative of the gradient of  $\tau_e$

$$k_\mu \equiv -\tau_{e|\mu}; \quad (5.47b)$$

and the prime on the last  $\mu$  index indicates that the covariant derivative is to be taken holding  $\tau_e$  constant.

This notation makes straightforward the geometric-optics expansion of the propagation equation (5.33), the Lorentz gauge condition (5.20), and our auxiliary gauge condition (5.43). The result of those expansions is:

$$\begin{aligned} \epsilon^{-2}\ddot{h}_{\alpha\beta}^{[0]}k_\mu k^\mu + \epsilon^{-1}(-2\dot{h}_{\alpha\beta|\mu'}^{[0]}k^\mu - \dot{h}_{\alpha\beta}^{[0]}k^\mu{}_{|\mu} + \ddot{h}_{\alpha\beta}^{[1]}k_\mu k^\mu) + \epsilon^0(2R_{\mu\alpha\nu\beta}^B h^{[0]\mu\nu} \\ + h_{\alpha\beta|\mu'}^{[0]|\mu'} - 2\dot{h}_{\alpha\beta|\mu'}^{[1]}k^\mu - \dot{h}_{\alpha\beta}^{[1]}k^\mu{}_{|\mu} + \ddot{h}^{\alpha\beta[2]}k_\mu k^\mu) + \text{O}(\epsilon) = 0; \end{aligned} \quad (5.48a)$$

$$-\epsilon^{-1}\dot{h}_{\alpha\beta}^{[0]}k^\beta + \epsilon^0(h_{\alpha\beta}^{[0]|\beta'} - \dot{h}_{\alpha\beta}^{[1]}k^\beta) + \text{O}(\epsilon) = 0; \quad (5.48b)$$

$$h_\alpha^{[0]\alpha} + \epsilon h_\alpha^{[1]\alpha} + \epsilon^2 h_\alpha^{[2]\alpha} + \text{O}(\epsilon^3) = 0. \quad (5.48c)$$

By equating to zero the leading two orders in (5.48a) and the leading order in (5.43b,c), we obtain the geometric-optics equations that govern  $h_{\alpha\beta}^{[0]}$ :

$$k_\mu k^\mu = 0, \quad h_{\alpha\beta|\mu'}^{[0]}k^\mu = -1/2k^\mu{}_{|\mu}h_{\alpha\beta}^{[0]}, \quad h_{\alpha\beta}^{[0]}k^\beta = 0, \quad h_\alpha^{[0]\alpha} = 0. \quad (5.49)$$

The higher-order terms in (5.48) govern the post-geometric-optics corrections to the propagation.

The first of Eqs. (5.49) tells us that the wave vector  $\mathbf{k} = -\nabla\tau_e$  is null, as it surely should be since we chose  $\tau_e$  to be retarded time. By taking the gradient of  $k_\mu k^\mu = 0$ , then noting that  $k_{\mu|\nu} = -\tau_{e|\mu\nu} = -\tau_{e|\nu\mu} = k_{\nu|\mu}$ , we deduce that  $k_{\nu|\mu}{}^{|\mu} = 0$ . Thus, the wave vector is the tangent vector to a null geodesic. That null geodesic is a *ray* of the propagating waves.

The second of Eqs. (5.49) tells us how the field  $h_{\alpha\beta}^{[0]}$  propagates along its rays. Note that, because  $\tau_e$  is constant along any ray, we do not need the prime on the gradient in this propagation equation: with or without the prime, the left-hand side of the propagation equation is sensitive only to the changes in  $h_{\alpha\beta}$  that hold  $\tau_e$  constant.

The third of Eqs. (5.49) tells us that the field  $h_{\alpha\beta}^{[0]}$  is orthogonal to its wave vector; and the fourth tells us it is trace-free.

Henceforth we shall ignore all post-geometric-optics corrections, and shall use  $h_{\alpha\beta}^{[0]}$  as a high-accuracy approximation to  $h_{\alpha\beta}$ . Accordingly, we shall rewrite the equations (5.49) governing it as

$$k_\mu k^\mu = 0, \quad k_{\nu|\mu} k^\mu = 0, \quad (5.50a)$$

$$h_{\alpha\beta} k^\beta = 0, \quad h_\alpha{}^\alpha = 0, \quad (5.50b)$$

$$h_{\alpha\beta|\mu} k^\mu = -1/2 k^\mu{}_{|\mu} h_{\alpha\beta}. \quad (5.50c)$$

Notice that the curvature-coupling term  $R_{\mu\alpha\nu\beta}^B h^{\mu\nu}$ , which appeared in the original propagation equation (5.33), is gone in the geometric-optics limit. It shows up only as a post-geometric-optics correction [the  $O(\epsilon^0)$  part of Eq. (5.48a), where the coupling of  $h_{\alpha\beta}^{[0]}$  to the curvature helps generate the tiny correction  $h_{\alpha\beta}^{[1]}$ ]. Because that curvature coupling is gone, in the geometric-optics limit  $h_{\alpha\beta}$  satisfies the wave equation  $\square h_{\alpha\beta} = 0$ ; and because the waves' Riemann tensor is a linear sum of gradients of  $h_{\alpha\beta}$  [Eq. (5.13)], it also satisfies the wave equation:

$$\square R_{\alpha\beta\gamma\delta}^{\text{GW}} = 0. \quad (5.51)$$

This is the propagation equation (4.5) which was derived in a very different manner in Sec. 4.A and was used as the foundation for the description of gravitational radiation in Chap. 4. Note, further, that in the geometric-optics approximation the waves' Riemann tensor (5.13) takes the form

$$R_{\alpha\beta\gamma\delta}^{\text{GW}} = 1/2(\ddot{h}_{\alpha\delta} k_\beta k_\gamma + \ddot{h}_{\beta\gamma} k_\alpha k_\delta - \ddot{h}_{\alpha\gamma} k_\beta k_\delta). \quad (5.52)$$

This is identical in form to expression (4.27), except that here the field used is the geometric-optics approximation to the trace-free, Lorentz-gauge metric perturbation  $h_{\alpha\beta}$ , while in Chap. 4 the field used was the “gravitational-wave field”  $h_{\alpha\beta}^{\text{GW}}$ . Recall that in Chap. 4 there was a separate gravitational-wave field  $h_{\alpha\beta}^{\text{GW}}$  associated with each nearly Lorentz reference frame, but that all those fields, when inserted into (5.52), produced the same frame-invariant Riemann tensor. In fact, in any specific small region of spacetime, one can adjust  $h_{\alpha\beta}$  to be the same as the  $h_{\alpha\beta}^{\text{GW}}$  of any desired nearly Lorentz frame there by a gauge change with a generator that has the geometric-optics form

$$\xi_\alpha = \xi_\alpha(\tau_e/\epsilon, x^\mu), \quad \text{where } \xi_\alpha k^\alpha = 0 \text{ and } \xi_{\alpha|\mu} k^\mu = 0. \quad (5.53)$$

This gauge change, in fact, has precisely the same effect as the transverse-traceless projection process introduced in Eq. (4.50). Correspondingly, in the chosen nearly Lorentz frame the gravitational-wave field is

$$h_{jk}^{\text{GW}} = (h_{jk})^{\text{TT}}, \quad (5.54)$$

where the superscript TT means “perform the TT projection process of Eq. (4.50)”.



We are ready, now, to make contact with the vacuum, geometric-optics propagation laws presented in Sec. 5.A: The field (5.2i) constructed there is the solution  $h_{\alpha\beta}$  of the equations of propagation (5.50). To verify this is straightforward, except for one detail: it is necessary to know that the cross sectional area  $\Delta A$  of a bundle of rays obeys the differential equation

$$\Delta A_{|\mu} k^\mu = k^\mu_{|\mu} \Delta A . \quad (5.55)$$

This is proved, for example, in Exercise 22.13 of MTW.

Finally, we note that for this geometric-optics solution (5.2i) to the propagation equations, Isaacson's gravitational-wave stress-energy tensor (5.38) reduces to

$$T_{\alpha\beta}^{\text{GW}} = \frac{1}{16\pi} \langle (\dot{h}_+)^2 + (\dot{h}_\times)^2 \rangle k_\alpha k_\beta = \frac{1}{16\pi r^2} \langle (\dot{Q}_+)^2 + (\dot{Q}_\times)^2 \rangle k_\alpha k_\beta , \quad (5.56)$$

in accord with an assertion made in Chap. 4 [Eq. (4.32)].

### 5.E. Interaction with Matter

In developing the geometric optics formalism for gravitational-wave propagation, we ignored the coupling of the waves to the matter and nongravitational fields through which they propagate; i.e., we introduced the “vacuum approximation”. In this section we shall study the coupling to matter, and in the next section, the coupling to electromagnetic fields. These studies will show that the vacuum approximation is highly accurate in the real astrophysical universe: the coupling to matter and electromagnetic fields can change only slightly the properties of the propagating waves. The sole exception is for waves emerging from the Planck era of the big bang. Near the Planck era, individual elementary particles and gravitons were so energetic that they could interact significantly (Sec. 7.2 of Zel'dovich and Novikov, 1983).

When gravitational waves pass through matter, they can be absorbed and scattered, and can develop dispersion (frequency-dependent propagation speeds). In this section we shall study absorption and dispersion, and shall describe and give references for scattering.

In our studies of absorption and dispersion, initially we shall confine attention to matter which, before the waves arrive, is static and has isotropic stresses and self-gravity that is negligible on lengthscales somewhat larger than the waves' reduced wavelength. More specifically, we shall assume that in the region of spacetime we are studying there exists a local Lorentz frame of  $g_{\alpha\beta}^{\text{B}}$  with size  $\mathcal{D} \gg \lambda$  in which

$$T_{\text{B}}^{00} = \rho_{\text{B}} , \quad T_{\text{B}}^{0j} = 0 , \quad T_{\text{B}}^{jk} = p_{\text{B}} \delta^{ij} , \quad (5.57)$$

with  $\rho_{\text{B}}$  (the density) and  $p_{\text{B}}$  (the pressure) independent of time  $t = x^0$  but possibly dependent on  $x^j$ ; and we shall insist that throughout this frame the gravitational interactions of the matter are negligible. By “negligible interactions” I mean that (i)  $g_{\alpha\beta}^{\text{B}}$  can be approximated by  $\eta_{\alpha\beta}$ , and (ii) when the matter is perturbed on scales  $\lesssim \mathcal{D}$ , the gravitational influence of one element of matter on any other can be ignored. This rules out, for example, using our analysis to study the coupling of gravitational waves to quadrupolar

normal modes of the earth; but it permits a study of coupling to short-wavelength sound waves inside the earth, to the quadrupolar modes of resonant-bar gravitational-wave detectors, and to primordial plasma in the early universe. Note that our local Lorentz frame must always be small compared with the background radius of curvature,  $\mathcal{D} \ll \mathcal{R}$ , since one can never approximate  $g_{\alpha\beta}^{\text{B}}$  by  $\eta_{\alpha\beta}$  on scales of order  $\mathcal{R}$ .

Specific examples that we shall study are a homogeneous perfect fluid (subsection *a* below), a homogeneous viscous fluid (subsection *b*), an inhomogeneous elastic medium, e.g., the earth (subsection *c*), a medium made of a large number of quadrupolar oscillators (subsection *d*), and a plasma (subsection *e*).

We presume that gravitational waves propagate into our local Lorentz frame from very far away, and thus are plane fronted on the scale of our frame. To simplify our calculations, we shall describe the waves in a gauge that is TT as the waves enter our frame. Since, as we shall see, interaction with the matter has only a tiny effect on the waves, on the right-hand side of the wave equation (5.33) we can treat the waves as having the undisturbed TT form

$$\bar{h}_{00} = \bar{h}_{0j} = 0, \quad \bar{h}_{jk} = h_{jk}^{\text{GW}}(t - n_j x^j). \quad (5.58a)$$

Here  $n_j$  is a unit vector in the propagation direction, and  $h_{jk}^{\text{GW}}$  is the transverse-traceless gravitational-wave field

$$h_{jk}^{\text{GW}} n^k = 0, \quad h_{jk}^{\text{GW}} \delta^{jk} = 0. \quad (5.58b)$$

This form of  $\bar{h}_{\alpha\beta}$  has  $\bar{h} = 0$ , and when contracted into the background stress-energy tensor (5.57) it gives  $\bar{h}_{\alpha\beta} T_{\text{B}}^{\alpha\beta} = 0$ , thereby bringing the wave equation (5.33) into the form

$$\square \bar{h}_{\alpha\beta} + 2R_{\mu\alpha\nu\beta}^{\text{B}} \bar{h}^{\mu\nu} = -16\pi \mathcal{T}_{\alpha\beta}. \quad (5.59)$$

[Our original definition (5.7) of  $\mathcal{T}_{\alpha\beta}$  was carefully crafted so that it alone would remain on the right-hand side of (5.59). If we had used the more naive definition  $\mathcal{T}_{\alpha\beta} = T_{\alpha\beta} - T_{\alpha\beta}^{\text{B}}$ , then the right-hand side of (5.59) would have contained an additional term  $16\pi p_{\text{B}} \bar{h}^{\alpha\beta}$ , thereby complicating our calculations but, of course, not changing their final physical conclusions.]

Notice that in (5.59) only the TT part of  $\mathcal{T}_{\alpha\beta}$  can contribute to the physically measurable waves. All other parts (e.g.,  $\mathcal{T}_{00}$  and  $\mathcal{T}_{jk} n^k$ ) produce changes in  $\bar{h}_{\alpha\beta}$  that are pure gauge, i.e., that contribute nothing to the waves' Riemann tensor and thus can be removed by a gauge transformation.

In the equation of motion (5.42) for the matter, as on the right-hand side of the wave equation, we can use the undisturbed wave field (5.58). When Eqs. (5.58) and (5.57) are inserted into Eq. (5.42), all terms on the right-hand side are found to vanish, leaving only

$$\mathcal{T}^{\alpha\mu}{}_{|\mu} = 0. \quad (5.60)$$

At first sight one might think that this equation of motion implies the waves have no influence at all on the matter. On the contrary, as we shall see, there is a coupling of waves and matter embodied in  $\mathcal{T}^{\alpha\beta}$  and hence in (5.60). Equation (5.60) governs the

dynamical response of the matter to that coupling, and (5.59) governs the response of the waves.

Although Eqs. (5.59) and (5.60) are valid only in a local Lorentz frame of size  $\mathcal{D} \ll \mathcal{R}$ , they can be used to study wave propagation on scales  $\gtrsim \mathcal{R}$ : All one need do is string a series of local Lorentz frames together along the route of the waves, and as the waves enter each frame transform them to that frame's TT gauge.

To make these remarks more concrete and to get physical insight into wave-matter coupling, we shall now study several specific situations.

### *a. Homogeneous perfect fluid*

The coupling of gravitational waves to a homogeneous, perfect fluid has been studied by a number of researchers over the years. The analysis which I like most is that of Gayer and Kennel (1979). The following calculation is patterned on it.

For a homogeneous perfect fluid, the stress-energy tensor in the full spacetime has the general form

$$T^{\alpha\beta} = (\rho + p)u^\alpha u^\beta + pg^{\alpha\beta} \quad (5.61)$$

(see, e.g., Sec. 22.3 of MTW). Here  $u^\alpha$  is the fluid 4-velocity, and  $\rho$  and  $p$  are the density and pressure as measured in the fluid's local rest frame. Our background stress-energy tensor (5.57) has this form with  $u_B^0 = 1$  and  $u_B^j = 0$ . Suppose that the fluid is perturbed slightly, so that a particle originally at location  $x^j$  gets moved to coordinate location  $x^j + \xi^j$ . This displacement produces a fractional increase in fluid volume  $\delta V/V = \xi^j{}_{|j}$ ; and correspondingly (by energy conservation), the density changes by  $\delta\rho = -(\rho_B + p_B)\xi^j{}_{|j}$ , and the pressure changes by  $\delta p = -K\xi^j{}_{|j}$ , where  $K$  is the fluid's bulk modulus. The time-dependent displacement  $\xi^j$  also produces a first-order change  $\delta u^0 = 0$ ,  $\delta u^j = \dot{\xi}^j$  in the 4-velocity, where the dot denotes  $\partial/\partial t$ . These perturbations, together with  $\delta g^{\alpha\beta} = -h^{\alpha\beta}$ , all contribute to the stress-energy perturbation

$$T^{\alpha\beta} - T_B^{\alpha\beta} = (\delta\rho + \delta p)u_B^\alpha u_B^\beta + 2(\rho_B + p_B)u^{(\alpha}\delta u^{\beta)} + \delta p g_B^{\alpha\beta} - ph^{\alpha\beta a}. \quad (5.62)$$

Our definition (5.7a) of  $\mathcal{T}^{\alpha\beta}$  has been carefully crafted so that the wave-dependent term  $-ph^{\alpha\beta a}$  will drop out of it. More specifically, by combining Eqs. (5.62) and (5.7a) and inserting the above values of  $\delta\rho$ ,  $\delta p$ , and  $\delta u^\alpha$ , we obtain

$$\mathcal{T}^{00} = -(\rho_B + p_B + K)\xi^i{}_{|i}, \quad \mathcal{T}^{0j} = (\rho_B + p_B)\dot{\xi}^j, \quad \mathcal{T}^{jk} = -K\xi^i{}_{|i}\delta^{jk}. \quad (5.63)$$

Notice that nowhere at all in this  $\mathcal{T}^{\alpha\beta}$  is there any gravitational-wave field  $\bar{h}^{\alpha\beta}$ , and recall that there is no explicit appearance of the wave field in the fluid's equation of motion (5.60). Correspondingly, as Gayer and Kennel (1979) conclude (see also p. 420 of Grishchuk and Polnarev, 1980 and references therein; XXXXXXXX), *a gravitational wave cannot couple to a homogeneous, perfect fluid*. This is true in two senses: (i) When a wave hits the fluid, it leaves  $\xi^i = 0$  and  $\mathcal{T}^{\alpha\beta} = 0$ ; and correspondingly, the wave propagates through the fluid in accord with the standard, vacuum propagation equation

$\square \bar{h}_{\alpha\beta} + 2R_{\mu\alpha\nu\beta} \bar{h}^{\mu\nu} = 0$ . (ii) When sound waves, governed by  $\mathcal{T}^{\alpha\mu}{}_{|\mu} = 0$ , propagate through the fluid, they carry a nonzero  $\mathcal{T}_{\alpha\beta}$  [Eq. (5.63)] whose spatial part (at first order in the fluid displacement) is a pure trace. Correspondingly, they generate via (5.59), a  $\bar{h}^{\alpha\beta}$  wave whose spatial part is pure trace, and hence is pure gauge: it can be removed by a subsequent gauge transformation. In other words, pressure waves in a homogeneous perfect fluid cannot radiate gravitational radiation, at first order in the fluid displacement. [KIP: HOW ABOUT HIGHER ORDERS? I THINK IT IS REPUTED TO VANISH THERE ALSO.]

*b. Homogeneous, viscous fluid*

If our homogeneous fluid has shear viscosity as well as pressure and density, then its full stress-energy tensor (5.61) is augmented by  $-2\eta\sigma^{\alpha\beta}$ , where  $\eta$  is the coefficient of shear viscosity and  $\sigma_{\alpha\beta}$  is the fluid's rate of shear (the symmetric, trace-removed part of the gradient of the 4-velocity, projected orthogonal to the 4-velocity); see, e.g., Exercise 22.6 of MTW. For the unperturbed fluid, with 4-velocity  $u_B^0 = 1$  and  $u_B^j = 0$ , the shear vanishes and the stress-energy tensor  $T_B^{\alpha\beta}$  has the form (5.57) considered above. However, when the fluid undergoes the displacement  $\xi^j$  and a gravitational wave of the form (5.58) is passing, the fluid experiences a rate of shear

$$\sigma_{00} = \sigma_{0j} = 0, \quad \sigma_{jk} = \xi_{(j|k)} - 1/3\xi^i{}_{|i}\delta_{jk} + 1/2\dot{h}_{jk}^{\text{GW}}. \quad (5.64)$$

(The term  $1/2\dot{h}_{jk}^{\text{GW}}$  arises from a connection coefficient  $\Gamma^0{}_{jk}$  in the computation of the gradient of the 4-velocity.) Correspondingly, the stress-energy perturbation  $\mathcal{T}_{\alpha\beta}$  has the standard form for a slightly perturbed viscous fluid in flat spacetime, augmented by the coupling term

$$\delta\mathcal{T}_{jk} = -\eta\dot{h}_{jk}^{\text{GW}}. \quad (5.65)$$

This term has a nonzero TT part. Thus, it produces a genuine coupling of the fluid to the gravitational waves.

The influence of this term on the waves can be studied by inserting it onto the right-hand side of the wave equation (5.59), taking the TT part of that wave equation so as to get rid of all extraneous, pure-gauge parts, and dropping the tiny curvature-coupling term (which we shall study in Sec. 5.G below). The result is

$$\square h_{jk}^{\text{GW}} = 16\pi\eta\dot{h}_{jk}^{\text{GW}}. \quad (5.66)$$

A straightforward solution shows that the time-derivative term on the right-hand side produces a damping of the waves: The amplitude of the waves dies out as  $\exp(-l/2l_{\text{atten}})$ , and the energy dies out as  $\exp(-l/l_{\text{atten}})$ , where  $l$  is the distance travelled and  $l_{\text{atten}}$  is the energy attenuation length

$$l_{\text{atten}} = \frac{1}{32\pi\eta}. \quad (5.67)$$

By restoring the factors of  $G$  and  $c$ , i.e., converting to cgs units via Eqs. (4.3), we bring this attenuation length into the form

$$l_{\text{atten}} = \frac{c^6/G}{32\pi\eta} = (4.2 \times 10^{18} \text{ lt yr}) \left( \frac{1 \text{ poise}}{\eta} \right). \quad (5.67')$$

When we recall that 1 poise is 1 dyne cm sec<sup>-2</sup>, and that the viscosity of water is about 0.01 poise, we recognize that the gravitational waves' viscosity-induced attenuation length is exceedingly long.

Where does the gravitational waves' energy go? Into the fluid, of course. The wave-induced rate of shear,  $\sigma_{jk} = 1/2\dot{h}_{jk}^{\text{GW}}$ , working against the viscosity, produces heat, thereby increasing the background energy density of the fluid at a rate  $\partial\rho_{\text{B}}/\partial t = 2\eta\sigma_{jk}\sigma^{jk}$  (MTW, Exercise 22.7). This rate of heating is precisely equal to the rate of loss of gravitational-wave energy,

$$\frac{\partial\rho_{\text{B}}}{\partial t} = -T_{\text{GW}|j}^{0j} = \frac{T_{\text{GW}}^{0j}n_j}{l_{\text{atten}}}, \quad (5.68)$$

as one can readily verify using expression (4.33) for the gravitational-wave energy flux and expression (5.67) for the waves' attenuation length. Notice, moreover, that this energy-balance relation (5.68) is just the general law of energy-momentum conservation (5.37), specialized to the present situation.

In order to estimate the magnitude of the attenuation length (5.67), we must consider the microscopic, particulate nature of the fluid. If the fluid is made of particles that move with mean speed  $v$  and that scatter off each other after traveling, on average, a mean free path  $s \ll \lambda$  (inhomogeneity scale of the perturbed fluid), then kinetic theory dictates that  $\eta \sim \rho_{\text{B}}vs$ ; see, e.g., XXXX. If  $s \gtrsim \lambda$ , the diffusion approximation which underlies the theory of viscous fluids breaks down, but one can show that the above formula for viscous heating remains valid in order of magnitude if we set  $\eta \sim \rho_{\text{B}}vs(\lambda/s)^2$ . These expressions for the viscosity  $\eta$ , together with the fact that the fluid produces a background radius of curvature  $\mathcal{R} \sim 1/(\text{Riemann tensor due to fluid})^{1/2} \sim 1/(\text{Einstein tensor due to fluid})^{1/2} \sim 1/(\text{energy density } \rho_{\text{B}} \text{ due to fluid})^{1/2}$ , implies that

$$\frac{l_{\text{atten}}}{\mathcal{R}} \sim \frac{\mathcal{R}}{\lambda} \frac{1}{v} \max\left(\frac{\lambda}{s}, \frac{s}{\lambda}\right). \quad (5.69)$$

The magnitudes of the terms on the right-hand side are  $\mathcal{R}\lambda \gg 1$  by virtue of the definition of a gravitational wave,  $1/v \geq 1$  since the fluid's particles cannot travel faster than light, and  $\max(\lambda/s, s/\lambda) \gtrsim 1$ . Consequently, the attenuation length is always much larger than the background radius of curvature of spacetime  $\mathcal{R}$  produced by the fluid. Since the size of the fluid cannot exceed by much the radius of curvature  $\mathcal{R}$  (when it reaches a size a bit larger than  $\mathcal{R}$ , it curls space up into closure around itself), this means that *no viscous fluid can produce significant attenuation of gravitational radiation*.

For more detailed treatments of the interaction between a viscous fluid and gravitational waves see, e.g., Esposito (1971a,b), Papadopoulos and Esposito (1985), Szekeres (1971), Sec. 4.2 of Grishchuk and Polnarev (1980) [KIP: CHECK THESE REFERENCES].

*c. Inhomogeneous, elastic medium*

For an inhomogeneous, elastic medium (e.g., a resonant-bar gravitational-wave detector), the background stress-energy tensor  $T_B^{\alpha\beta}$  has the standard form (5.57), and the stress-energy perturbation  $\mathcal{T}^{\alpha\beta}$  is that of a perfect fluid (5.61), augmented by a shear restoring force

$$\delta\mathcal{T}^{\alpha\beta} = -2\mu\Sigma^{\alpha\beta} , \quad (5.70a)$$

where  $\mu$  is the shear modulus and  $\Sigma^{\alpha\beta}$  is the shear (the time integral of the rate of shear  $\sigma^{\alpha\beta}$ ). By time integrating expression (5.64) we obtain

$$\Sigma_{00} = \Sigma_{0j} = 0 , \quad \Sigma_{jk} = \Sigma_{jk}^\xi + 1/2h_{jk}^{\text{GW}} , \quad (5.70b)$$

where  $\Sigma_{jk}^\xi$  is the part of the shear produced by the displacement  $\xi^i$

$$\Sigma_{jk}^\xi = \xi_{(j|k)} - 1/3\xi^i{}_{|i}\delta_{jk} . \quad (5.70c)$$

By augmenting (5.70) onto the  $\mathcal{T}_{\alpha\beta}$  of Eq. (5.63) and then inserting that  $\mathcal{T}^{\alpha\beta}$  into the equation of motion (5.60) and specializing to the nearly Newtonian regime  $p_B \ll \rho_B$ ,  $K \ll \rho_B$ , we obtain

$$\rho_B \ddot{\xi}_j - (K\xi^i{}_{|i})_{|j} - 2(\mu\Sigma_{jk}^\xi)^{|k} = \mu^{|k}h_{jk}^{\text{GW}} . \quad (5.71)$$

This is the standard equation of motion for a slightly perturbed, inhomogeneous, nonrelativistic elastic medium, augmented by the gravitational-wave driving term  $\mu^{|k}h_{jk}^{\text{GW}}$ . This equation was first derived by Dyson (1969) and was subsequently generalized and studied in more elegant ways by Carter and Quintana (1977) and Carter (1983). Notice that *the waves drive the medium only through inhomogeneities of its shear modulus*.

For an elastic body that is small compared to  $\lambda$  (e.g., a resonant-bar gravitational-wave detector), one can study the waves' influence using the TT-gauge equation of motion (5.71), or one can study it in the body's proper reference frame, where the full metric  $g_{\alpha\beta} = g_{\alpha\beta}^B + h_{\alpha\beta}$  has the form (4.39). In the proper reference frame, the body's equation of motion will be the same as (5.71) but with the driving term  $\mu^{|k}h_{jk}^{\text{GW}}$  replaced by the standard gravitational-wave driving term  $-1/2\rho_B \ddot{h}_{jk}^{\text{GW}} x^k$  [Eqs. (4.12) and (4.15)]. The two driving terms look completely different, and they give different displacement functions  $\xi^j$ . The reason is that the spatial coordinates of the TT gauge wiggle dynamically relative to those of the proper reference frame, thereby producing

$$\xi_j^{\text{TT}} = \xi_j^{\text{PRF}} - 1/2h_{jk}^{\text{GW}} x^k . \quad (5.72)$$

If one wants to be able to rely on ordinary physical intuition, one should use spatial coordinates that are as rigid as possible: proper reference-frame coordinates. However, if one wants only to solve the equations of motion of the medium without referring to elementary physical intuition, one is free to use either approach, proper-reference-frame or TT. If the medium is large compared to a reduced wavelength (e.g., for studies of the interaction of kilohertz waves with the earth's crust), one is stuck: only the TT

analysis [Eq. (5.71)] is valid. The proper-reference-frame analysis fails. See the discussion in Sec. 4.F.

Turn attention from the influence of the waves on the medium to the influence of a homogeneous, elastic medium on the waves. The shear stress  $\mathcal{T}_{jk} = -\mu h_{jk}^{\text{GW}}$ , acting back on the waves, produces dispersion; in addition, if there is viscosity, it will give rise to a shear stress  $\mathcal{T}_{jk} = -\eta \dot{h}_{jk}^{\text{GW}}$  [Eq. (5.65)] that damps the waves. We can see this quantitatively with the help of the waves' propagation equation (5.59). By (i) inserting into that propagation equation the above elastic and viscous contributions to  $\mathcal{T}_{jk}$  along with the fluid contributions (5.63), (ii) taking the transverse-traceless part of the resulting equation [in accord with the paragraph following Eq. (5.59)], and (iii) ignoring the tiny curvature-coupling term, we obtain

$$\square h_{jk}^{\text{GW}} = 16\pi(\mu h_{jk}^{\text{GW}} + \eta \dot{h}_{jk}^{\text{GW}}). \quad (5.73)$$

For waves with the sinusoidal form  $h_{jk}^{\text{GW}} \propto e^{i(kz - \omega t)}$ , Eq. (5.73) gives the dispersion relation

$$\omega^2 = k^2 + 16\pi(\mu - i\omega\eta). \quad (5.74)$$

Since, as we shall see,  $16\pi|\mu - i\omega\eta|$  is always extremely small compared to  $\omega^2 \cong k^2 = 1\lambda^2$ , this dispersion relation corresponds to (i) an attenuation of the waves with an energy attenuation length the same as for a viscous fluid [Eq. (5.67)]

$$l_{\text{atten}} = \frac{1}{32\pi\eta}, \quad (5.75)$$

and (ii) propagation with phase velocity  $v_{\text{ph}} = \omega/k$  and group velocity  $v_{\text{gp}} = \partial\omega/\partial k$  given by

$$v_{\text{ph}} = 1 + 8\pi\lambda^2, \quad v_{\text{gp}} = 1 - 8\pi\lambda^2. \quad (5.76)$$

Ordinary solid bodies have  $\eta \sim 10^3 \text{ g cm}^{-1} \text{ sec}^{-1}$  and  $\mu \sim 10^{10} \text{ dyne cm}^{-2}$  which, by virtue of  $c = 3 \times 10^{10} \text{ cm sec}^{-2} = 1$  and  $G/c^2 = 0.7 \times 10^{-28} \text{ cm/g} = 1$ , is the same as  $\eta \sim 10^{-36} \text{ cm}^{-1}$  and  $\mu \sim 10^{-39} \text{ cm}^{-2}$ . Correspondingly, *when propagating through an ordinary solid such as the earth, the gravitational waves' attenuation length is  $l_{\text{atten}} \sim 10^{34} \text{ cm} \sim 10^6$  Hubble distances; and their phase and group velocities differ from the speed of light by fractional amounts  $\sim 10^{-24}(\lambda/100 \text{ km})^2$ . Thus, kilohertz-frequency gravitational waves would have to propagate through earth-type matter a distance  $l_{\text{disp}} \sim 10^{24} \sim 10^{31} \text{ cm} \sim 10^3$  Hubble distances in order for dispersion to cause their phase to slip by just one radian.*

More generally, because the velocity of propagation of shear waves in any elastic medium is  $\simeq \sqrt{\mu/\rho_{\text{B}}}$  and cannot exceed light speed, it should always be true that  $\mu \lesssim \rho_{\text{B}} \sim 1/\mathcal{R}^2$ . This means that gravitational waves in *any* elastic medium will have their phase shifted by one radian due to dispersion only after traveling a distance

$$l_{\text{disp}} \sim \frac{1}{\lambda} \gtrsim \mathcal{R} \frac{\mathcal{R}}{\lambda}. \quad (5.77)$$

Since the medium cannot be much larger than  $\mathcal{R}$ , and since gravitational radiation by definition must have  $\lambda/\mathcal{R} \ll 1$ , *dispersion in an elastic medium can never produce a slippage of phase by even one radian.* Similarly, as was shown in Eq. (5.69), *attenuation can never be significant in an elastic medium.*

*d. Medium made of quadrupolar oscillators*

Turn, next, to the attenuation of gravitational radiation by that type of medium which, so far as I am aware, is the most effective of all realistic media for absorbing gravitational radiation: a medium made of a large number of “quadrupolar oscillators” with internal damping. By “quadrupolar oscillator”, I mean a solid body with size  $L \lesssim \lambda$  and with a normal mode of oscillation that has a quadrupolar shape. Examples include resonant-bar gravitational-wave detectors, planets like the earth, stars like the sun, neutron stars, and black holes.

We can estimate the attenuation length in such a medium as  $l_{\text{atten}} = 1/n\sigma$ , where  $\sigma$  (not to be confused with the rate of shear of a fluid) is the cross section for an individual oscillator to absorb gravitational-wave energy and  $n$  is the number density of oscillators. To evaluate the cross section  $\sigma$  we compute the response of an oscillator to a passing, monochromatic gravitational wave. That response, in the oscillator’s proper reference frame (*not* in TT gauge), is governed by the equation

$$\frac{d^2\delta L}{dt^2} + \frac{1}{\tau_*} \frac{d\delta L}{dt} + \omega_o^2 \delta L \simeq L \frac{d^2 h_+}{dt^2}; \quad (5.78)$$

cf. Exercise 37.10 of MTW. Here  $\delta L$  is the generalized coordinate of the oscillator’s quadrupolar normal mode, so normalized as to be equal to the physical displacement of a representative piece of the oscillator’s surface, and  $h_+$  is the gravitational-wave field evaluated at the oscillator’s location. (Since the oscillator is smaller than a reduced wavelength of the waves,  $L \lesssim \lambda$ , spatial variations of  $h_+$  are unimportant inside the oscillator.) The left-hand side of (5.78) is the standard harmonic-oscillator equation for the normal mode’s generalized coordinate, and the right-hand side is an order-of-magnitude estimate of the gravitational-wave driving force, based on Eqs. (4.12), (4.16) and (4.25). The parameter  $\omega_o$  is the eigenfrequency of the normal mode,  $\tau_*$  is its damping time,  $L$  is the oscillator’s linear size, and below we shall denote by  $M$  the oscillator’s mass and by  $Q \equiv \omega_o\tau_*/\pi$  the normal mode’s “quality factor”.

The approximate equation of motion (5.78) and the order-of-magnitude analysis that follows are valid for bodies with strong self-gravity (e.g., neutron stars and black holes) as well as weak (the earth or a resonant-bar gravitational-wave detector).

By setting  $h_+ = h e^{-i\omega t}$  (where  $\omega = 1/\lambda$  is the wave’s angular frequency and  $h$  is its amplitude), solving (5.78) for  $\delta L$ , then computing the energy of oscillation  $E_{\text{osc}} \sim 1/2 M \omega_o^2 \times (\text{amplitude of } \delta L)^2$ , and then multiplying by  $1/\tau_*$ , we obtain the rate that energy is fed into internal damping of the oscillator—a rate which, in this steady-state situation, must equal the power absorbed by the oscillator from the gravitational wave,  $P_{\text{abs}}$ . By equating this  $P_{\text{abs}}$  to the product of the cross section  $\sigma$  and the waves’ energy flux  $(1/16\pi)\omega^2 h^2$  [Eq. (4.34)], we obtain the following expression for the oscillator’s cross section

$$\sigma(\omega) \sim \frac{ML^2\omega^2/\tau_*}{\omega^2 - \omega_o^2 + (2\tau_*)^2}. \quad (5.79)$$

We shall return to the frequency dependence of this expression in Chap. 10, when discussing gravitational-wave detectors. For now, in order to put an upper limit on the effects of



absorption, we shall suppose that the waves are precisely on resonance,  $\omega = \omega_o$ . Then  $\sigma$  achieves its maximum value of

$$\sigma_{\max} \sim \frac{M}{L} \frac{L}{\lambda^-} Q L^2, \quad (5.80)$$

and the attenuation length achieves its minimum possible value,  $l_{\text{atten}} = 1/n\sigma_{\max}$ . Expressed in terms of the radius of curvature of the background spacetime produced by the attenuating oscillators,  $\mathcal{R} \sim 1/\rho^{1/2} = (1/nM)^{1/2}$ , this works out to be

$$\frac{l_{\text{atten}}}{\mathcal{R}} \sim \frac{\mathcal{R}}{\lambda^-} \left(\frac{\lambda^-}{L}\right)^2 \frac{1}{Q}. \quad (5.81)$$

The first term,  $\mathcal{R}\lambda^-$ , is  $\gg 1$  by the definition of a gravitational wave. The second term,  $(\lambda^-/L)^2$ , is equal to the speed of light divided by the velocity of sound inside the oscillating body, squared, and thus is always  $\gtrsim 1$ . [For a black hole  $(\lambda^-/L)^2 \sim 1$ , for a neutron star  $(\lambda^-/L)^2 \sim 10$ , for a white dwarf  $(\lambda^-/L)^2 \sim 10^4$ , for normal stars like the sun  $(\lambda^-/L)^2 \sim 10^6$ , for the earth or a resonant-bar gravitational-wave detector  $(\lambda^-/L)^2 \sim 10^{10}$ .] By contrast, the third term,  $1/Q$ , is generally  $\ll 1$ . However, for realistic astrophysical situations  $1/Q$  is never sufficiently small to make up for the large product of the first two terms. Moreover, when the resonant angular frequencies of the many oscillators are spread out randomly over a band  $\Delta\omega_o \sim \omega_o$ , only a fraction  $\sim 1/Q$  of the oscillators will be near enough resonance to have  $\sigma \sim \sigma_{\max}$ ; and correspondingly the factor  $1/Q$  in (5.81) will be replaced by unity. Thus, *although, in principle, gravitational waves could be attenuated significantly by a medium of quadrupolar oscillators, in realistic situations the attenuation length greatly exceeds the radius of curvature  $\mathcal{R}$  produced by the oscillators; and thus, as in the case of a viscous medium, attenuation cannot be astrophysically important.*

A simple extension of this argument shows that dispersion also cannot be significant: the total phase shift, due to dispersion, in traveling the distance  $\mathcal{R}$  through a realistic astrophysical medium is generally  $\ll 1$ ; see Sec. 2.4.3 of Thorne (1983). It is instructive and fun, however, to imagine and study theoretically an unrealistic form of matter (“respondium”) with such strong dispersion that it actually reflects gravitational waves (Press 1979).

The specific problem of the absorption and scattering of gravitational waves by black holes has been studied in extensive detail. Those studies reveal a great richness of scattering phenomena (superradiant scattering, “glories”, rotation of the waves’ polarization, . . .); see De Logi and Kovacs (1977), Matzner and Ryan (1978), Matzner *et al.* (1985), Futterman, Handler, and Matzner (1988), and references therein. For studies of absorption and scattering by neutron stars and other stars see Linet (1984). For a study of how the energy levels of atoms are shifted by the tidal gravity of passing gravitational waves [fractional shifts no larger than  $h \times (\text{size of atom})^2 \lambda^2$ , which is almost certainly too small in the real universe to be measurable], see Leen, Parker, and Pimentel (1983).

#### *e. Plasmas*

The most astrophysically ubiquitous of all media is a magnetized plasma. Careful studies of the propagation of gravitational waves through plasmas are only now in process

(Ehlers, Prasanna, and Breuer, 1986; Bondi and Pirani, 1988), and there are no definitive results at this writing, with one exception: Gayer and Kennel (1979), and Grishchuk and Polnarev (1980, p. 420 – KIP: CHECK) have shown that in an unmagnetized plasma, as in the media studied above, dispersion is so extremely small that there is no hope for particles with mass to “ride along with the crests” of a gravitational wave and produce Landau damping. *Landau damping of gravitational radiation in a plasma is totally negligible.* This result, and intuition built up from the above calculations for other media, make me rather confident that a magnetized plasma cannot have any significant influence on gravitational waves that propagate through it. Nevertheless, there are likely to be a number of fascinating but tiny effects of the waves on the plasma and the plasma on the waves.

## 5.F. Interaction with Electromagnetic Fields

Turn attention from propagation of gravitational waves through matter, to propagation through electromagnetic fields.

Because gravitational and electromagnetic waves should propagate with the same speed, they can interact in a coherent way (Gertsenshtein, 1962). The interaction is so weak, however, that a substantial transformation of one into the other requires propagation over a distance of order the radius of curvature  $\mathcal{R}$  of the background spacetime which their own energy density produces. Thus, such coherent interaction is not likely ever to be important in the real universe—except possibly in gravity-wave detectors; see Sec. 12.A below. For a review of the extensive literature on this subject see Grishchuk and Polnarev (1980). For a brief pedagogical discussion see Sec. 17.9 of Zel’dovich and Novikov (1983).

The situation in which one might have expected the strongest resonant interaction is for electromagnetic and gravitational waves propagating parallel to each other through an otherwise empty spacetime. Remarkably, in this situation there is no interaction whatsoever (Braginsky and Grishchuk, 1977 KIP: LEONYA CLAIMS THIS PAPER DOES NOT EXIST AND SAYS TO CITE BRAGINSKY ET AL 1973; Grishchuk, 1977b – KIP: LEONYA SAYS THIS REFERENCE IS NOT NECESSARY). It is easy to see why, for the special issue of whether the stress-energy tensor of a propagating electromagnetic wave generates a gravitational wave propagating along with it. That stress-energy tensor, in a local Lorentz frame of the background metric, has the form

$$T^{00} = T^{0z} = T^{z0} = T^{zz} = \frac{E_o^2}{4\pi} \cos^2 \omega(t - z) , \quad (5.82)$$

where  $E_o$  is the amplitude of oscillation of the electric field and the wave is presumed to be plane polarized and to propagate in the  $z$ -direction. The oscillatory part of  $T^{\mu\nu}$ , which one might expect to generate gravitational waves, is

$$\mathcal{T}^{00} = \mathcal{T}^{0z} = \mathcal{T}^{z0} = \mathcal{T}^{zz} = \frac{E_o^2}{8\pi} \cos 2\omega(t - z) . \quad (5.83)$$

When fed into the wave equation (5.33) (with the coupling of  $\bar{h}_{\alpha\beta}$  to the background fields  $R_{\alpha\beta\gamma\delta}^B$  and  $T_{\alpha\beta}^B \equiv \langle T_{\alpha\beta} \rangle$  ignored because it can be important only over the extremely

long lengthscale  $\mathcal{R}$ ), this  $\mathcal{T}^{\alpha\beta}$  produces a trace-reversed metric perturbation  $\bar{h}_{\alpha\beta}$  that propagates along with the electromagnetic waves at the speed of light, growing linearly with the distance traveled. However, this  $\bar{h}_{\alpha\beta}$ , like the  $\mathcal{T}_{\alpha\beta}$  that generates it, is purely longitudinal; i.e., it has  $00$ ,  $0z$ ,  $z0$ , and  $zz$  components but no components in transverse directions. This implies that this wavelike  $\bar{h}_{\alpha\beta}$  is “pure gauge”: it can be transformed to zero by a change of gauge, as one can see most easily by noting that its transverse-traceless projection (4.50) vanishes and therefore that it is associated with a vanishing gravitational-wave field  $h_{jk}^{\text{GW}}$ .

To achieve a resonant interaction between parallelly propagating electromagnetic and gravitational waves, one can send them through a time-independent (“DC”) electric or magnetic field (Gertsenshtein, 1962). As a simple example, let a pure electromagnetic wave, with electric field  $\mathbf{E} = E_o \cos \omega(t - z)\mathbf{e}_x$ , propagate from vacuum at  $z < 0$  into a region of homogeneous, DC field  $\mathbf{E} = E_{\text{DC}}\mathbf{e}_x$  at  $z > 0$ ; and assume that  $E_{\text{DC}} \gg E_o$ . Then the beating of the wave’s electric field against the DC field produces an oscillating stress-energy tensor which has (among others) the transverse components

$$\mathcal{T}_{xx} = -\mathcal{T}_{yy} = \frac{E_{\text{DC}}E_o}{4\pi} \cos \omega(t - z) \quad \text{for } z > 0. \quad (5.84)$$

Fed into the wave equation (5.33) (with background-coupling effects neglected as above), these  $\mathcal{T}_{\alpha\beta}$  generate a trace-reversed metric perturbation

$$\bar{h}_{xx} = -\bar{h}_{yy} = \frac{2E_{\text{DC}}E_o}{\omega} z \sin \omega(t - z) \quad \text{for } z > 0. \quad (5.85)$$

The TT projection of this  $\bar{h}_{\alpha\beta}$  [Eq. (4.50)] gives a gravitational-wave field

$$h_+ = \frac{2E_{\text{DC}}E_o}{\omega} z \sin \omega(t - z), \quad h_\times = 0 \quad \text{for } z > 0. \quad (5.86)$$

The amplitude of this wave grows linearly with the distance  $z$  travelled, and correspondingly its energy density grows quadratically. It is easy to verify that the ratio of the energy in the growing gravitational wave to that in the original electromagnetic wave is of order  $(z/\mathcal{R})^2$ , where  $\mathcal{R}$  is the background radius of curvature produced by the DC field. By virtue of total energy conservation, there is a back-action on the electromagnetic wave which saps energy from it as the gravitational wave grows. A detailed analysis (XXXXX) shows that, once all the wave energy has been fed into the gravitational wave, the beating of that gravitational wave against the DC field begins to regenerate the electromagnetic wave. The wave energy thereafter sloshes back and forth between electromagnetic and gravitational waves, with a sloshing lengthscale of order  $\mathcal{R}$ . [KIP: SEE GRISHCHUK’S REFS. PRIVATELY HE SAYS ZEL’DOVICH JETP 65, 1311 (1973), SOV PHYS JETP 38, 652 (1974); ALSO GERLACH PRL 32, 1023 (1974)]

Because the background field cannot have a longitudinal extent much larger than  $\mathcal{R}$  (see above), the sloshing cannot continue for more than a few cycles. And, for realistic laboratory or astrophysical parameters, there cannot be any sloshing at all; there is only a fractionally tiny interconversion of one wave type into the other.

A specific, well-studied example of the above process is the interconversion of gravitational and electromagnetic waves as they propagate near an electrically charged black hole (XXXXXX). Another cute application is a proof that in principle (though never in practice) this interconversion, plus interaction of the electromagnetic waves with thermal matter, can be used to thermalize initially nonthermal gravitational radiation (Garfinkle and Wald, 1985). A third application is to gravitational-wave detectors in which a strong, DC field (e.g., the electric field in a parallel-plate capacitor) is driven by incoming gravitational waves to produce a tiny amount of electromagnetic radiation (Braginsky *et al.*, 1973; Sec. 12.A, below).

Interactions between gravitational and electromagnetic waves can be catalyzed not only by a background, DC electromagnetic field, but also in other ways: (i) Parallely propagating electromagnetic and gravitational waves can be coupled by a dielectric medium, but the coupling is proportional to  $n - 1$  where  $n$  is the dielectric's index of refraction, and the coupling is so weak that it probably is of no practical interest (Grigor'ev, 1982). (ii) When electromagnetic and gravitational waves propagate through vacuum in nonparallel directions, they interact weakly. For example, if the wavelength of the gravitational wave is much longer than that of the electromagnetic wave, then the gravitational wave can produce electromagnetic polarization (Polnarev, 1985), it can rotate the plane of electromagnetic polarization (Cruise, 1983), and it can produce fluctuations in the frequency, intensity, and direction of the electromagnetic wave (Zipoy, 1966; Bergman, 1971; Bertotti and Catenacci, 1975; Adams, Hellings, and Zimmerman, 1984). Such interactions have only minuscule influence on either the gravitational or the electromagnetic wave; but, thanks to high-precision technology, the tiny electromagnetic effects can be used in a variety of promising ways for gravitational-wave detection (Sec. 12.C).

### 5.G. Catalog of Vacuum Wave-Propagation Effects

Having seen that the interaction of gravitational waves with matter and electromagnetic fields is almost never significant, we now return to the vacuum approximation. There are a number of peculiarities of vacuum wave propagation. Some show up in the equations of geometric optics, while others are removed by the approximations that underlie the geometric-optics formalism. In this section we shall discuss the most interesting and important of the vacuum propagation phenomena, and we shall examine their relationship to geometric optics and their relevance to the real universe.

#### *a. Scattering by background curvature, and tails of waves*

Gravitational waves can sometimes encounter regions of spacetime where the background radius of curvature becomes comparable to or shorter than the reduced wavelength,  $\mathcal{R} \lesssim \lambda^-$ . When this happens, not only do the shortwave and geometric optics formalisms break down, but the very concept of a gravitational wave becomes meaningless. Nevertheless, one can continue to analyze the evolution of the metric perturbations  $h_{\alpha\beta}$  using the formalism of Sec. 5.B.

Of particular interest when  $\mathcal{R} \lesssim \lambda^-$  is the scattering of the perturbations by the background curvature. Such scattering shows up in the vacuum wave equation  $\square \bar{h}^{\alpha\beta} +$

$2R_{\mu\alpha\nu\beta}^B \bar{h}^{\mu\nu} = 0$  [Eq. (5.24)] as a result not only of the curvature-coupling term, but also of the influence of the background on the wave operator  $\square$ . This scattering is very important in some sources of waves, as the waves are trying to form. For example, it is responsible for the normal-mode vibrations of black holes (Press, 1971; Goebel, 1972; Sec. 6.J), and it leads to the formation of “tails” of the waves in a source’s near zone (Price, 1972a,b; Thorne, 1972; Cunningham, Price, and Moncrief, 1979) and to radiative tails in the wave zone (Leaver, 1986; Blanchet, 1987b; XXXX)—which, though they are very important in principle (Newman and Penrose, 1965; Blanchet and Damour, 1988a), are not likely ever to be observationally important. Remarkably, in a homogeneous cosmological model filled with perfect fluid with vanishing pressure or with pressure equal to 1/3 the energy density, there is no backscatter off the spacetime curvature whatsoever (Janis, 1985; Gayer and Kennel, 1979).

#### *b. Parametric amplification by background curvature*

In regions of a dynamical spacetime (e.g., the expanding universe) in which the characteristic wavelength  $\lambda$  of gravitational waves is larger than or comparable to the background radius of curvature  $\mathcal{R}$ ,  $\lambda \gtrsim \mathcal{R}$ , the waves can be parametrically amplified by interaction with the dynamical background (Grishchuk, 1974, 1975a,b, 1977a; Grishchuk and Polnarev, 1980; Allen, 1988; Sec. 9.D). Viewed quantum mechanically, the interaction causes stimulated emission of new gravitons (XXXX). Viewed classically, the interaction can be analyzed using the standard, perturbed, vacuum Einstein equation  $\square \bar{h}^{\alpha\beta} + 2R_{\mu\alpha\nu\beta}^B = 0$ ; and the parametric amplification comes about because of the time dependence not only in  $R_{\mu\alpha\nu\beta}$  but also in the background connection coefficients that appear in the wave operator. Such parametric amplification may well have enabled the expansion of the universe to take gravitational vacuum fluctuations that emerged from the Planck era of the big-bang, and enlarge them into a strong, stochastic background of gravitational waves today; see Sec. 9.D below.

#### *c. Gravitational focusing*

Lumps of background curvature associated with black holes, stars, star clusters, and galaxies will focus gravitational waves in precisely the same manner as they focus electromagnetic waves; i.e., they act as “gravitational lenses” for the waves. Just as this focusing is observationally important for the light and radio waves from a few very distant quasars, so it might also be important for distant discrete sources of gravitational waves. Focusing by the sun, in the case of waves with sufficiently short wavelength, can be significant, but not at earth; the focal point lies farther out in the solar system, near the orbit of Jupiter (Cyranski and Lubkin, 1974). Gravitational focusing shows up clearly in the waves’ geometric-optics propagation: A bundle of rays, along which the waves are propagating, is focussed gravitationally. This causes the bundle’s cross sectional area  $\Delta A$  and radial variable  $r$  [Eq. (5.2d)] to decrease, and the  $h_+$  and  $h_\times$  of Eq. (5.2e) to increase.

#### *d. Diffraction*

Near the focal point of a gravitational lens, the radii of curvature of the wave fronts are no longer huge compared to the waves' reduced wavelength. As a result, the waves cease to propagate along null rays and begin to diffract, thereby lessening the strength of the focusing. The analysis of this is no different for gravitational waves than for electromagnetic or scalar waves, since polarization plays no important role. The analysis can be carried out using the flat-spacetime wave equation  $\square h_{\alpha\beta} = 0$  in a nearly Lorentz frame of the focal region. One switches from geometric optics to this wave equation as the waves near the focal point. Then, once the waves are well past the focal point, one can return to geometric optics. One thereby finds that diffraction almost completely wipes out the effects of gravitational focusing, unless the waves' reduced wavelength  $\lambda$  is small compared to the lens's gravitational radius  $2GM/c^2 = 3\text{ km}(M/M_\odot)$ . (Here  $M$  is the lens's mass.) This criterion applies whether the lens is a black hole, or a star like the sun, or a galaxy. For an order of magnitude discussion see, e.g., Sec. 2.6.1 of Thorne (1983); for full details see Bontz and Haugan (1981).

*e. Nonlinear wave-wave coupling (frequency doubling, etc.)*

Because general relativistic gravity is nonlinear, there is a nonlinear self-coupling of gravitational waves ("wave-wave coupling"). In principle this leads to such nonlinear conversion processes as frequency doubling. One can compute the effects of nonlinearities using an explicit version of Eq. (5.32c). Such a calculation shows that in practice wave-wave coupling effects are not important in regions where the waves *are* waves (where  $\lambda \ll \mathcal{L}$ ). This is because, in such regions, the dimensionless amplitude  $h$  of the waves is small compared to unity [Eq. (5.41) above]. For details see Sec. 2 of Thorne (1985). However, in idealized situations where  $\lambda$  becomes temporarily  $\sim \mathcal{L}$  and  $h$  becomes temporarily of order unity, significant frequency doubling can occur. An example is the focusing of beams of gravitational radiation into a region so small (of order  $\lambda$ ) and with such great beam intensity ( $h \sim 1$ ) that the focused radiation almost but not quite forms a black hole. Upon diffracting and reexploding, the radiation shows significant frequency doubling (Abrahams, 1987).

Even when the waves' amplitude  $h$  becomes of order unity (and, as a result, the distinction between background curvature and wave curvature begins to break down), there is no evidence in any calculations to date for a steepening of the waves to form gravitational shocks (discontinuities in the waves' Riemann tensor). This remains true even when one adds additional nonlinearities to the Einstein field equation by augmenting the Einstein-Hilbert Lagrangian by terms quadratic in the curvature tensor (Tomimatsu, 1987).

*f. Generation of background curvature by the waves*

The generation of background curvature by the stress-energy of the waves [Isaacson, 1968b; MTW Sec. 35.15; Eq. (5.38) above] is important in cosmological models in any epoch when the waves are sufficiently strong that their energy density is comparable to that of matter, or larger; see, e.g., Hu (1978) and Chap. 17 of Zel'dovich and Novikov (1983). It is also important in a gravitational "geon"—i.e., a bundle of gravitational waves that is held

together by its own gravitational pull on itself (Wheeler, 1962; pp. 409–438 of Wheeler, 1964; Brill and Hartle, 1964). But geons surely do not exist in the real universe. There is no reason to expect them to form, and if they did form they would quickly disrupt due to a large-scale, global instability (XXXXXX). Nevertheless, geons are important theoretical entities: they are useful for exploring issues in fundamental physics.

*g. Nonlinear effects in collisions of gravitational waves*

The head-on collisions of precisely planar gravitational waves (with infinite transverse extent) have been studied using exact, rather than approximate solutions of the vacuum Einstein field equation; see Sec. 5.H below. These solutions, and exact theorems about them, reveal a number of interesting nonlinear features: (i) The background curvature produced by each wave acts as a lens to focus the other wave. Because the waves have infinite transverse extent, diffraction does not occur, and each focussed wave converges onto its focal plane to produce a spacetime singularity (Kahn and Penrose, 1971; Szekeres, 1972; Nutku and Halil, 1977; Tipler, 1980; Matzner and Tipler, 1984). (ii) The singularity has an “inhomogeneous Kasner structure” with infinite tidal squeezing along two spatial axes and infinite stretching along the third (Yurtsever, 1987a, 1988). (iii) For special forms of the pre-collision waves, some or all of the singularity gets replaced by a “Cauchy horizon”. However, those special forms are nongeneric: arbitrarily weak changes in them cause the collision to produce an all-embracing singularity rather than a Cauchy horizon (Chandrasekhar and Xanthopoulos, 1986, 1987; Yurtsever, 1987a, 1988).

Exact theorems show that, in the more realistic case of colliding waves that are almost planar but die out slowly at large transverse distances, if the transverse size is sufficiently large compared to the initial wave amplitude, then the focusing still drives the amplitude up far enough, before diffraction can act, to make nonlinear effects take over and produce singularities (Yurtsever, 1987b, 1988). If the “cosmic censorship conjecture” is correct, those singularities must be hidden inside one or two black-hole horizons; but it has not yet been possible to determine whether this is so. Unfortunately, the wave size required to produce a singularity is so huge that wave-wave collisions almost certainly do not form singularities in the real universe, except possibly near the big bang (Yurtsever, 1987b, 1988).

Collisions of gravitational waves produce not only focusing, but also a rotation of the polarization axes of one wave by the gravitational action of the other—a phenomenon discovered in collisions of cylindrical waves by Piran and Safer (1985).

## **5.H. Asymptotic Analyses and Exact Solutions**

We conclude this chapter with a brief description of studies of gravitational-wave propagation in special circumstances.

*a. Asymptotic analyses*

Much has been learned about the geometric properties of gravitational radiation by studying the idealized problem of the propagation of waves outward from a source

that resides alone in an otherwise empty and asymptotically flat spacetime: In analyses that were central to building up confidence in our understanding of gravitational waves, Bondi (1960), Bondi, van der Burg, and Metzner (1962), and Sachs (1962, 1963) expanded the spacetime curvature along the outgoing light cone in inverse powers of the distance to the source. Their expansions, carefully formulated and combined with conformal transformations that bring “infinity” in to finite locations (Penrose 1963a,b) revealed an elegant asymptotic structure for waves in asymptotically flat spacetime. The study of this asymptotic structure has been pursued with vigor in recent years; for reviews and references see Newman and Todd (1980), Ashtekar (1981, 1984), Walker (1983), Schmidt (1979, 1986), Hobill (1984), Penrose and Rindler (1986), Friedrich (1986), Blanchet and Damour (1986), Blanchet (1987a), Winicour (1988), and Ashtekar and Schmidt (1990).

*b. Exact solutions to the vacuum Einstein field equation*

Much insight into gravitational radiation has come from exact solutions to the vacuum Einstein field equation.

One broad class of exact solutions, called “boost-rotation symmetric spacetimes”, describes an idealized class of gravitational-wave sources that radiate into a (nearly) asymptotically flat spacetime.

The sources are axially symmetric and invariant under a Lorentz-like “boost”. They include such idealized configurations as two black holes with a spring between them, which forces them to accelerate uniformly away from each other (the “C-metric”, discovered by Levi-Civita, 1918 and explored and interpreted physically by Kinnersley and Walker, 1970; Bonnor, 1983; and others). The spacetime into which these special sources radiate is asymptotically flat (like Minkowskii spacetime), except for a weak, cosmic-string-type structure (circumference, divided by  $2\pi \times$  radius, equal to a constant slightly less than one) along the direction of acceleration (the symmetry axis). For the general theory and reviews of boost-rotation-symmetric spacetimes see Bičak (1968); Bičak, Hoenselaers and Schmidt (1983); Bičak and Schmidt (1984); and Bičak (1985, 1988).

Although there are no other known exact solutions describing waves that propagate out into asymptotically flat spacetime, there is a general formalism for a much broader and more realistic class of solutions—a formalism sufficiently powerful to permit proof of interesting theorems and to give promise of ultimately producing exact solutions. This formalism, due to Robinson and Trautman (1962), describes wave-carrying spacetimes whose rays are “geodesic and hypersurface orthogonal” (properties shared by the rays of geometric optics) and in addition are free of shear. [KIP: CHECK - HOW CAN THEY BE SHEAR-FREE?] Among the important, rigorous theorems that have been proved for such spacetimes is one which says that the waves must die out at late times, leaving behind the Schwarzschild spacetime of a nonrotating black hole (Forster and Newman, 1967; Lucacs *et al.*, 1984). For reviews and references on the Robinson-Trautman formalism see, e.g., Kramer *et al.* (1980) and Schmidt (1987). For a first step in generalizing the Robinson-Trautman theory to spacetimes whose rays have “twist”, see Chinea (1988).

Nonlinear interactions of gravitational waves with themselves and each other have been studied extensively using exact solutions which are plane symmetric or cylindrically



symmetric—and, thus, which extend outward infinitely far in one or two transverse directions. Powerful, soliton-theoretic techniques for generating such exact solutions have been devised by Belinsky and Zakharov (XXXX); and other solution-generating techniques have been developed by Chandrasekhar (1986 and refs. therein) and by Ernst, Garcia, and Hauser (1988). For applications of these techniques see, e.g., Cespedes and Verdaguer (1987); Garriga and Verdaguer (1987); and Ferrari, Ibanez, and Bruni (1987). The physical properties of cylindrical gravitational waves have been explored, e.g., by Einstein and Rosen (1936) and Weber and Wheeler (1957), who pioneered the subject; and by Thorne (1965a,b), Schmidt (1981), Piran, Safer, and Katz (1986), Chandrasekhar and Ferrari (1987), and others. For detailed studies of planar gravitational waves see Rosen (1937), Bondi, Pirani, and Robinson (1959), and Ehlers and Kundt, 1962 (the pioneering papers), and, more recently, the papers cited in Sec. 5.G.g in connection with gravitational-wave collisions.

Insight into cosmological gravitational waves originating in the early universe comes from a family of exact solutions generated by the Belinsky-Zakharov (XXXX) technique. These solutions describe universes which, at early times, contain “frozen-in” inhomogeneities. As the cosmological horizon expands and becomes larger than the inhomogeneities’ reduced wavelength, the inhomogeneities unfreeze and are smoothly transformed into gravitational radiation propagating dynamically through an otherwise homogeneous universe. For specific solutions of this type see Carr and Verdaguer (1983), Belinsky and Francaviglia (1984), and Adams, Hellings, and Zimmerman (1985).

A final type of exact solution which is useful for insight is the extreme limit of geometric optics, where the wavelength becomes so short that the radiation is compacted into a *gravitational shock wave*. For the exact theory of gravitational shocks see, e.g., Pirani (1957), Papapetrou (1977), and references therein.

# The Scientific Case for Advanced LIGO Interferometers

Kip S. Thorne

CaRT, California Institute of Technology, Pasadena, CA 91125

*in consultation with*

Lars Bildsten, Alessandra Buonanno, Curt Cutler, Lee Samuel Finn, Craig Hogan, Vassiliki Kalogera, Benjamin J. Owen, E. Sterl Phinney, Thomas A. Prince, Frederic A. Rasio, Stuart L. Shapiro, Kenneth A. Strain, Greg Ushomirsky and Robert V. Wagoner.

January 22, 2001

*LIGO Document Number P-000024-00-D*

## 1 Introduction and Overview

Throughout our 1989 proposal for LIGO, all our planning of LIGO, and all our presentations to review committees and the National Science Board, we envisioned and proposed a two-stage process for opening up the gravitational-wave window onto the universe. The first stage (often called “LIGO-I”) was to build the facilities for LIGO and install in them a conservatively designed set of interferometers, capable of reaching a sensitivity “ $10^{-21}$ ” at which it is plausible, but not probable, that gravitational waves will be detected. A several year search with these *initial interferometers* will give us the experience necessary for moving to the second stage, and might produce the first firm detection of gravitational waves. The second stage (sometimes called “LIGO-II”) is to upgrade the interferometers, bringing them to the best sensitivities robustly achievable with the mid 2000’s technology — sensitivities at which it is probable that we will detect a number of sources and begin extracting rich information about the gravitational-wave universe. This proposal is for R&D and construction of these *advanced interferometers* in LIGO.

The advanced (“LIGO-II”) interferometers (IFOs) described in this proposal (i) will lower the amplitude noise by a factor  $\sim 15$  at the frequencies of best sensitivity  $f \sim 100\text{--}200$  Hz, (ii) will widen the band of high sensitivity at both low frequencies (pushing it down to  $\sim 20$  Hz) and high frequencies (pushing it up to  $\sim 1000$  Hz), and (iii) will be capable of *reshaping* the noise curve (lowering it at some frequencies at the price of raising it at others) so as to optimize the sensitivity to specific sources; see Fig. 1. The lowered noise at optimal frequencies will increase the event rate for distant, extragalactic sources by a factor  $\sim 15^3 \simeq 3000$ . Opening up lower and higher frequency bands will bring us into the domains of new sources: colliding, massive black holes and stochastic background at low frequencies; low-mass X-ray binaries, fast pulsars and tidal disruption of neutron stars by black holes at high frequencies. Noise-curve reshaping can be used, for example, to reduce the noise by a factor  $\sim 3$  to  $5$  within some chosen narrow frequency band  $\Delta f/f \sim 0.2$  in which targeted periodic sources (e.g. low-mass X-ray binaries) are expected to lie. We shall refer to this as “narrow-band tuning” of the IFO.

More specifically, as illustrated in Fig. 1:

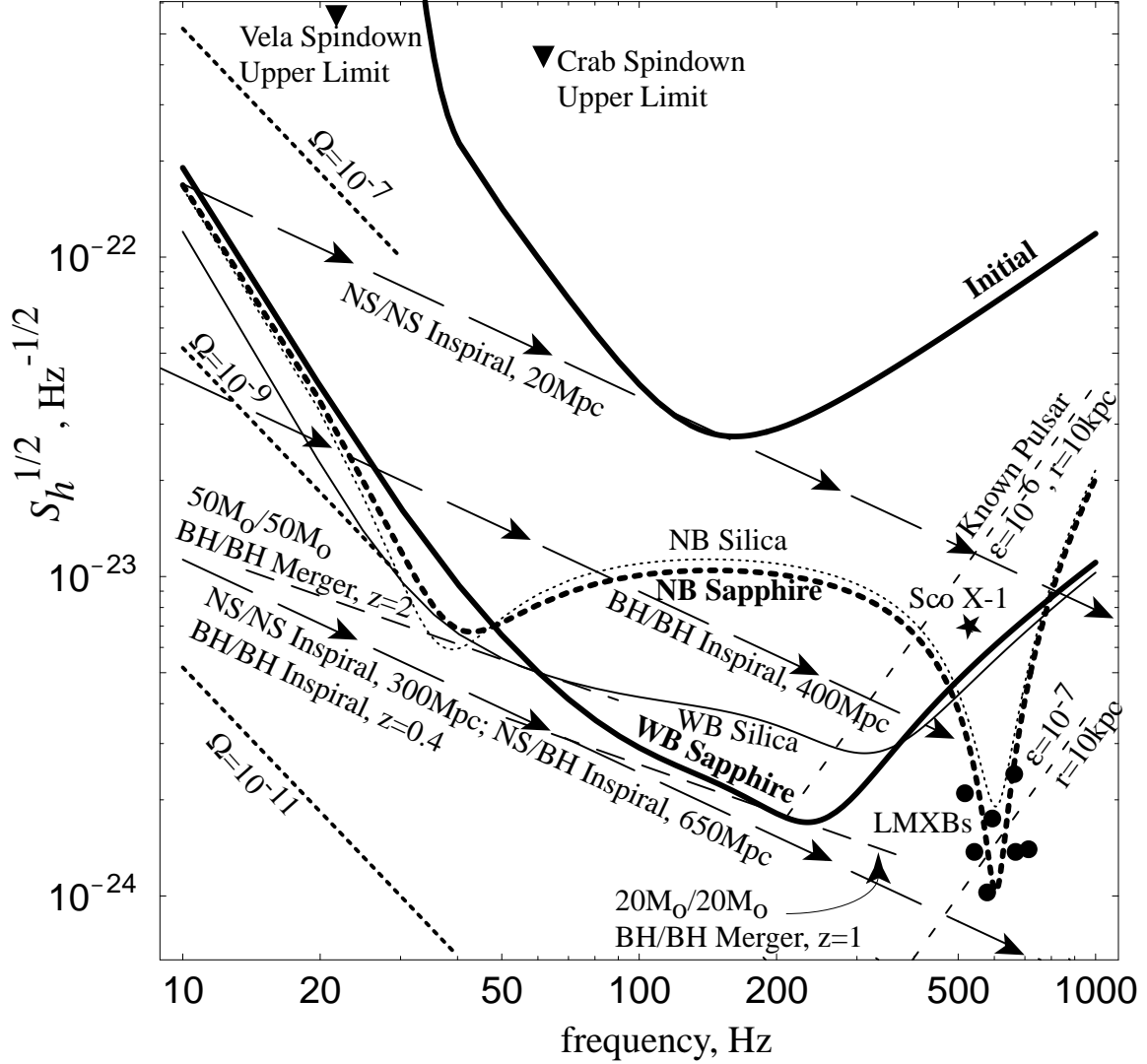


Figure 1: The noise  $\tilde{h}(f)$  in several LIGO interferometers plotted as a function of gravity-wave frequency  $f$ , and compared with the estimated signal strengths  $\tilde{h}_s(f)$  from various sources. The signal strength  $\tilde{h}_s(f)$  is defined in such a way that, *wherever a signal point or curve lies above the interferometer's noise curve, the signal, coming from a random direction on the sky and with a random orientation, is detectable with a false alarm probability of less than one per cent*; see the text for greater detail and discussion.

We have two options for the test-mass material for the *advanced* IFOs, sapphire (our preference) and fused silica (our fallback). Whichever is chosen, we will be able to shape the noise curves by adjusting the position and reflectivity of a signal-recycling mirror, so as to optimize the noise for various kinds of signals (a capability absent in the *initial* IFOs). The figure shows noise curves [square root of the spectral density of an IFO’s arm-length difference as a function of frequency, i.e. “strain per root Hertz”  $\tilde{h}(f) \equiv \sqrt{S_{\Delta L/L}(f)}$ ] for two such optimizations: (i) Advanced IFOs optimized to search for waves from inspiraling neutron-star / neutron-star binaries (thick solid curve labeled **WB Sapphire** for “wide-band, Sapphire” and thin solid curve labeled WB Silica for “wide-band, Silica”). (ii) Advanced IFOs optimized to search for pulsars and low-mass X-ray binaries in the vicinity of  $f = 600$  Hz (thick dotted curve labeled **NB Sapphire** and thin dotted curve labeled NB Silica, where NB means “narrow-band”). In general, the sapphire IFO is capable of somewhat lower noise than the fused-silica one, because of lower total thermal noise in its test masses. [The fact that the specific Silica IFO in Fig. 1 has better noise performance at low frequencies than the Sapphire one is a price that has been paid in the Sapphire IFO: the noise curve has been shaped to produce the lowest possible noise at its minimum, around 200 Hz, at the price of worsened noise below  $\sim 50$  Hz.] In our discussion of the science, we will describe the performance of the sapphire IFOs, keeping in mind that, if we are forced to the fused-silica fallback, there will be a modest (a few tens of per cent) loss of signal to noise and corresponding factor  $\sim 2$  loss of event rate for typical sources.

Figure 1 shows, along with the noise curves, the estimated signal strengths  $\tilde{h}_s(f)$  for various sources. These signal strengths are defined in such a way [1] that the ratio  $\tilde{h}_s(f)/\tilde{h}(f)$  is equal to the ratio of signal  $S$  to noise threshold  $T$ , rms averaged over source directions and orientations,  $\tilde{h}_s(f)/\tilde{h}(f) = \langle S^2/T^2 \rangle^{1/2}$ , with the threshold being that at which the false alarm probability is one per cent when using the best currently known, practical data analysis algorithm. (For broad-band sources, the algorithm is assumed to integrate over a bandwidth equal to frequency and to use the output from LIGO’s two 4km IFOs and one 2km IFO [2], thereby removing all non-Gaussian noise. For periodic sources such as spinning neutron stars, the algorithm uses data from only one 4 km IFO, usually narrow banded, the noise again is assumed Gaussian, and the signal is integrated for  $10^7$  sec, except in cases such as Low Mass X-Ray Binaries where there is little gain from integrating so long.) This definition of  $\tilde{h}_s(f)$  means that, *wherever a signal point or signal curve lies above the IFO noise curve, the signal, coming from a random direction on the sky and with a random orientation, is detectable with a false alarm probability of less than one per cent.*

In this introductory section, we shall discuss the sources briefly, in turn, and then in subsequent sections we shall discuss them in greater detail, focusing on the likelihood of detection and the science we expect to extract from detected waves. Box 1 gives a brief summary of the various sources and their detectability.

The three arrowed, long-dashed lines in Fig. 1 represent the signal  $\tilde{h}_s(f)$  from **neutron-star (NS) and black-hole (BH) binaries in the last few minutes of their inspiral**, assuming masses  $M = 1.4M_\odot$  for each NS and  $M = 10M_\odot$  for each BH. These sources are best searched for by the method of matched filters [4]. Using matched filters, LIGO’s initial IFOs can detect NS/NS inspirals (with a 1 per cent false alarm probability) out to a distance of 20 Mpc [top arrowed line]; the wide-band advanced IFOs can do so 15 times farther, out to 300 Mpc for NS/NS and out to 650 Mpc for NS/BH [bottom arrowed line]. (The wide-band IFOs can integrate up the signal over a wide range of frequencies, thereby achieving detection even though the signal curve in Fig. 1 is a little below the noise curve.) For BH/BH inspiral, the wide-band IFOs can see so far that cosmological effects are important. For definiteness, throughout this

### Box 1

#### Brief Summary of Detection Capabilities of Advanced LIGO Interferometers

• **Inspirals of NS/NS, NS/BH and BH/BH Binaries:** The table below [15, 2] shows estimated rates  $\mathcal{R}_{\text{gal}}$  in our galaxy (with masses  $\sim 1.4M_{\odot}$  for NS and  $\sim 10M_{\odot}$  for BH), the distances  $\mathcal{D}_{\text{I}}$  and  $\mathcal{D}_{\text{WB}}$  to which initial IFOs and advanced WB IFOs can detect them, and corresponding estimates of detection rates  $\mathcal{R}_{\text{I}}$  and  $\mathcal{R}_{\text{WB}}$ ; Secs. 1.1 and 1.2.

	NS/NS	NS/BH	BH/BH in field	BH/BH in clusters
$\mathcal{R}_{\text{gal}}, \text{yr}^{-1}$	$10^{-6}$ – $5 \times 10^{-4}$	$\lesssim 10^{-7}$ – $10^{-4}$	$\lesssim 10^{-7}$ – $10^{-5}$	$\sim 10^{-6}$ – $10^{-5}$
$D_{\text{I}}$	20 Mpc	43 Mpc	100	100
$\mathcal{R}_{\text{I}}, \text{yr}^{-1}$	$3 \times 10^{-4}$ – 0.3	$\lesssim 4 \times 10^{-4}$ – 0.6	$\lesssim 4 \times 10^{-3}$ – 0.6	$\sim 0.04$ – 0.6
$D_{\text{WB}}$	300 Mpc	650 Mpc	$z = 0.4$	$z = 0.4$
$\mathcal{R}_{\text{WB}}, \text{yr}^{-1}$	1 – 800	$\lesssim 1$ – 1500	$\lesssim 30$ – 4000	$\sim 300$ – 4000

• **Tidal disruption of NS by BH in NS/BH binaries:** First crude estimates suggest WB IFOs can measure onset of disruption at 140Mpc well enough to deduce the NS radius to 15% accuracy (compared to current uncertainties of a factor  $\sim 2$ ); see table above for rates; Sec. 1.3.

• **BH/BH merger and ringdown:** Rough estimates suggest detectability, by WB IFOs out to the cosmological distances shown in Fig. 2(b); rates for BH/BH total mass  $\sim 20M_{\odot}$  are in table above; rates for much larger masses are unknown; Sec. 1.4.

• **Low-Mass X-Ray Binaries:** If accretion’s spin-up torque on NS due is counterbalanced by gravitational-wave-emission torque, then WB IFOs can detect Sco X-1, and NB IFOs can detect  $\sim 6$  other known LMXB’s; Secs. 1.1, 1.5.

• **Fast, Known Spinning NS’s (Pulsars with pulse frequency above 100 Hz):** Detectable by a advanced NB IFO in 3 months’ integration time, if NS ellipticity is  $\epsilon \gtrsim 2 \times 10^{-8}(100\text{Hz}/f)^2(r/10\text{kpc})$ , where  $f$  is gravity wave frequency (twice the pulsar frequency) and  $r$  is distance; actual ellipticities are unknown, but plausible range is  $\epsilon \lesssim 10^{-6}$ .

• **Fast, Unknown Spinning NS’s:** Unknown frequency wandering and doppler shifts degrade the detectable ellipticity  $\epsilon$  by a factor of a few to  $\sim 15$ , so detection with a NB IFO requires  $\epsilon \gtrsim (0.6 \text{ to } 3) \times 10^{-5}(100\text{Hz}/f)^2(r/10\text{kpc})$ ; Secs. 1.1 and 1.5.

• **R-Modes in Newborn NS’s with Initial Spin Rates Faster than  $\sim 100$  Hz:** Estimates suggest detectability out to  $\sim 15\text{Mpc}$  (the Virgo cluster) with WB or NB IFOs; NS birth rate in Virgo is a few per year, but initial spins are unknown; Secs. 1.5 and 1.6;

• **Centrifugally Hung-Up Proto Neutron Stars in White-Dwarf Accretion-Induced Collapse and in Supernovae:** Dynamics of star very poorly understood; if instability deforms star into tumbling bar, may be detectable by WB IFOs to  $\sim 20$  Mpc (the Virgo Cluster), and possibly farther; event rates uncertain but could be enough for detection; Sec. 1.6.

• **Convection of Supernova Core:** May be detectable by WB IFOs, via correlations with neutrinos, for supernovae in our Galaxy and possibly Magellanic Clouds; Sec. 1.6

• **Gamma Ray Bursts:** If triggered by NS/BH mergers, a few per year could be detectable by WB IFOs; if none are seen individually, statistical studies could nevertheless confirm gravity-wave emission by the gamma-burst triggers; Sec. 1.7.

• **Stochastic Background:** Detectable by cross correlating Hanford and Livingston 4km detector outputs, if  $\Omega = (\text{gravitational-wave energy in } \Delta f \sim f \sim 40 \text{ Hz}) \gtrsim 8 \times 10^{-9}$ ; there are many possible sources of such waves in very early universe, all very speculative; Sec. 1.8.

proposal we assume a Hubble expansion rate  $H_o = 65$  km/s/Mpc, a cold-matter density 0.4 of that required to close the universe  $\Omega_M = 0.4$ , and a vacuum energy density (cosmological constant) 0.6 of closure  $\Omega_\Lambda = 0.6$  [3]. Then the wide-band IFOs can see ( $10M_\odot/10M_\odot$ ) BH/BH inspirals out to a cosmological redshift  $z = 0.4$ . The binary inspiral rates at these advanced IFO distances are likely to be many per year; see Box 1. The middle arrowed line is the signal from BH/BH inspiral at 400Mpc, where the geometric mean of the event-rate estimates for BH/BH field binaries is three per year (third column of table in Box 1).

The **tidal disruption of a NS by its BH companion** at the endpoint of NS/BH inspiral should produce gravitational waves that carry detailed information about the NS structure and equation of state. The advanced IFOs may detect these waves and extract their information; see Sec. 3. This tidal disruption is a promising candidate for the **trigger of gamma-ray bursts**, as is the final merger of the two NS's in a NS/NS binary. A gamma-burst / gravitational-wave coincidence would be of great value in revealing the nature of gamma-burst sources; see Sec. 7

For BH/BH binaries much heavier than  $\sim 10M_\odot/10M_\odot$ , most of the gravitational signal is likely to come from the **black holes' merger and the vibrational ringdown of the final black hole**, rather than from the inspiral. Rough estimates discussed in Sec. 4 suggest that, if the holes are rapidly spinning (within a few per cent of the fastest spin allowed, i.e.  $a/m \gtrsim 0.98$  in the jargon of relativity theorists), then the wide-band IFOs can see the merger waves from two  $20M_\odot$  holes out to  $z = 1$  and two  $50M_\odot$  holes out to  $z = 2$ ; see the down-sloping, non-arrowed, dashed lines in Fig. 1. The event rates at these distances could well be many per year, and the waves from such mergers will carry rich physical and astrophysical information; see Sec. 4.

The triangles, star, large dots, and up-sloping short-dashed lines in Fig. 1 represent signals from **slightly deformed, spinning neutron stars**. The most interesting of these is a class of objects called **low-mass X-ray binaries (LMXB's)**. These are neutron stars that are being torqued by accretion from a companion, but that seem to be locked into spin periods in the range  $\sim 300 - 600$  revolutions per second. The most plausible explanation for this apparent locking is that the accretion is producing an asymmetry that radiates gravitational waves, which torque the star's spin down at the same rate as accretion torques it up [5, 6]. Assuming this to be true, one can deduce an LMXB's wave strength  $\hat{h}_s$  from its measured X-ray flux and its spin frequency [with the frequency inferred, sometimes to within a few Hz but not better, from nearly coherent oscillations (NCOs) in type-I X-ray bursts, or less reliably from frequency splittings of quasiperiodic (QPO) X-ray oscillations[7].] The spin frequency, and thence the gravitational-wave frequency, will wander somewhat due to fluctuations in accretion (which can be estimated by monitoring the X-ray flux) and due to poorly known orbital parameters. As a result, in searching for an LMXB's waves one can only perform coherent integrations for about 20 days; thereafter, one must stack the signals incoherently, allowing for unknown shifts of the wave frequency [8]. When one uses this "stack-slide" method of data analysis, the resulting signal strengths improve only slightly for integration times longer than 20 days [8].

Assuming 20 days of integration using a single 4-km IFO, the estimated signal strengths and frequencies for the strongest known LMXB's are shown by the big dots and the star in Fig. 1. The estimated strengths assume a steady-state balance of accretion torque by gravitational-wave torque, which is expected if density inhomogeneities produce the gravitational waves [5]. However, if sloshing fluid motions ("r-modes") produce the waves [9], then temperature-dependent viscosity could trigger long-term ( $\gtrsim$  a few hundred year) oscillations in the gravitational-wave emission, with short epochs of enhanced emission and long epochs of little or no emission [10]; a recent estimate [11] suggests a factor  $\sim 10$  enhancement of wave strength above those shown in Fig. 1 for  $\sim 10\%$  of the time. The estimated wave frequencies are also somewhat uncertain: The figure assumes density inhomogeneities, which means the wave frequency is twice

the NS rotation frequency; if r-mode sloshing produces the waves, then they will be at  $\simeq 4/3$  the rotation frequency ( $\sim 400$  Hz rather than 600 Hz). For every LMXB in Fig. 1 except the weakest one, the estimated rotation frequency is based on QPO splittings rather than NCOs, which means that about half of the frequencies might be double these estimates:  $\sim 1200$  Hz for density inhomogeneities and  $\sim 800$  Hz for r-mode sloshing, rather than  $\sim 600$  Hz. Doubling the frequency above 600 Hz reduces the emission amplitude by a factor 2 (at fixed X-ray flux assuming a steady-state torque balance), and increases the amplitude noise in a advanced NB IFO by a factor  $\simeq \sqrt{2}$ . As a result, at  $\sim 1200$  Hz frequency, Sco X-1 would still be readily detectable in a NB IFO but not in a WB IFO, and the strongest of the other LMXB's would be marginal. By contrast, if the frequencies are  $\sim 600$  Hz or  $\sim 400$  Hz and the waves are in a steady state, then Sco X-1 should be very easily detected by a WB IFO, and several LMXB's should be detectable by narrow banding (NB).

The large number of caveates and uncertainties in these LMXB estimates (which, however, generally leave at least Sco X-1 detectable) illustrate a very important point: Gravitational-wave observations have the potential to probe a rich range of complex physical processes in neutron stars; see Sec. 5 for further discussion.

The advanced IFOs can perform interesting searches for waves from **known radio pulsars**, such as the **Crab and Vela** for which the current upper limits (based on the pulsars' observed spindown rates) are shown as triangles. A Crab search, using coherent integrations based on the star's observed (slightly wandering) rotation period, could improve the limit on the Crab's wave amplitude by a factor 100 and constrain the star's gravitational ellipticity to  $\epsilon \lesssim 7 \times 10^{-6}$  — which is approaching the realm of physically plausible ellipticities,  $\epsilon \lesssim 10^{-6}$  [6].

More interesting will be searches for waves from **known, fast pulsars**, since the signal strength scales as  $\tilde{h}_s \propto \epsilon f^2/r$  (where  $r$  is distance to the source). The up-sloping short-dashed lines in Fig. 1 show some examples of signal strengths. With a narrow-band IFO tuned to the vicinity of such a fast pulsar, the waves would be detectable when  $\epsilon \gtrsim 2 \times 10^{-6}(100\text{Hz}/f)^2(r/10\text{kpc})$ , which is in the realm of plausible ellipticities for pulsars throughout our galaxy so long  $f$  exceeds 100 Hz, i.e. the spin frequency exceeds 50 Hz.

Also of great interest will be searches for **previously unknown spinning neutron stars**, for which the signal strengths  $\tilde{h}_s$  will be reduced by a factor of a few to  $\sim 15$  by the lack of prior information about the frequency and its evolution and the direction to the source (which determines the time-evolving doppler shift produced by the earth's motion) [12, 8]. A tunable, narrow-band IFO will be crucial to such searches. One can search more deeply by a factor of several, using a narrow-banded IFO that dwells on a given frequency and its neighborhood for a few days or weeks and then moves on to another frequency, than using a broad-interferometer that collects signal at all frequencies simultaneously for a year. Such searches will be in the band of physically plausible ellipticities, for stars throughout our galaxy, if  $f \gtrsim 200$  Hz (spin frequency above  $\sim 100$  revolutions per second).

One can search for a **stochastic background** of gravitational waves by cross correlating the outputs of LIGO's two 4 km detectors [13]. For such a search the signal strengths  $\tilde{h}_s(f)$  are shown in Fig. 1 as downward-sloping dotted lines, assuming a cross-correlation of 4 months of (not necessarily contiguous) data, and isotropic waves. The lines are labeled by the waves' energy density  $\Omega$  in a bandwidth equal to frequency and in units of the density to close the universe,  $\Omega = (fdE_{\text{GW}}/df)/\rho_{\text{closure}}$ . Unfortunately, the frequency of optimal *a priori* sensitivity,  $f \sim 70$  Hz (where the noise curve is parallel to the dotted  $\Omega$  lines), is near the center of a dead band for LIGO. This dead band arises from the fact that  $1/70\text{Hz} \simeq 14$  ms is about the round-trip gravity-wave travel time between the two LIGO sites [14]. The result is a net debilitation of the stochastic background sensitivity by a factor of a few: the initial IFOs can detect an

isotropic background with  $\Omega$  down to  $\sim 10^{-5}$ , while advanced, wide-band IFOs can reach down to  $\Omega \sim 5 \times 10^{-9}$ , and a factor  $\sim 2$  lower than this if it is reoptimized for low frequencies. These are interesting sensitivities, able to test a wide range of speculations about the physics of the early universe and perhaps even detect waves. Such a detection could have profound implications for physics and cosmology; see Sec. 8.

Other waves that advanced IFOs in LIGO will seek and may detect are those from **the stellar core collapse that triggers supernovae** and the **boiling of the nascent neutron star** and the endpoint of that collapse (Sec. 6), **accretion induced collapse of white dwarfs** (Sec. 6), and **totally unknown sources** (Sec. 9).

We turn, now, to a discussion of each of the above sources, focusing especially on event rate estimates and the information that the waves may bring.

## 2 Inspiring NS and BH Binaries with $M_{BH} \lesssim 10M_{\odot}$

As we have discussed, wide-band advanced LIGO IFOs can detect the waves from NS/NS inspirals out to 300Mpc, NS/BH out to 650 Mpc, and BH/BH out to  $z = 0.4$ . The event rates out to these distances can be estimated from observational data in our own galaxy [15], and an extrapolation out through the universe based on the density of massive stars (which can be deduced by several different methods) [16]. The resulting rates are quite uncertain but very promising; see Box 1.

For NS/NS binaries, the event rate in our galaxy is constrained by the results of radio astronomers’ searches for binary pulsars that will merge, due to gravitational radiation emission, in less than the age of the universe, and by other aspects of pulsar searches [15]. The resulting constraints,  $10^{-6}/\text{yr} \lesssim \mathcal{R}_{\text{gal}} \lesssim 5 \times 10^{-4}/\text{yr}$ , extrapolate to a NS/NS event rate for advanced IFOs between 1/yr and 800/yr. Searches in our galaxy for NS/BH binaries in which the NS is a pulsar have failed to find any as yet, so we must turn to much less reliable estimates based on “population synthesis” (simulations of the evolution of a population of progenitor binary systems to determine the number that make NS/BH binaries compact enough to merge in less than the universe’s age). Population synthesis gives a NS/BH event rate in our galaxy in the range  $\sim 10^{-7}/\text{yr} \lesssim \mathcal{R}_{\text{gal}} \lesssim 10^{-4}/\text{yr}$  [21], though it is possible the rate could be even less than this (hence the  $\lesssim 10^{-7}/\text{yr}$  in Box 1). Extrapolating out into the universe, we find a NS/BH rate in WB advanced IFOs between  $\lesssim 1/\text{yr}$  and about 1500/yr. A similar analysis for BH/BH binaries based on population synthesis (third column of the table in Box 1) gives a rate between  $\lesssim 30/\text{yr}$  and  $\sim 4000/\text{yr}$  [17]. Population synthesis ignores the likely role of globular clusters and other types of dense star clusters as “machines” for making BH/BH binaries [18]: single black holes, being heavier than most stars in a globular, sink to the center via tidal friction, find each other, and make binaries; then the BH/BH binaries get “hardened” (made more compact) by interaction with other black holes, reaching sizes where gravitational-wave emission will cause them to merge in less than the age of the universe; and further interactions will often eject the BH/BH binaries from the globular, to interstellar space where they merge. Simulations [18] suggest that each dense cluster will make a number of such BH/BH binaries, and extrapolations into the universe predict an event rate in WB advanced IFOs between  $\sim 300$  and  $\sim 4000/\text{yr}$  — though the uncertainties are probably larger than these numbers from the literature suggest [18, 15].

These event rates are very encouraging. They make it seem quite likely that the advanced IFOs will observe tens to thousands of BH and NS inspirals per year, while the initial IFOs will be lucky to observe  $\sim 1$  per year.



The observed inspiral waves will last for between  $\sim 1000$  and  $10,000$  cycles depending on the binary's masses, and will carry detailed information about the binary and about general relativistic deviations from Newtonian gravity. This information can be extracted with good precision using the method of matched filters. Specifically (denoting by  $M = M_1 + M_2$  the binary's total mass and  $\mu = M_1 M_2 / M$  its reduced mass):

(i) The binary's chirp mass  $M_c \equiv \mu^{3/5} M^{2/5}$  will typically be measured, from the Newtonian part of the signal's upward frequency sweep, to  $\sim 0.04\%$  for a NS/NS binary and  $\sim 0.3\%$  for a system containing at least one BH. (ii) *If* we are confident (e.g., on a statistical basis from measurements of many previous binaries) that the binary's spins are a few percent or less of the maximum physically allowed, then the reduced mass  $\mu$  will be measured to  $\sim 1\%$  for NS/NS and NS/BH binaries, and  $\sim 3\%$  for BH/BH binaries. (iii) Because the frequency dependences of the (relativistic)  $\mu$  effects and spin effects are not sufficiently different to give a clean separation between  $\mu$  and the spins, if we have no prior knowledge of the spins, then the spin/ $\mu$  correlation will worsen the typical accuracy of  $\mu$  by a large factor, to  $\sim 30\%$  for NS/NS,  $\sim 50\%$  for NS/BH, and a factor  $\sim 2$  for BH/BH. These worsened accuracies should be improved significantly (though we do not yet know how much) by waveform modulations due to spin-induced precession of the orbit [20], and even without modulational information, a certain combination of  $\mu$  and the spins will be determined to a few per cent. (iv) The distance to the binary (angle-effective distance at cosmological distances) can be inferred, from the observed waveforms, to a precision  $\sim 1/\rho \lesssim 10\%$ , where  $\rho$  is the amplitude signal-to-noise ratio in the total LIGO network (which must exceed about 8 in order that the false alarm rate be less than the threshold for detection). (v) With the aid of VIRGO and/or other international partners, the location of the binary on the sky can be inferred, by time of flight between the detector sites, to a precision of order one degree on the sky.

Advanced LIGO will likely produce a catalog of hundreds or thousands of binary inspirals and their inferred parameters; this catalog will be a valuable data base for observational astronomy and cosmology.

Important examples of the general relativistic effects that can be detected and measured with precision, in the inspiral waves, are these: (i) As the waves emerge from the binary, some of them get backscattered one or more times off the binary's spacetime curvature, producing wave *tails*. These tails act back on the binary, modifying its radiation reaction force and thence its inspiral rate in a measurable way. (ii) If the orbital plane is inclined to one or both of the binary's spins, then the spins drag inertial frames in the binary's vicinity (the "Lense-Thirring effect"), this frame dragging causes the orbit to precess, and the precession modulates the waveforms [20]. This precession and modulation should be very strong in a significant fraction of NS/BH binaries [21].

### 3 Tidal Disruption of a NS by a BH: Measuring the Nuclear Equation of State

As a NS/BH binary spirals inward, its NS experiences ever increasing tidal forces from the BH's gravitational field (its spacetime curvature). In many cases these tidal forces may tear the NS apart before it begins its final, quick plunge into the hole's horizon. The gravitational waves from this tidal disruption and from the termination of inspiral should carry detailed information about the NS's equation of state (the equation of state of bulk nuclear matter at  $\sim 10$  times the density of an atomic nucleus). The disruption waves lie largely in the frequency band  $\sim 300\text{Hz} \lesssim f \lesssim 1000 \text{ Hz}$ , where the wide-band, advanced IFOs have good sensitivity,

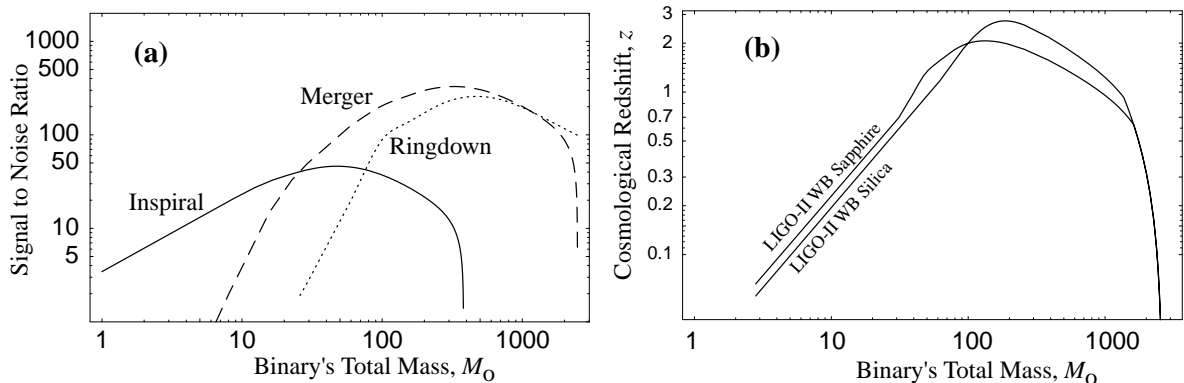


Figure 2: Characteristics of the gravitational waves from the inspiral, merger, and final ringdown of a BH/BH binary with equal masses  $M_1 = M_2 = M/2$  and large spins, as computed by combining the source estimates of Ref. [24] with the wide-band noise curves of Fig. 1. (a) The amplitude signal to noise ratio, as a function of the binary’s total mass  $M$  for a binary at 300 Mpc distance, and for the three phases of the binary’s evolution: inspiral, merger, and ringdown. (b) The cosmological redshift to which the binary can be seen by wide-band, advanced IFOs, as a function of its total mass  $M$ .

and where narrow-band or some other optimized IFO can do even better. This suggests that the advanced IFOs may be able to extract new information about the nuclear equation of state from the tidal-disruption waves. A first, crude estimate [22] suggests, for example, that for NS/BH binaries at 140 Mpc distance (where the event rate could be a few per year; see the table in Box 1), tidal-disruption observations may enable the NS radius  $R$  to be measured to a precision  $\sim 15\%$ , by contrast with its present uncertainty (for fixed NS mass) of about a factor 2. From the measured radii would follow the desired equation-of-state information. Detailed numerical-relativity simulations will be required to firm up this estimate, and will be essential as a foundation for interpreting any tidal-disruption waves that are observed.

The merger waves from NS/NS binaries, by contrast with NS/BH, are likely to lie outside the band of good advanced-IFO sensitivity — at frequencies  $f \gtrsim 1500$  Hz. However the onset of NS/NS merger, triggered by a plunge of the two NS’s toward each other, may produce a strong “cliff” in the waves’ spectrum, in a range  $f \sim 400$  — 1000 Hz of good sensitivity [23], and by measuring the cliff frequency we may learn about the nuclear equation of state.

## 4 BH/BH Mergers and Ringdown: Observing The Nonlinear Dynamics of Spacetime Curvature

Black holes are made not from ordinary matter, but rather from spacetime curvature. For a single, quiescent black hole, this curvature has a rich structure: a trumpet-horn-like curvature of space, a tornado-like whirling of space around the hole’s horizon, and a warpage of time that becomes so strong near the horizon that, in a certain sense, the flow of time grinds to a halt there. Even richer (and as yet only crudely understood) will be the spacetime curvature of a BH/BH binary, as its holes near each other and merge. Among other things, it should entail tornado-like whirlings of space around each of the two black holes caused by their spins, and a third whirl of space around the binary as a whole, caused its orbital angular momentum. In the half dozen years between now and the advanced IFOs’ first operation, numerical relativists

will perfect their techniques for simulating such BH/BH mergers, in preparation for comparison with LIGO’s observations. That comparison should bring a clear understanding of the highly nonlinear dynamics of warped spacetime.

The numerical simulations are not yet sufficiently advanced to tell us much about the predicted waves, so we must rely, for now, on crude insights from perturbation theory. Those insights suggest that, if the holes are rapidly spinning, then the wave strengths, quantified by the net signal to noise ratio in wide-band advanced IFOs, are as shown in Fig. 2(a). For total mass  $M \gtrsim 30M_\odot$ , the merger waves are stronger than the inspiral waves; for  $M \sim 100$  to  $2000M_\odot$ , the ringdown waves are comparable to the merger. Above  $M \sim 2000M_\odot$ , the waves are at too low frequency to be seen by the advanced IFOs. The distance to which the waves can be detected, expressed in terms of cosmological redshift (assuming  $H_o = 65$  km/s/Mpc,  $\Omega_M = 0.4$ ,  $\Omega_\Lambda = 0.6$ ) is shown in Fig. 2(b). For  $M \sim 100$  to  $1000M_\odot$ , the distance exceeds  $z = 1$ . We know little about what the event rate may be, when  $M \gtrsim 40M_\odot$ . It is unlikely that main sequence binaries form BH/BH binaries this massive; but they may well be formed by mergers of smaller holes in galactic nuclei in sufficient numbers to produce many mergers per year at  $z \sim 1$ [25]. LIGO’s observations may thereby bring us major new insights into the physics of galactic nuclei.

## 5 Spinning Neutron Stars

In Sec. 1.1 we discussed the signal strengths and search strategies for spinning neutron stars. As we saw, tunable, narrow-band IFOs have good possibilities to detect such stars’ waves, especially for LMXB’s.

For any detected waves, the features that can be measured include their frequency (or frequencies if several lines are seen), the time evolution of the frequencies, the wave amplitudes and their evolution, and correlations with electromagnetic observations of the same source (if any). These quantities are governed by a wide variety of rich physics in the neutron-star interior, and by the direction to the source. For example: (i) The modulation of the frequency due to the earth’s motion can reveal the source direction to an accuracy of order one arc second [26], enabling identification with electromagnetically observed objects. (ii) The ratio of the gravitational-wave frequency to the electromagnetically observed rotation frequency can reveal the nature of the inhomogeneities that emit the waves: for density inhomogeneities frozen into a spinning neutron star, e.g. those of a deformed crust or core,  $f_{\text{GW}} = 2f_{\text{rot}}$ . For a free-precessing (wobbling) star with frozen-in inhomogeneities, there will be a second line at  $f_{\text{GW}} = f_{\text{rot}} + f_{\text{precess}} \simeq f_{\text{rot}}$ . For r-mode oscillations of a star’s fluid mantle driven by gravitational radiation reaction [27],  $f_{\text{GW}} \simeq \frac{4}{3}f_{\text{rot}}$ . (iii) Depending on the nature of the inhomogeneities, each line’s frequency evolution and amplitude can be influenced by a wide variety of different physical processes in the neutron star, e.g., crust physics (thickness, elasticity moduli, breaking strain, ...), crust-core mechanical and thermal couplings, superfluid transition temperature, magnetic field strength, viscosity, etc. (iv) Correlated gravitational and electromagnetic observations after a frequency “glitch” might be particularly informative about the neutron-star physics. (v) For precessing pulsars, the gravitational-wave observations can determine the orientation of the pulsar angular momentum vector relative to the line of sight, and this can be used to test models of the pulsar emission mechanism, which depend on the angle between the rotation axis and the pulsar beam [28].

## 6 Supernovae and Accretion-Induced Collapse of White Dwarfs

Type-II supernovae are triggered by the violent collapse of a stellar core to form a NS or BH. The details of the collapse and NS or BH formation are poorly understood, and the optical display sheds little light on them because the photons are emitted  $\gtrsim 100,000$  km from the trigger and hours or more afterward. Neutrino observations provide one window on the trigger, with emphasis on the thermal structure of the collapsed core. Gravitational waves provide a complementary window, with emphasis on the compactness and density of the core, on its asymmetry, and on whether the final remnant is a BH or a NS.

Observations show that many type-II supernovae produce neutron stars and give them kicks of magnitude as large as  $\sim 1000$  km/s. Indeed, about half of all radio pulsars are born with a kick larger than 500 km/s [29]. The observed kicks suggest that at least some newborn proto-neutron-stars may be strongly asymmetric, perhaps due to fast rotation, and therefore could produce significant gravitational radiation. Rapidly rotating proto-neutron-stars may also be produced by the accretion-induced collapse of white dwarf stars (AIC) in some cases, depending on the white-dwarf composition, central density and accretion rate [30].

If the newborn proto-neutron-star in an AIC or supernova is spinning so fast that it hangs up centrifugally at a radius large compared to that of the final NS, then it may be dynamically (or at least secularly) unstable to deforming into a bar-shaped object that tumbles end-over-end, emitting gravitational waves in LIGO’s band of good sensitivity [31]. Recent simulations suggest that the bar will be long-lived, rather than just wrapping itself up into an axisymmetric shape and disappearing [32]. The simulations show that the waves from such a bar may sweep upward in frequency, due to a gradual shrinkage of the proto-neutron-star, or may sweep downward due to development of “Dedekind-like” internal circulation [33]. The discovery of the waves from such a proto-neutron-star and observations of their frequency evolutions (which should mirror the bar’s evolution) would teach us much. Though the strengths of the waves and the best signal processing techniques and thresholds are all ill-understood, a rough estimate [34] suggests that the advanced IFOs’ range for detection might be the distance of the VIRGO cluster of galaxies (about 15 Mpc) and conceivably significantly larger, suggesting event rates that could be some per year but might be far less.

Even if the proto-neutron-star does not hang up centrifugally, if it is born spinning faster than  $\sim 100$  revolutions per second, then its r-modes of oscillation (oscillatory, quadrupolar circulation patterns) may be driven unstable by gravitational radiation reaction. Estimates suggest that the r-modes may radiate for some months, gradually slowing the star’s rotation to  $\sim 100$  revolutions per second, and their waves may be detectable by LIGO’s wide-band or narrow-band IFOs out to the Virgo Cluster; cf. Sec. 5. Theoretical astrophysicists and relativists are struggling to understand the physics that governs and influences the r-modes [35], but it is so complex that a reliable understanding will likely only come from LIGO’s observations of (or failure to observe) the r-modes’ waves.

Numerical models of supernovae suggest that, even if it is slowly rotating, the newborn proto-neutron-star will be convectively unstable, and that the gravitational waves from the convective overturn in the first  $\sim$ one second of the star’s life may be detectable throughout our galaxy and its orbiting companions, the Magellanic Clouds [36]. Although the supernova rate is low in our galaxy and its companions ( $\lesssim 1/30$  yrs), one observed event could be very valuable scientifically: The bulk of the supernova’s neutrinos are thought to come from the same convecting material as produces the gravitational waves, so there should be correlations between the neutrinos and the waves, which could teach us much about the proto-neutron-star’s dynamics.

If the advanced WB IFOs detect no gravitational waves from a supernova at distance  $r$ ,

during a time  $T$  preceding the beginning of the optical outburst or over a time  $T$  during a neutrino outburst, then one can thereby place a limit on the emitted gravitational-wave energy. In the band from  $\sim 100$  to  $300$  Hz this limit is  $\Delta E_{\text{GW}} \lesssim 0.05(r/15\text{Mpc})^{1/2}(T/1\text{h})^{1/2}M_{\odot}$ . In the case of a neutrino-emitting supernova in our own galaxy, with  $T \sim 1$  sec, this limit is very impressive:  $\sim 10^{-9}M_{\odot}$ .

## 7 Gamma Ray Bursts

Cosmic gamma-ray bursts, observed  $\sim$  once per day by detectors on spacecraft, are believed to arise from shocks in a relativistic fireball, generated by rapid accretion onto a newly formed black hole [37]. The gamma-ray production must occur rather far from the BH ( $10^{13} - 10^{15}$  cm), making it difficult to test the BH involvement by conventional astronomical observations. Gravitational waves are more promising: The BH and its accretion flow are thought to form violently, by the collapse of a massive star (perhaps initiated by merger with a companion) [“a hypernova”], or by the merger of a binary made of compact objects: a NS/NS binary, a BH/NS binary, a BH/white-dwarf or a BH/He-core binary [37]. Statistical evidence points to several subclasses of gamma-ray bursts [38], so several of these “triggers” might occur in nature.

Each of these gamma-burst triggers should emit strong gravitational waves that carry detailed information about its source. NS/BH mergers and hypernovae are promising trigger candidates for *long bursts* (duration  $\gtrsim 2$  s), for which a number of distances have been measured via afterglows. From the measured distances and the distribution of gamma-burst fluences, one can estimate a long-burst event rate of  $\sim 1$  per year out to  $650$  Mpc — a distance at which advanced IFOs should be able to detect NS/BH inspirals but will likely not be able to detect the gravitational waves from hypernovae. NS/NS mergers are a promising trigger candidate for *short bursts* (duration  $\lesssim 2$  s). The distances to the short bursts are unknown (no after glows have been detected), but they could well be near enough (event rate  $\gtrsim 1/\text{yr}$  at  $300$  Mpc) for the advanced IFOs to detect the inspiral waves from a NS/NS trigger.

If gravitational waves are detected from one or more gamma-burst triggers, the waves will almost certainly reveal the physical nature of the trigger. Moreover, by comparing the arrival times of the gravitational waves and the earliest gamma rays, it should be possible to measure the relative propagation speeds of light and gravitational waves to an accuracy  $\sim 1 \text{ sec}/10^{10} \text{ yr} \sim 10^{-17}$ .

If no gravitational waves are detected from any individual gamma burst, the correlation between gamma bursts and gravitational waves might nevertheless be established by statistical studies of the advanced IFOs’ gravitational-wave data in narrow time windows preceding the gamma bursts [39].

## 8 Sources of Stochastic Background

The most plausible sources of a stochastic gravitational-wave background in LIGO’s frequency band are processes in the very early universe. The current best limit on the strength of such waves is  $\Omega \lesssim 10^{-5}$ ; a wave energy larger than this would have caused the universe to expand too rapidly through the era of primordial nucleosynthesis (universe age  $\sim$  a few minutes), thereby distorting the universal abundances of light elements away from their observed values. LIGO’s advanced interferometers would improve on this current limit by a factor  $\sim 10,000$ , to  $\Omega \simeq 5 \times 10^{-9}$  — an improvement enabling LIGO to test a number of current speculations about the very early universe. A positive detection would have profound consequences.

Inflationary models of the early universe predicts that vacuum fluctuations, created in the Planck era when the universe was being born, should have been parametrically amplified, during the first  $\sim 10^{-25}$  sec of the universe’s life, to produce a stochastic gravitational wave background in the LIGO band. Unfortunately, if “standard” inflation theory is correct, then the amplified waves are much too weak for LIGO to detect,  $\Omega \lesssim 10^{-15}$  [40]. The most plausible modifications of standard inflation push  $\Omega$  downward from this [40], but some less plausible modifications push it upward, to the point of detectability [41].

The first, tentative efforts to combine superstring theory with inflationary ideas have produced a new description of the very early universe called the “pre-big-bang model”, in which string effects cause the gravitational-wave spectrum to rise steeply at high frequencies — most likely at frequencies above LIGO’s band, but quite possibly in or below that band [42]. The result could be waves strong enough for LIGO to detect. A non-detection would significantly constrain the pre-big-bang model.

There are a wide variety of postulated mechanisms that could have produced strong gravitational waves, with wavelengths of order the horizon size, at various epochs in the very early universe. Those waves (if any) produced at (universe age)  $\sim 10^{-25}$  sec, corresponding to (universe temperature  $T$ )  $\sim 10^9$  GeV, would have been redshifted into the LIGO band today and might be detectable. The temperature (energy) region  $\sim 10^9$  GeV is *tera incognita*; LIGO’s advanced detectors will provide our first opportunity for a serious experimental exploration of it. Among the speculated wave-generating mechanisms that could operate there, and that LIGO could constrain (or discover!), are these:

- A first-order phase transition in the states of quantum fields at  $T \sim 10^9$  K. Such a phase transition would nucleate bubbles of the new phase that expand at near the speed of light and collide to produce gravitational waves; and their collisions would also generate turbulence that radiates waves. If the transition is strongly first order, the waves would be strong enough for LIGO’s advanced IFOs to detect. [43]
- Goldstone modes (coherent, classical excitations) of scalar fields that arise in supersymmetric and string theories. If strongly excited, these modes will entail coherent flows of energy that radiate gravitational waves strong enough for detection. [44]
- Coherent excitations of our 3+1 dimensional universe, regarded as a “brane” (defect surface) in a higher dimensional universe. The excitations could be of a “radion” field that controls the size or curvature of the additional dimensions, or they could be of the location and shape of our universe’s brane in the higher dimensions; in either case, if there is an equipartition of energy between these excitations, in the very early universe, and other forms of energy, then the excitations will produce gravitational waves easily strong enough for detection by LIGO’s advanced IFOs. LIGO would thereby probe one or two additional dimensions of size or curvature length  $\sim 10^{-10} - 10^{-13}$  mm; by contrast, LISA’s lower-frequency observations would probe lengths  $\sim 1 - 10^{-5}$  mm. If the number of extra dimensions is larger than 2, the probes reach to much smaller scales [45]

Cosmic strings (not to be confused with superstrings), produced in the early universe, were once regarded as candidates for seeding galaxy formation, but recent cosmological observations have ruled them out as seeds. Nevertheless, it remains possible that a network of vibrating cosmic strings too weak to seed galaxy formation was formed in the early universe. LIGO can search for the presence of such a network in two ways: (i) Via the stochastic background of gravitational waves that the strings’ vibrations produce; this background would be strong

enough for the advanced IFOs to detect if the strings' mass per unit length is  $\gtrsim 10^{-8}$ . [46]  
(ii) Via occasional non-Gaussian, strong bursts (“spikes”) of gravitational waves produced by kinks (cusps) in the string shapes. These bursts could be detectable even if the accompanying stochastic background is too weak for detection. [47]

## 9 Unknown Sources

Each of these cosmological speculations is plausible, though not highly likely. Perhaps their greatest value is to remind us of how terribly ignorant we are of physics and astrophysics in the domain that LIGO's advanced IFOs will probe. Our ignorance may well be even greater than that of the pioneering radio astronomers of 1940 and X-ray astronomers of 1960; and as there, so also here, the first waves to be discovered may well be from sources that were previously unknown. Advanced LIGO could bring us a revolution of insights into the universe, and even into gravity, comparable to the revolutions wrought by radio and X-ray astronomy.

## References

- [1] This  $\tilde{h}_s(f)$  is related to the *characteristic amplitude*  $h_c(f)$  widely used in the literature in the following way:  $h_c = \sqrt{5f}(T/N)\tilde{h}_s$ , where the  $\sqrt{5}$  comes from averaging over the sky, the  $\sqrt{f}$  is due to  $h_c$  being the signal strength in a bandwidth equal to frequency, and  $T/N$  is the ratio of the threshold to the rms noise at the endpoint of signal processing.
- [2] If, in its advanced (“LIGO-II”) incarnation, the 2km interferometer is replaced by a narrow-banded 4km interferometer, then for the most important wide-band sources, inspiraling binaries, the 3-IFO threshold will be lowered (improved) slightly and correspondingly the distances to which the sources can be seen will be increased slightly beyond those in Box 1. If the 2km interferometer is replaced by a wide-band 4km interferometer, then the threshold will be lowered by a factor 1.16, the binaries' observable distances will be increased correspondingly by 1.16, and the predicted event rates will go up by  $1.16^3 \simeq 1.5$ .
- [3] See, e.g., the review of cosmological observations by Michael S. Turner, in *Proceedings of Particle Physics and the Universe (Cosmo-98)*, ed. D. O. Caldwell, AIP, Woodbury, NY; astro-ph/9904051.
- [4] See, e.g., B.J. Owen and B.S. Sathyaprakash, Phys. Rev. D **60**, 022002 (1999), and references therein.
- [5] L. Bildsten, Astrophys. J. Lett., **501**, L89 (1998).
- [6] G. Ushomirsky, C. Cutler and L. Bildsten, astro-ph/0001136; and references therein.
- [7] M. van der Klis, Ann. Rev. Astron. Astrophys., **38**, 717 (2000); astro-ph/0001167.
- [8] P.R. Brady and T. Creighton, Phys. Rev. D **61**, 082001 (2000); see also M.A. Papa, B.F. Schutz and A.M. Sintes, in press, gr-qc/0011034.
- [9] Yu. Levin and G. Ushomirsky, Mon. Not. Roy. Astron. Soc., in press, astro-ph/0006028; and references therein.
- [10] Yu. Levin, Astrophys. J. **517**, 328 (1999).

- [11] J. Hennawi, J. Liu and R.V. Wagoner, paper in preparation.
- [12] P.R. Brady, T. Creighton, C. Cutler and B.F. Schutz, *Phys. Rev. D* **57**, 2101 (1998).
- [13] See, e.g., B. Allen and J.D. Romano, *Phys. Rev. D* **59**, 102001 (1999) and references therein.
- [14] See the discussion of the overlap reduction function in Sec. III.B of Ref. [13], especially Fig. 2.
- [15] The NS/NS numbers in this table are taken from V. Kalogera, R. Narayan, D. Spergel, and J.H. Taylor, *Astrophys. J.*, submitted, astro-ph/0012038 — as augmented slightly by a new channel for NS/NS formation analyzed by K. Belczynski and V. Kalogera, *Astrophys. J. Lett* submitted, astro-ph/0012172 — and with adjustment of  $\mathcal{D}_{\text{WB}}$  from 350 Mpc (appropriate for three 4 km interferometers) to 300 Mpc (for one 2 km and two 4 km interferometers; see Ref. [2]). The NS/BH and BH/BH numbers are based on Kalogera’s survey of all estimates of  $\mathcal{R}_{\text{gal}}$  [V. Kalogera, in *Gravitational Waves, Proceedings of the Third Edoardo Amaldi Conference*, AIP Conference Proceedings Vol. 523, ed. Sydney Meshkov (American Institute of Physics, 2000), astro-ph/9911532; and V. Kalogera in *Astrophysical Sources of Gravitational Radiation for Ground-Based Detectors*, ed. J.M. Centrella (AIP, Woodbury NY), submitted, astro-ph/0101047] — extrapolated into the distant universe by the B-band method of Phinney as updated by Kalogera et. al. [16]. The last column is based on the estimates by Portegeis Zwart and McMillan [18]. The numbers preceded by “ $\lesssim$ ” represent Kalogera’s personal best estimate of the lower limit with the “ $<$ ” being a warning that some researchers have argued for lower numbers.
- [16] See the B-band extrapolation technique developed by E.S. Phinney, *Astrophys. J.* **380**, L17 (1991) as updated by V. V. Kalogera, R. Narayan, D. Spergel, and J.H. Taylor, *Astrophys. J.*, submitted, astro-ph/0012038; also the cosmological evolution effects estimated by P. Madau, astro-ph/9902228.
- [17] When extrapolating out to cosmological distances,  $z \gtrsim 0.1$ , we must take account of cosmological effects. We assume a cosmological model with  $H_o = 65$  km/s/Mpc,  $\Omega_M = 0.4$ ,  $\Omega_\Lambda = 0.6$  [3], and we take account of the evolution of the numbers of massive stars and thence BH/BH binaries using Eq. (4) of Madau, Ref. [16]; the result is an event rate, inside redshift  $z$ , that scales as  $z^3$  for  $0 < z < 4$ , aside from an enhancement by a factor  $\sim 2$  near  $z = 1$  and a decrement by a factor  $\sim 2$  at  $z \sim 2.5 - 4$ .
- [18] S. McMillan and S. Portegies-Zwart, *Astrophys. J. Lett.* **528**, L17 (2000).
- [19] E. Poisson and C.M. Will, *Phys. Rev. D*, **52**, 848 (1995).
- [20] T.A. Apostolatos, C. Cutler, G.J. Sussman and K.S. Thorne, *Phys. Rev. D* **49**, 6274 (1994); L.E. Kidder, *Phys. Rev. D* **52**, 821 (1995); T.A. Apostolatos, *Phys. Rev. D* **52**, 605 (1995).
- [21] V. Kalogera, *Astrophys. J.* **541**, 319 (2000).
- [22] M. Vallisneri, *Phys. Rev. Lett.* **84**, 3519 (2000).
- [23] See, e.g., J.A. Faber, F.A. Rasio and J.B. Manor, gr-qc/0006078; also J. A. Faber and F. A. Rasio, in *Astrophysical Sources of Gravitational Waves*, ed. J.M. Centrella (AIP, Woodbury NY), gr-qc/0101074; and references therein.
- [24] E.E. Flanagan and S.A. Hughes, *Phys. Rev. D* **57**, 4535 (1998).



- [25] G.D. Quinlan and S.L. Shapiro, *Astrophys. J.* **356**, 483 (1990). Note also the tentative evidence for a  $\gtrsim 500M_{\odot}$  black hole in a region of active star formation in the star-burst galaxy M82 which is believed to have experienced a recent two-galaxy merger: P. Kaaret et. al. *Mon. Not. Roy. Astron. Soc.*, in press, astro-ph/0009211; H. Matsumoto et. al., *Astrophys. J. Lett.*, in press, astro-ph/0009250.
- [26] P. Jaranowski and A. Krolak, *Phys. Rev. D* **59**, 063003 (1999).
- [27] For a recent review of the extensive literature on r-modes, see N. Andersson and K.D. Kokkotas, gr-qc/0010102.
- [28] See, e.g., A.G. Lyne and R.N. Manchester, *Mon. Not. Roy. Astron. Soc.* **234**, 477 (1988)
- [29] See, e.g., <http://online.itp.ucsb.edu/online/neustars00/chernoff/>, especially slide 34.
- [30] K. Nomoto, in *Proc. 13th Texas Symposium on Relativistic Astrophysics*, ed. M. Ulmer (World Scientific: Singapore); K. Nomoto and Y. Kondo, *Astrophys. J. Lett.* **367**, L19.
- [31] See, e.g., recent simulations of dynamical bar formation by M. Shibata, T.W. Baumgarte and S.L. Shapiro, *Astrophys. J.* **542**, 453 (2000), and M. Saijo, J. Shibata, T.W. Baumgarte and S.L. Shapiro, *Astrophys. J.* in press, astro-ph/0010201, and references therein. These recent simulations show that general relativity enhances the instability to bar formation.
- [32] K.C.B. New, J.M. Centrella and J.E. Tohline, *Phys. Rev. D* **62**, 064019 (2000); D. Brown, *Phys. Rev. D* **62**, 084024 (2000).
- [33] D. Lai and S.L. Shapiro, *Astrophys. J.* **442**, 259 (1995).
- [34] In order to shrink to normal neutron-star size, the proto-neutron-star must get rid of its excess angular momentum. In the idealized case that (i) the angular momentum is lost solely to gravitational waves and not to hydrodynamic or magnetic processes, and (ii) the LIGO data are analyzed by optimal signal processing, the integrated signal strength depends primarily on the excess angular momentum and not on the ellipticity of the bar, and the distance to which the signal can be seen is of order 150Mpc (about half that for a NS/NS binary whose mass is twice as large). A factor ten reduction of amplitude signal to noise (factor 100 reduction of power signal to noise), due to non-optimal signal processing and to loss of angular momentum via non-gravitational-wave channels, would still leave the source detectable at  $\sim 15$  Mpc, the distance of Virgo.
- [35] See, e.g, the following references and others cited therein: L. Lindblom, J.E. Tohline, and M. Vallisneri, astro-ph/0010653; L. Lindblom, B.J. Owen and G. Ushomirsky, *Phys. Rev. D* **62** 084030 (2000); Y. Wu, C.D. Matzner and P. Arras, astro-ph/0006123; Yu. Levin and G. Ushomirsky, astro-ph/0006028.
- [36] See, e.g., A. Burrows, J. Hayes and B. Fryxell, *Astrophys. J.* **450**, 830 (1995).
- [37] See, e.g., P. Mészáros, M.J. Rees and R.A.M.J. Wijers, *New Astron.* **4**, 303 (1999).
- [38] See, e.g., S. Mukherjee *et. al.*, *Astrophys. J.* **508**, 314 (1998).
- [39] L.S. Finn, S.D. Mohanty and J. Romano, *Phys. Rev. D* **60**, 121101 (1999).
- [40] See, e.g., M.S. Turner, *Phys. Rev. D* **55**, 435 (1997).

- [41] L.P. Grishchuk, Sov. Phys. JETP **40**, 409 (1975); L.P. Grishchuk, gr-qc/0002035 and references therein.
- [42] R. Brustein, M. Gasperini, M. Giovannini and G. Veneziano, Phys. Lett. B **361**, 45 (1995). For a review of more recent literature, see M. Maggiore, Phys. Rep. **331** 283 (2000).
- [43] See, e.g., M. Kamionkowski, A. Kosowsky and M.S. Turner, Phys. Rev. D **49**, 2837 (1994) and references therein.
- [44] See, e.g., C.J. Hogan, Phys. Rev. Lett **74**, 3105 (1995), and C.J. Hogan, astro-ph/9809365.
- [45] C.J. Hogan, Phys. Rev. Lett **85**, 2044 (2000); Phys. Rev. D, submitted, astro-ph/0009136.
- [46] See, e.g., B. Allen and J.D. Romano, Phys. Rev. D **59**, 102001 (1999).
- [47] T. Damour and A. Vilenkin, gr-qc/0004075.

Published in Gravitational Radiation, eds. N. Deruelle  
& T. Piran (North Holland, Amsterdam, 1983) pp 1-57.

REF C  
QAP-647

THE THEORY OF GRAVITATIONAL RADIATION: AN INTRODUCTORY REVIEW\*

KIP S. THORNE

W. K. Kellogg Radiation Laboratory  
California Institute of Technology, Pasadena, California 91125  
and  
Institute for Theoretical Physics  
University of California, Santa Barbara, California 93106

ABSTRACT

This is the written version of lectures presented at the Workshop on Gravitational Radiation, Ecole d'Ete de Physique Theorique, Les Houches, France, June 1982.

These lectures are an introduction to and a progress report on the effort to bring gravitational-wave theory into a form suitable for astrophysical studies — a form for use in the future, when waves have been detected and are being interpreted.

Much of the viewpoint embodied in these lectures I have adopted or developed since 1972 when Misner, Wheeler, and I completed Gravitation. If I were rewriting the gravitational-wave parts of Gravitation today, I would do so along the lines of these lectures.

---

\*Supported in part by the National Science Foundation [AST79-22012 and PHY77-27084].

---

ONE OF THE ORANGE AID PREPRINT SERIES  
IN NUCLEAR, ATOMIC & THEORETICAL ASTROPHYSICS

September 1982



## TABLE OF CONTENTS

1. INTRODUCTION AND OVERVIEW
  - 1.1 The nature of these lectures
  - 1.2 What is a gravitational wave?
  - 1.3 Regions of space around a source of gravitational waves
  - 1.4 Organization of these lectures; Notation and conventions
  
2. THE PROPAGATION OF GRAVITATIONAL WAVES
  - 2.1 Gravitational waves in metric theories of gravity: Description and propagation speed
  - 2.2 Plane waves on a flat background in metric theories with  $c_{\text{GW}} = c_{\text{EM}}$ 
    - 2.2.1 Bianchi identities and dynamical degrees of freedom
    - 2.2.2 Local inertial frames (side remarks)
    - 2.2.3 Physical description of plane-wave polarizations
  - 2.3 Plane waves on a flat background in general relativity
    - 2.3.1 The gravitational-wave field  $h_{\text{jk}}^{\text{TT}}$
    - 2.3.2 Behavior of  $h_{\text{jk}}^{\text{TT}}$  under Lorentz transformations
    - 2.3.3 Relationship of  $h_{\text{jk}}^{\text{TT}}$  to Bondi news function
  - 2.4 Weak perturbations of curved spacetime in general relativity
    - 2.4.1 Metric perturbations and Einstein field equations
    - 2.4.2 Wave propagation on a curved vacuum background
    - 2.4.3 Absorption and dispersion of waves by matter
    - 2.4.4 Scattering of waves off background curvature, and tails of waves
    - 2.4.5 The stress-energy tensor for gravitational waves
  - 2.5 Wave propagation in the geometric optics limit
    - 2.5.1 Differential equations of geometric optics
    - 2.5.2 Solution of geometric optics equations in local wave zone
    - 2.5.3 Solution of geometric optics equations in distant wave zone
    - 2.5.4 Example: Propagation through a Friedmann universe
  - 2.6 Deviations from geometric optics
    - 2.6.1 Diffraction
    - 2.6.2 Nonlinear effects in wave propagation
  
3. THE GENERATION OF GRAVITATIONAL WAVES
  - 3.1 Foundations for multipole analyses
    - 3.1.1 Multipole moments of a stationary system in linearized general relativity
    - 3.1.2 Relation of STF tensors to spherical harmonics
    - 3.1.3 The Einstein equations in de Donder (harmonic) gauge
    - 3.1.4 Multipole moments of a fully relativistic, stationary system
  - 3.2 Gravitational wave generation by slow-motion sources:  $\lambda \gg L \gtrsim M$ 
    - 3.2.1 Metric in the weak-field near zone
    - 3.2.2 Metric in the induction zone and local wave zone
    - 3.2.3 Gravitational-wave field in local wave zone
    - 3.2.4 Slow-motion method of computing wave generation
    - 3.2.5 Example: Rigidly rotating neutron star
    - 3.2.6 Example: Compact binary system
    - 3.2.7 Example: Torsional oscillations of a neutron star
  - 3.3 Multipole decomposition of arbitrary waves in the local wave zone
    - 3.3.1 The radiation field
    - 3.3.2 The energy, momentum, and angular momentum carried by the waves
    - 3.3.3 Order-of-magnitude formulas

- 3.4 Radiation reaction in slow-motion sources
  - 3.4.1 Method of conservation laws
  - 3.4.2 Radiation reaction potential
  - 3.4.3 PN, P<sup>2</sup>N, and P<sup>2.5</sup>N iteration of the field equations
- 3.5 Gravitational-wave generation by fast-motion sources:  $\lambda \lesssim L$
- 4. THE DETECTION OF GRAVITATIONAL WAVES
  - 4.1 Detectors with size  $L \ll \lambda$ 
    - 4.1.1 The proper reference frame of an accelerated, rotating laboratory
    - 4.1.2 Examples of detectors
    - 4.1.3 Methods of analyzing detectors
    - 4.1.4 Resonant bar detectors
  - 4.2 Detectors with size  $L \gtrsim \lambda$
- 5. CONCLUSION

# 1. INTRODUCTION AND OVERVIEW

## 1.1 The nature of these lectures

These lectures are an introduction to and a progress report on the effort to bring gravitational-wave theory into a form suitable for astrophysical studies — a form for use in the future, when waves have been detected and are being interpreted. I will not describe all aspects of this effort. Several of the most important aspects will be covered by other lecturers, elsewhere in this volume. These include the computation of waves from models of specific astrophysical sources (lectures of Eardley); the techniques of numerical relativity — our only way of computing waves from high-speed, strong-gravity, large-amplitude sources (lectures of York and Piran); and a full analysis of radiation reaction and other relativistic effects in binary systems such as the binary pulsar — our sole source today of quantitative observational data on the effects of gravitational waves (lectures of Damour).

My own lectures will provide a sort of framework for those of Eardley, York and Piran, and Damour: I shall present the mathematical description of gravitational waves in a form suitable for astrophysical applications (§2); I shall describe a variety of methods for computing the gravitational waves emitted by astrophysical sources (§3); I shall describe methods for analyzing the propagation of waves from their sources, through our lumpy universe, to earth (§2); and I shall describe methods of analyzing the interaction of gravitational waves with earth-based and solar-system-based detectors (§4). Here and there in my lectures I shall sketch derivations of the methods of analysis and of the formulas presented; but in most places I shall simply refer the reader to derivations elsewhere in the literature and/or pose the derivations as exercises for the reader.

## 1.2 What is a gravitational wave?

A gravitational wave is a ripple in the curvature of spacetime, which propagates with the speed of light (Fig. 1). In the real universe gravitational waves propagate on the back of a large-scale, slowly changing spacetime curvature created by the universe's lumpy, cosmological distribution of matter. The background curvature is characterized, semiquantitatively, by two length scales

$$R \equiv \left( \begin{array}{l} \text{radius of curvature} \\ \text{of background spacetime} \end{array} \right) \equiv \left| \begin{array}{l} \text{typical component } R_{\hat{\alpha}\hat{\beta}\hat{\gamma}\hat{\delta}} \\ \text{tensor of background in a local Lorentz frame} \end{array} \right|^{-\frac{1}{2}},$$

$$L \equiv \left( \begin{array}{l} \text{inhomogeneity scale of} \\ \text{background curvature} \end{array} \right) \equiv \left( \begin{array}{l} \text{length scale on which} \\ R_{\hat{\alpha}\hat{\beta}\hat{\gamma}\hat{\delta}} \text{ varies} \end{array} \right) \lesssim R; \quad (1.1)$$

and the gravitational waves are characterized by one length scale

$$\lambda \equiv \left( \begin{array}{l} \text{reduced wavelength of} \\ \text{gravitational waves} \end{array} \right) = \frac{1}{2\pi} \times (\text{wavelength } \lambda). \quad (1.2)$$

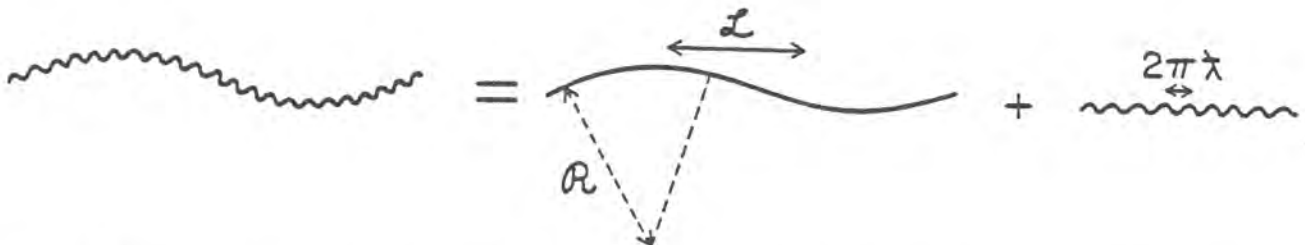


Fig. 1 A heuristic embedding diagram for the decomposition of curve spacetime into a background spacetime plus gravitational waves.

(Of course  $\lambda$ ,  $\mathcal{L}$ , and  $\mathcal{R}$  are not precisely defined; they depend on one's choice of coordinates or reference frame. But in typical astrophysical situations there are preferred frames - e.g. the "asymptotic rest frame" of the source of the waves, or the "mean local rest frame" of nearby galaxies; and these permit  $\lambda$ ,  $\mathcal{L}$ , and  $\mathcal{R}$  to be defined with adequate precision for astrophysical discussion.) The separation of spacetime curvature into a background part  $R_{\alpha\beta\gamma\delta}^{(B)}$  and a wave part  $R_{\alpha\beta\gamma\delta}^{(W)}$  depends critically on the inequality

$$\lambda \ll \mathcal{L}. \quad (1.3)$$

The waves are the part that varies on the lengthscale  $\lambda$ ; the background is the part that varies on the scale  $\mathcal{L}$ ; the separation is impossible if  $\lambda \sim \mathcal{L}$ . See Figure 1.

In constructing the theory of gravitational waves one typically expands the equations of general relativity in powers of  $\lambda/\mathcal{L}$  and  $\lambda/\mathcal{R}$ . In the real universe these expansions constitute perturbation theory of the background spacetime (these lectures and that of Yvonne Choquet). In an idealized universe consisting of a source surrounded by vacuum (so that  $\mathcal{L} \equiv r = \text{distance to source}$ ) these expansions constitute "asymptotic analyses of spacetime structure near future timelike infinity  $\mathcal{J}^+$ " (lectures of Martin Walker).

### 1.3 Regions of space around a source of gravitational waves

I shall characterize any source of gravitational waves, semiquantitatively, by the following length scales as measured in the source's "asymptotic rest frame":

$$L \equiv \left( \begin{array}{l} \text{size of} \\ \text{source} \end{array} \right) = \left( \begin{array}{l} \text{radius of region inside which the stress-energy } T^{\alpha\beta} \\ \text{and all black-hole horizons are contained} \end{array} \right),$$

$$2M \equiv \left( \begin{array}{l} \text{gravitational} \\ \text{radius of source} \end{array} \right) = \left( \begin{array}{l} 2 \times \text{mass of source in} \\ \text{units where } G = c = 1 \end{array} \right),$$

$$\lambda \equiv \left( \begin{array}{l} \text{reduced wavelength of the waves emitted} \end{array} \right), \quad (1.4)$$

$$\left. \begin{array}{l} r_I \equiv \left( \begin{array}{l} \text{inner radius of local wave zone} \end{array} \right) \\ r_O \equiv \left( \begin{array}{l} \text{outer radius of local wave zone} \end{array} \right) \end{array} \right\} \text{(see below).}$$

Corresponding to these length scales, I shall divide space around a source into the following regions (Fig. 2):

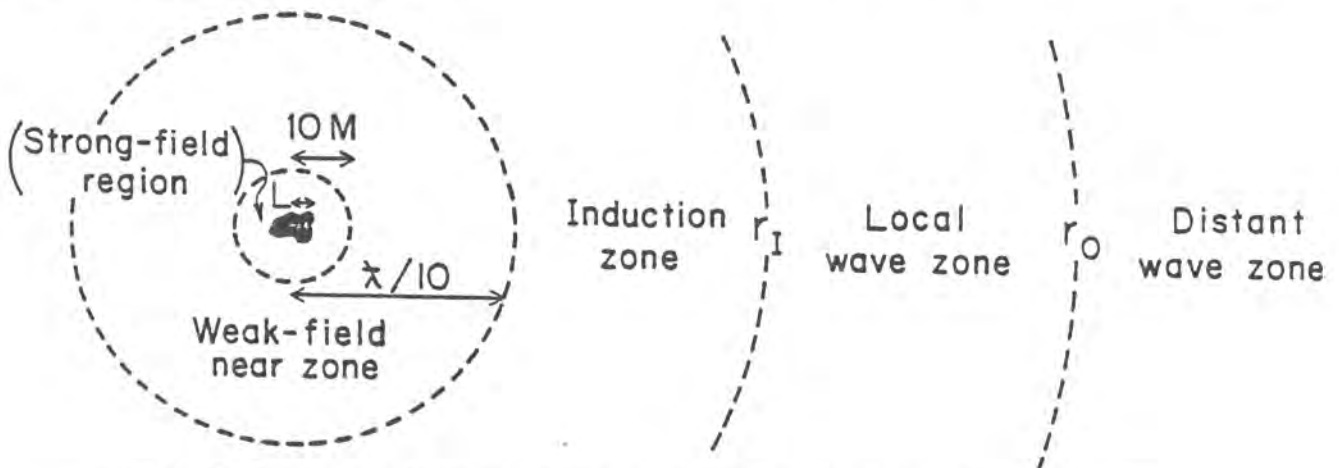


Fig. 2 Regions of space around a source of gravitational waves.



$$\begin{aligned}
\text{Source:} & \quad r \lesssim L, \\
\text{Strong-field region:} & \quad r \lesssim 10 M \text{ if } 10 M \gtrsim L, \\
& \quad \text{typically does not exist if } L \gg 10 M, \\
\text{Weak-field near zone:} & \quad L < r, 10 M < r < \lambda/10, \\
\text{Induction zone:} & \quad L < r, \lambda/10 < r < r_I \\
\text{Local wave zone:} & \quad r_I < r < r_0 \\
\text{Distant wave zone:} & \quad r_0 < r.
\end{aligned} \tag{1.5}$$

Although Figure 2 suggests the lengthscale ordering  $L < 10 M < \lambda/10$ , no such ordering will be assumed in these lectures. Thus, we might have  $\lambda \gg L$  and  $M$  ("slow-motion source"), or  $\lambda \ll L$  and  $M$  (high-frequency waves from some small piece of a big source; weak field near zone does not exist), or  $\lambda \sim L$  or  $M$ ; and we might have  $L \gg M$  or perhaps  $L \sim M$ .

At radius  $r$  outside the source ( $r > L$ ) the background curvature due to the source has lengthscales

$$R_s \approx (r^3/M)^{1/2}, \quad \lambda_s \approx r. \tag{1.6}$$

Consequently, the dynamically changing part of the curvature can be regarded as "gravitational waves" (i.e. has  $\lambda \ll \lambda_s$ ) only in the "wave zone"  $r \gg \lambda$ . I split the wave zone up into two parts, the local wave zone and the distant wave zone, so as to facilitate a clean separation of two mathematical problems: the generation of waves by the source, and the propagation of those waves through the lumpy, real universe to earth. The local wave zone ( $r_I \lesssim r \lesssim r_0$ ) will serve as a matching region for the two problems: the theory of wave generation will cover the local wave zone and all regions interior to it; the theory of wave propagation will cover the local wave zone and its exterior.

To facilitate the matching I shall choose  $r_I$  and  $r_0$  in such a manner that throughout the local wave zone the background curvature can be ignored and the background metric can thus be approximated as that of flat Minkowskii spacetime. More specifically, the inner edge of the local wave zone ( $r_I$ ) is the location at which one or more of the following effects becomes important: (i) the waves cease to be waves and become a near-zone field, i.e.,  $r$  becomes  $\lesssim \lambda$ ; (ii) the gravitational pull of the source produces a significant red shift, i.e.,  $r$  becomes  $\sim 2M =$  (Schwarzschild radius of source); (iii) the background curvature produced by the source distorts the wave fronts and backscatters the waves significantly, i.e.,  $(r^3/M)^{1/2}$  becomes  $\lesssim \lambda$ ; (iv) the outer limits of the source itself are encountered, i.e.,  $r$  becomes  $\lesssim L =$  (size of source). Thus, the inner edge of the local wave zone is given by

$$\begin{aligned}
r_I &= \alpha \times \max \{ \lambda, 2M, (M\lambda^2)^{1/3}, L \}, \\
\alpha &\equiv \left( \begin{array}{c} \text{some suitable number} \\ \text{large compared to unity} \end{array} \right).
\end{aligned} \tag{1.7}$$

The outer edge of the local wave zone  $r_0$  is the location at which one or more of the following effects becomes important: (i) a significant phase shift has been produced by the "M/r" gravitational field of the source, i.e.,  $(M/\lambda) \times \ln(r/r_I)$  is no longer  $\ll \pi$ ; (ii) the background curvature due to nearby masses or due to the external universe perturbs the propagation of the waves, i.e.,  $r$  is no longer  $\ll R_u =$  (background radius of curvature of universe). Thus, the outer edge of the local wave zone is given by

$$r_0 = \min[r_I \exp(\lambda/\beta M), R_u/\gamma], \quad (1.8)$$

$$\beta, \gamma = \left( \begin{array}{l} \text{some suitable numbers} \\ \text{large compared to unity} \end{array} \right).$$

Of course, we require that our large numbers  $\alpha, \beta, \gamma$  be adjusted so that the thickness of the local wave zone is very large compared to the reduced wavelength:

$$r_0 - r_I \gg \lambda. \quad (1.9)$$

In complex situations the location of the local wave zone might not be obvious. Consider, for example, a neutron star passing very near a supermassive black hole. The tidal pull of the hole sets the neutron star into oscillation, and the star's oscillations produce gravitational waves [Mashhoon (1973); Turner (1977)]. If the hole is large enough, or if the star is far enough from it, there may exist a local wave zone around the star which does not also enclose the entire hole. Of greater interest — because more radiation will be produced — is the case where the star is very near the hole and the hole is small enough ( $M_h \lesssim 100 M_\odot$ ) to produce large-amplitude oscillations, and perhaps even disrupt the star. In this case, before the waves can escape the influence of the star, they get perturbed by the background curvature of the hole. One must then consider the entire star-hole system as the source, and construct a local wave zone that surrounds them both.

\* \* \* \* \*

Exercise 1. Convince yourself that for all astrophysical sources except the big-bang singularity (e.g., for the neutron-star/black-hole source of the last paragraph)  $\alpha, \beta$ , and  $\gamma$  can be so chosen as to make condition (1.9) true.

#### 1.4 Organization of these lectures; Notation and conventions

Section 2 of these lectures will discuss the propagation of gravitational waves from the local wave zone out through our lumpy universe to the earth. Section 3 will discuss the generation of gravitational waves, including their propagation into the local wave zone where they can be matched onto the propagation theory of Section 2. Section 4 will discuss the detection of gravitational waves on earth and in the solar system.

My notation and conventions are those of Misner, Thorne, and Wheeler (1973) (cited henceforth as "MTW"): I use geometrized units ( $c = G = 1$ ); Greek indices range from 0 to 3 (time and space), Latin indices from 1 to 3 (space only); the metric signature is +2;  $\eta_{\alpha\beta} \equiv \text{diag}(-1, 1, 1, 1)$  is the Minkowski metric;  $\epsilon_{\alpha\beta\gamma\delta}$  and  $\epsilon_{ijk}$  are the spacetime and space Levi-Civita tensors with  $\epsilon_{0123} > 0$  in a right-hand-oriented basis; and the signs of the Riemann, Ricci, Einstein, and stress-energy tensors are given by

$$\begin{aligned} R^\alpha_{\beta\gamma\delta} &= \Gamma^\alpha_{\beta\delta,\gamma} - \Gamma^\alpha_{\beta\gamma,\delta} + \text{"IT"} - \text{"IT"}, & R_{\alpha\beta} &\equiv R^\mu_{\alpha\mu\beta}, \\ G_{\alpha\beta} &\equiv R_{\alpha\beta} - \frac{1}{2} R g_{\alpha\beta} = 8\pi T_{\alpha\beta}, & T^{00} &> 0. \end{aligned} \quad (1.10)$$

Much of the viewpoint embodied in these lectures I have adopted or developed since 1972 when Misner, Wheeler and I completed MTW. However, many of the new aspects of my viewpoint are contained in my 1975 Erice lectures (Thorne 1977) and/or in a recent Reviews of Modern Physics article (Thorne 1980a; cited henceforth as "RMP").

## 2. THE PROPAGATION OF GRAVITATIONAL WAVES

### 2.1 Gravitational waves in metric theories of gravity: Description and propagation speed

Gravitational waves are not unique to Einstein's theory of gravity. They must exist in any theory which incorporates some sort of local Lorentz invariance into its gravitational laws. Many such theories have been invented; see, e.g., Will (1982) for examples and references.

Among the alternative theories of gravity there is a wide class - the so-called "metric theories" - whose members are so similar to general relativity that a discussion of their gravitational waves brings the waves of Einstein's theory into clearer perspective. Thus, I shall initiate my discussion of wave propagation within the framework of an arbitrary metric theory, and then shall specialize to Einstein's general relativity.

A metric theory of gravity is a theory (i) in which gravity is characterized, at least in part, by a 4-dimensional, symmetric spacetime metric  $g_{\alpha\beta}$  of signature +2; and (ii) in which the Einstein equivalence principle is satisfied - i.e., all the nongravitational laws of physics take on their standard special relativistic forms in the local Lorentz frames of  $g_{\alpha\beta}$  (aside from familiar complications of "curvature coupling"; chapter 16 of MTW).

Examples of metric theories are: general relativity [ $g_{\alpha\beta}$  is the sole gravitational field]; the Dicke-Brans-Jordan theory (e.g., Dicke 1964) [contains a scalar gravitational field  $\phi$  in addition to  $g_{\alpha\beta}$ ; matter generates  $\phi$  via a curved-spacetime wave equation; then  $\phi$  and the matter jointly generate  $g_{\alpha\beta}$  via Einstein-like field equations]; and Rosen's (1973) theory [a "bimetric" theory with a flat metric  $\eta_{\alpha\beta}$  in addition to the physical metric  $g_{\alpha\beta}$ ; the matter generates  $g_{\alpha\beta}$  via a flat-spacetime wave equation whose characteristics are null lines of  $\eta_{\alpha\beta}$ ]. See Will (1982) for further details, references, and other examples.

The Einstein equivalence principle guarantees that in any metric theory, as in general relativity, freely falling test particles move along geodesics of  $g_{\alpha\beta}$ , and that the separation vector  $\xi^\alpha$  between two nearby test particles (separation  $\ll \lambda$ ) is governed by the equation of geodesic deviation:

$$D^2 \xi^\alpha / d\tau^2 + R^\alpha_{\beta\gamma\delta} u^\beta \xi^\gamma u^\delta = 0. \quad (2.1a)$$

Here  $u^\alpha$  is the 4-velocity of one of the test particles;  $\tau$  is proper time measured by that particle;

$$D^2 \xi^\alpha / d\tau^2 \equiv (\xi^\alpha_{;\beta} u^\beta)_{;\gamma} u^\gamma \quad (2.1b)$$

is the relative acceleration of the particles; and  $R^\alpha_{\beta\gamma\delta}$  is the Riemann curvature tensor associated with  $g_{\alpha\beta}$ . Throughout Sections 2 (wave propagation) and 3 (wave generation) I shall use geodesic deviation and the Riemann tensor to characterize the physical effects of gravitational waves. Only in Section 4 (wave detection) will I discuss other physical effects of waves.

The Riemann tensor  $R_{\alpha\beta\gamma\delta}$  contains two parts: background curvature and wave curvature

$$R_{\alpha\beta\gamma\delta} = R^{(B)}_{\alpha\beta\gamma\delta} + R^{(W)}_{\alpha\beta\gamma\delta}. \quad (2.2)$$

As discussed in §1.2  $R^{(B)}_{\alpha\beta\gamma\delta}$  varies on a long lengthscale  $\mathcal{L}$ , while  $R^{(W)}_{\alpha\beta\gamma\delta}$  varies on a short lengthscale  $\lambda$ . Consequently, if by  $\langle \rangle$  we denote an average over spacetime regions somewhat larger than  $\lambda$  but much smaller than  $\mathcal{L}$  ("Brill-Hartle average";

Exercise 35.14 of MTW), then we can write

$$R_{\alpha\beta\gamma\delta}^{(B)} \equiv \langle R_{\alpha\beta\gamma\delta} \rangle, \quad R_{\alpha\beta\gamma\delta}^{(W)} \equiv R_{\alpha\beta\gamma\delta} - \langle R_{\alpha\beta\gamma\delta} \rangle. \quad (2.3a)$$

Similarly we can define the background metric, of which  $R_{\alpha\beta\gamma\delta}^{(B)}$  is the Riemann tensor, by

$$g_{\alpha\beta}^{(B)} \equiv \langle g_{\alpha\beta} \rangle. \quad (2.3b)$$

[For a discussion of delicacies which require the use of "steady coordinates" in the averaging of  $g_{\alpha\beta}$  see Isaacson (1968), or more briefly §35.13 of MTW.]

In general relativity and in the Dicke-Brans-Jordan theory gravitational waves propagating through vacuum are governed by the wave equation

$$R_{\alpha\beta\gamma\delta}^{(W)} |_{\mu\nu} g^{\mu\nu} = 0, \quad (2.4)$$

whereas in Rosen's theory they are governed by

$$R_{\alpha\beta\gamma\delta, \mu\nu} \eta^{\mu\nu} = 0. \quad (2.5)$$

Here " $|$ " denotes covariant derivative with respect to  $g^{\mu\nu}_{(B)}$  while " $,$ " denotes covariant derivative with respect to the flat metric  $\eta^{\mu\nu}$ . These equations imply that in general relativity and in Dicke-Brans-Jordan theory gravitational waves propagate through vacuum with precisely the speed of light,  $c_{GW} = c_{EM}$ , but in Rosen's theory they propagate with a different speed,  $c_{GW} \neq c_{EM}$ . As a rough rule of thumb, whenever a theory of gravity possesses "prior geometry" such as a flat auxiliary metric (MTW, §17.6), it will have  $c_{GW} \neq c_{EM}$ ; often when there is no prior geometry,  $c_{GW} = c_{EM}$ .

High-precision experiments to test  $c_{GW} = c_{EM}$  will be possible if and when electromagnetic waves and gravitational waves are observed from outbursts in the same distant source. For example, for a supernova in the Virgo cluster of galaxies (about  $4 \times 10^7$  light years from earth; distance at which several supernovae are seen each year) one can hope to discover the light outburst within one day (of retarded time) after the explosion is triggered by gravitational collapse. If gravitational waves from the collapse are observed, then a test is possible with precision

$$\left| \frac{\Delta c}{c} \right| = \left| \frac{c_{GW} - c_{EM}}{c} \right| \sim \frac{1 \text{ day}}{4 \times 10^7 \text{ yr}} \simeq 1 \times 10^{-10}. \quad (2.6)$$

Actually, there already exists strong observational evidence that gravitational waves do not propagate more slowly than light. If they did, then high-energy cosmic rays with speeds  $v$  in the range  $c_{GW} < v < c_{EM}$  would emit gravitational Cerenkov radiation very efficiently and would be slowed quickly by gravitational radiation reaction to  $v = c_{GW}$ . Since cosmic rays are actually detected with  $v$  as large as  $c_{EM} \times (1 - 10^{-18})$ ,  $c_{GW}$  presumably is no smaller than this. (For further details and for a discussion of whether we really understand gravitational Cerenkov radiation in alternative theories of gravity see Caves (1980); also earlier work by Aichelburg, Ecker, and Sexl (1971).

## 2.2 Plane waves on a flat background in metric theories with $c_{GW} = c_{EM}$

Henceforth I shall restrict attention either to metric theories that have  $c_{GW} = c_{EM}$  always (e.g., general relativity and Dicke-Brans-Jordan); or, for theor-

ies like Rosen's, to regions of spacetime where  $c_{GW}$  happens to equal  $c_{EM}$ .

In this section and the next several, I shall make a further restriction to spacetime regions of size  $\ll \mathcal{R}$  (but  $\gg \lambda$ ). In such regions with good accuracy I can ignore the curvature of the background; i.e., I can and will introduce global Lorentz frames of the background metric, in which

$$g_{\alpha\beta}^{(B)} = \eta_{\alpha\beta} . \quad (2.7)$$

Far from their source gravitational waves will have wave fronts with radii of curvature large compared to  $\lambda$ , i.e., they will be locally plane fronted. Thus, with good accuracy I can and shall approximate  $R_{\alpha\beta\gamma\delta}^{(W)} = R_{\alpha\beta\gamma\delta}$  as precisely plane fronted; and by correctly orienting my spatial axes I shall make the waves propagate in the  $x^3 = z$  direction. Since they propagate with the speed of light, the waves are then functions of  $t - z$ :

$$R_{\alpha\beta\gamma\delta} = R_{\alpha\beta\gamma\delta}(t-z) . \quad (2.8)$$

The analysis of such waves in arbitrary metric theories of gravity, as described below, is due to Eardley, Lee, Lightman, Wagoner, and Will (1973), cited henceforth as ELLWW. For greater detail see Eardley, Lee, and Lightman (1973).

### 2.2.1 Bianchi identities and dynamical degrees of freedom

Because the Riemann tensor of any metric theory is derivable from a metric  $g_{\alpha\beta}$ , it must satisfy the Bianchi identities  $R_{\alpha\beta}[\gamma\delta;\epsilon] = 0$ . For the plane-wave Riemann tensor (2.8) on a flat background (2.7) the total content of the Bianchi identities is

$$\begin{aligned} R_{\alpha\beta 12,0} = 0 & \Rightarrow R_{\alpha\beta 12} = 0 , \\ R_{\alpha\beta 13,0} - R_{\alpha\beta 10,3} = 0 & \Rightarrow R_{\alpha\beta 13} = -R_{\alpha\beta 10} , \\ R_{\alpha\beta 23,0} - R_{\alpha\beta 20,3} = 0 & \Rightarrow R_{\alpha\beta 23} = -R_{\alpha\beta 20} . \end{aligned} \quad (2.9)$$

Recalling the pair-wise symmetry  $R_{\mu\nu\alpha\beta} = R_{\alpha\beta\mu\nu}$  we see from (2.9) that any purely spatial pair of indices (12 or 13 or 23) either vanishes or can be converted into a space-time pair (10 or 20 or 30). This means that the six quantities

$$R_{i0j0}(t-z) = R_{j0i0}(t-z) \quad (2.10)$$

are a complete set of independent components of our plane-wave Riemann tensor. All other components of Riemann can be expressed algebraically in terms of these.

In a general metric theory of gravity these six quantities represent six independent degrees of freedom of the gravitational field - i.e., six independent polarizations of a gravitational wave.

In the special case of general relativity a vacuum gravitational wave must have vanishing Ricci tensor

$$R_{\mu\nu} = R^{\alpha}{}_{\mu\alpha\nu} = 0 \quad (2.11)$$

(Einstein field equations). One can show easily that this reduces the number of independent degrees of freedom from six to two:

$$R_{x0x0} = -R_{y0y0} \quad \text{and} \quad R_{x0y0} = R_{y0x0} . \quad (2.12)$$

\* \* \* \* \*

Exercise 2. Show that the Bianchi identities for a plane wave on a flat background imply equations (2.9) and that they, in turn, guarantee that  $R_{i0j0}$  are a complete set of independent components of the Riemann tensor.

Exercise 3. Show that the vacuum Einstein field equations (2.11) reduce the independent plane-wave components of Riemann to (2.12).

### 2.2.2 Local inertial frames (side remarks)

In the next section I shall use geodesic deviation to elucidate the physical nature of the six gravity-wave polarizations. But as a foundation for that discussion I must first remind you of the mathematical and physical details of local inertial frames (LIF); see, e.g., §§8.6, 11.6, and 13.6 of MTW.

Physically an LIF is the closest thing to a global inertial frame that an experimenter can construct. The central building block of an LIF is a freely falling test particle ("fiducial particle"), which carries with itself three orthogonally pointing gyroscopes. The experimenter attaches a Cartesian coordinate grid to the gyroscopes. Because of spacetime curvature, this grid cannot be precisely Cartesian; but deviations from Cartesian structure can be made second order in the spatial distance  $r$  from the fiducial particle:

$$g_{\alpha\beta} = \eta_{\alpha\beta} + O(r^2 R_{\mu\nu\rho\sigma}) . \quad (2.13)$$

From an experimental viewpoint the details of the  $O(r^2 R_{\mu\nu\rho\sigma})$  corrections often are unimportant. Those corrections actually produce geodesic deviation, if one calculates geodesics directly from  $g_{\alpha\beta}$ ; but geodesic deviation is more clearly described as the effect of  $R_{\mu\nu\rho\sigma}$  in the geodesic deviation equation (2.1a), which now reads for a test particle at spatial location  $x^j = \xi^j =$  (separation from fiducial test particle) and, as always in geodesic deviation, with velocity  $|dx^j/dt| \ll 1$ :

$$d^2 x^j / dt^2 = -R_{j0k0} x^k . \quad (2.14)$$

It is this "experimenter's version" of geodesic deviation to which I shall appeal in discussing gravitational waves.

\* \* \* \* \*

Exercise 4. Show that in an LIF with metric (2.13) the fiducial particle (at rest at the spatial origin) moves along a geodesic. Show further that if  $\xi^j = x^j$  is the separation vector between the fiducial test particle and another test particle, the equation of geodesic deviation (2.1a) takes on the form (2.14).

Exercise 5. One realization of an LIF is a "Fermi normal coordinate system" obtained by letting the spatial coordinate axes be spacelike geodesics that start out along the directions of the three gyroscopes. Show that in such a coordinate system

$$ds^2 = -dt^2 (1 + R_{0l0m} x^l x^m) dt^2 - \frac{4}{3} R_{0l0m} x^l x^m dt dx^j + (\delta_{ij} - \frac{1}{3} R_{iljm} x^l x^m) dx^i dx^j . \quad (2.15)$$

For details see, e.g., §13.6 of MTW.

Exercise 6. Show that in the de Donder gauge of §3.1.3 below and in the vacuum of general relativity a mathematical realization of an LIF is

$$ds^2 = -dt^2(1 + R_{0l0m} x^l x^m) dt^2 - \frac{4}{3} R_{0ljm} x^l x^m dt dx^j + \delta_{ij}(1 - R_{0l0m} x^l x^m) dx^i dx^j. \quad (2.16)$$

(Note: neither this nor (2.15) requires any assumption of a plane-wave Riemann tensor.) For details see, e.g., Hartle and Thorne (1983).

### 2.2.3 Physical description of plane-wave polarizations

Consider a cloud of test particles surrounding a central, fiducial test particle. Initially the cloud resides in flat spacetime, all its particles are at rest with respect to each other, and its shape is precisely spherical with radius  $a$ . Then a gravitational wave hits and deforms the cloud. The deformations can be analyzed using the equation of geodesic deviation only if the cloud is small compared to the inhomogeneity scale of the Riemann tensor,  $a \ll \lambda$ . Assume this to be the case, and analyze the cloud's deformations in the LIF of the fiducial particle:

$$d^2 x^j / dt^2 = -R_{j0k0}(t) x^k. \quad (2.17)$$

Here  $x^j(t)$  is the location, in the LIF, of some specific test particle at time  $t$ ; and  $R_{j0k0}(t-z)$  is evaluated at the fiducial particle's location  $(x, y, z) = 0$ . Consider, in turn, and with the help of Figure 3, the six independent polarizations of the wave (further details in ELLWW):

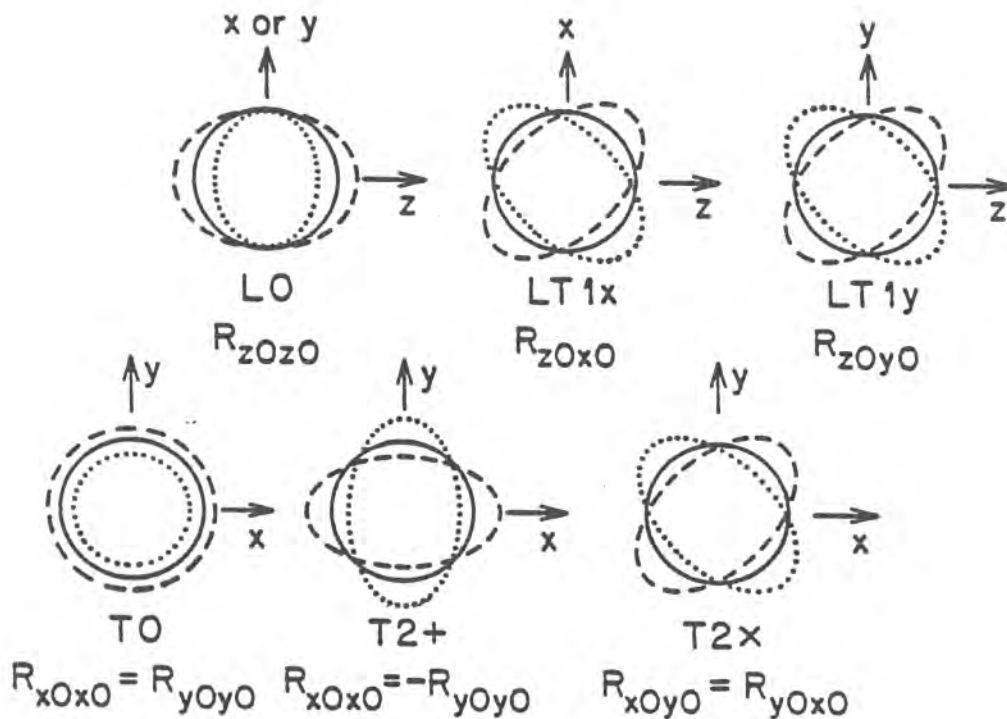


Fig. 3. The deformations of a sphere of test particles produced by gravitational waves with each of six polarizations. As the wave oscillates, the sphere (solid) first gets deformed in the manner shown dashed; then in the manner shown dotted.

$R_{z0z0}$  produces deformations

$$\ddot{x} = 0, \ddot{y} = 0, \ddot{z} = -R_{z0z0}z. \quad (2.18a)$$

As  $R_{z0z0}(t)$  alternately oscillates negative and positive this expands and then squeezes the sphere longitudinally (i.e., along the direction of wave propagation,  $z$ ), while leaving its transverse cross section unchanged. In this sense the wave is "purely longitudinal". At any moment of time the deformed sphere is invariant under rotations about the propagation direction  $\vec{e}_z$ . This means, in the language of "canonical field theory", that the wave has "spin zero" (or "helicity zero"). These properties are summarized by saying that the wave is "LO" (longitudinal and spin zero).

$R_{z0x0} = R_{x0z0}$  produces deformations

$$\ddot{x} = -R_{x0z0}z, \ddot{y} = 0, \ddot{z} = -R_{x0z0}x. \quad (2.18b)$$

As  $R_{x0z0}(t)$  oscillates this expands and then squeezes the sphere at a 45 degree angle to  $\vec{e}_z$  in the "logitudinal-transverse"  $z$ - $x$  plane, while leaving it undeformed in the  $y$  direction. At any moment the deformed sphere is invariant under a  $360^\circ$  rotation about the propagation direction, a property that it shares with the electric or magnetic field of an electromagnetic wave. Thus, this gravitational wave like an electromagnetic wave has spin one - but whereas the electromagnetic wave is "T1" (transverse, spin one), this gravitational wave is "LT1" (longitudinal-transverse, spin one).

$R_{z0y0} = R_{y0z0}$  produces deformations

$$\ddot{x} = 0, \ddot{y} = -R_{y0z0}z, \ddot{z} = -R_{y0z0}y, \quad (2.18c)$$

and is thus also "LT1". It is the LT1 polarization orthogonal to  $R_{z0x0}$ .

A wave with  $R_{x0x0} = R_{y0y0}$  and all other  $R_{j0k0}$  zero produces deformations

$$\ddot{x} = R_{x0x0}x, \ddot{y} = R_{x0x0}y, \ddot{z} = 0. \quad (2.18d)$$

This wave alternately expands and compresses the sphere in the transverse plane while leaving it transversely circular and leaving it totally unchanged in the longitudinal direction. Thus, this wave is T0 ("transverse, spin-zero").

A wave with  $R_{x0x0} = -R_{y0y0}$  and all other  $R_{j0k0}$  zero produces deformations

$$\ddot{x} = -R_{x0x0}x, \ddot{y} = +R_{x0x0}y, \ddot{z} = 0. \quad (2.18e)$$

As  $R_{x0x0}(t)$  oscillates this wave expands the sphere in the  $x$  direction and squeezes it in  $y$ , then expands it in  $y$  and squeezes it in  $x$ . Thus the deformations are purely transverse, and at any moment the deformed sphere is invariant under a  $180^\circ$  rotation about the propagation direction. The "spin" ("helicity")  $S$  of any wave which propagates with the speed of light is determined by the angle  $\Theta$  of rotations about the propagation direction that leave all momentary physical effects of the wave unchanged:

$$S = 360^\circ / \Theta.$$

Thus, this wave has spin  $S = 2$ , i.e., it is a T2 ("transverse, spin 2) wave. The orientation of the polarization is identified as "+" ( $x$  and  $y$ ; horizontal and



vertical).

$R_{x_0y_0} = R_{y_0x_0}$  produces deformations

$$\ddot{x} = R_{x_0y_0} \ddot{y}, \quad \ddot{y} = R_{x_0y_0} \ddot{x}, \quad \ddot{z} = 0 \quad (2.18f)$$

which are also T2; but the orientation of the polarization is "X". This is the T2 wave orthogonal to "+".

That the spin 0 waves have just one polarization state while the spin 1 and spin 2 waves each have two orthogonal polarization states is familiar both from quantum mechanics and from canonical, classical field theory. It is a consequence of the fact that the waves propagate with the speed of light - i.e., their quanta have zero rest mass.

This familiar feature is deceptively reassuring. Actually, a nasty surprise awaits us if we try to check the fundamental tenet of canonical field theory that the spin of a wave must be Lorentz invariant. If we begin in one Lorentz frame with a gravitational wave that is pure T0 or pure T2, we will find it to be pure T0 or pure T2 in all other Lorentz frames. However, if we begin with a pure LT1 wave in one frame, we will find a mixture of LT1, T0, and T2 in other frames; and if we begin with pure L0 in one frame, we will find a mixture of L0, LT1, T0, and T2 in other frames. See Eardley, Lee, and Lightman (1973) for proofs.

This means that any metric theory of gravity possessing L0 or LT1 waves violates the tenets of canonical field theory and cannot be quantized by canonical methods, even in the weak-gravity limit. Rosen's theory is an example (in the special case  $c_{GW} = c_{EM}$  to which our discussion applies; when  $c_{GW} \neq c_{EM}$  there exist eight polarizations, not six [C. M. Caves, private communication]). By contrast, metric theories with purely transverse, speed-of-light gravity waves obey the canonical tenets and are quantizable by canonical means, at least in the weak-gravity limit. Examples are general relativity which has pure T2 waves (Exercise 3 above) and the Dicke-Brans-Jordan theory which has both T2 waves and T0 waves.

\* \* \* \* \*

Exercise 7. Verify the claims made above about the behavior of polarization states under Lorentz transformations. (See Eardley, Lee, and Lightman 1973 for solution.)

## 2.3 Plane waves on a flat background in general relativity

### 2.3.1 The gravitational-wave field $h_{jk}^{TT}$

Specialize now and henceforth to general relativity. Then a plane wave on a flat background has precisely two orthogonal polarization states: T2+ and T2X (denoted simply "+" and "X" henceforth).

Choose a specific Lorentz frame of the flat background space, and in that frame define a "gravitational-wave field"  $h_{jk}^{TT}$  by

$$R_{j_0k_0}(t-z) = -\frac{1}{2} h_{jk,tt}^{TT} \quad (2.19)$$

with  $h_{jk}^{TT} = 0$  before any waves ever arrive. Then the waves are fully characterized equally well by  $R_{j_0k_0}$  or by  $h_{jk}^{TT}$ . Note that the only nonzero components of  $h_{jk}^{TT}$  are

$$h_{xx}^{TT} = -h_{yy}^{TT} \equiv A_+(t-z), \quad h_{xy}^{TT} = h_{yx}^{TT} = A_X(t-z), \quad (2.20)$$

$A_+$  being the "amplitude function" for the + polarization state and  $A_\times$  being that for the  $\times$  state. Note that  $h_{jk}^{TT}$  is purely spatial, symmetric, transverse to the propagation direction  $\vec{n} = \vec{e}_z$ , and also traceless (hence the TT superscript)

$$h_{jk}^{TT} = h_{kj}^{TT}, \quad h_{jk}^{TT} n^k = 0, \quad \delta^{jk} h_{jk}^{TT} = 0. \quad (2.21)$$

Note further that the experimenter's version of the equation of geodesic deviation (eq. 2.17) can be integrated to give

$$\delta x^j = \frac{1}{2} h_{jk}^{TT} x^k \quad (2.22)$$

for the change in location, in an LIF, of a test particle initially at  $x^k$ . This equation suggests the common interpretation of  $h_{jk}^{TT}$  as a "dimensionless strain of space".

### 2.3.2 Behavior of $h_{jk}^{TT}$ under Lorentz transformations

A single gravitational wave is described, in different Lorentz frames of the flat background, by different  $h_{jk}^{TT}$  fields, each one purely spatial and TT in its own frame. How are these gravitational-wave fields related to each other? I shall state the answer in this section, leaving the proof as an exercise for the reader.

Begin in some fiducial background Lorentz frame, in which  $h_{jk}^{TT}$  is described by equations (2.20) above. Define

$$\psi \equiv t - z = \text{"retarded time"}, \quad (2.23a)$$

regard  $\psi$  as a scalar field in spacetime (a sort of "phase function" for the wave), and regard the amplitude functions  $A_+$  and  $A_\times$  of equations (2.20) as scalar fields which are known functions of  $\psi$ . From the scalar field  $\psi$  construct the "propagation vector"

$$\vec{k} \equiv -\vec{\nabla}\psi, \quad \text{so } k^0 = k^z = 1, \quad k^x = k^y = 0 \text{ in fiducial frame.} \quad (2.23b)$$

This propagation vector and the basis vector  $\vec{e}_x$ , which determines the orientations of the + and  $\times$  polarization states, together define a "fiducial 2-flat" (plane)

$$\vec{f} \equiv \vec{k} \wedge \vec{e}_x \equiv (2\text{-flat spanned by } \vec{k} \text{ and } \vec{e}_x). \quad (2.23c)$$

Now choose some other background Lorentz frame with 4-velocity  $\vec{u}'$ . In that frame define basis vectors

$$\begin{aligned} \vec{e}_{0'} &\equiv \vec{u}', & \vec{e}_{z'} &\equiv \left[ \begin{array}{l} \text{unit vector obtained by projecting } \vec{k} \\ \text{orthogonal to } \vec{u}' \text{ and renormalizing} \end{array} \right], \\ \vec{e}_{x'} &\equiv \left[ \begin{array}{l} \text{unit vector lying in } \vec{f} \text{ and orthogonal to } \vec{u}' \end{array} \right], \\ \vec{e}_{y'} &\equiv \left[ \begin{array}{l} \text{unit vector such that } \vec{e}_{0'}, \vec{e}_{x'}, \vec{e}_{y'}, \vec{e}_{z'} \\ \text{are a right-hand oriented, orthonormal frame} \end{array} \right]. \end{aligned} \quad (2.24a)$$

Then in this basis the gravitational-wave field has components

$$h'_{x'x'}{}^{TT} = -h'_{y'y'}{}^{TT} = A_+(\psi), \quad h'_{x'y'}{}^{TT} = h'_{y'x'}{}^{TT} = A_\times(\psi), \quad (2.24b)$$

where  $A_+$  and  $A_\times$  are the same scalar fields as describe the waves in the fiducial

frame. Note, however, that  $\psi$  is not  $t'-z'$ ; rather, it differs from  $t'-z'$  by the standard doppler-shift factor:

$$\psi = t-z = (v'/v)(t'-z'), \quad (2.24c)$$

$$\frac{v'}{v} = \left[ \begin{array}{l} \text{ratio of frequencies of photons, propagating in } \vec{k} \text{ direction,} \\ \text{as measured in the two reference frames} \end{array} \right].$$

Thus, under a Lorentz transformation the gravitational-wave frequencies get doppler shifted just like those of light, but the amplitude functions are left unchanged and the polarization directions change only by a projection that keeps them spatial (eq. 2.24a for  $\vec{e}_x$ ). The fact, that  $h_{jk}^{TT}$  is a "spin-2" quantity with amplitude functions  $A_+$  and  $A_\times$  that are Lorentz invariant is embodied in the statement that " $A_+ + iA_\times$  has spin-weight 2 and boost-weight 0" [language of Geroch, Held, and Penrose (1973);  $i \equiv \sqrt{-1}$ ].

It is often convenient to define polarization tensors

$$\vec{e}_+^{\leftrightarrow} \equiv \vec{e}_x \otimes \vec{e}_x - \vec{e}_y \otimes \vec{e}_y, \quad \vec{e}_\times^{\leftrightarrow} \equiv \vec{e}_x \otimes \vec{e}_y + \vec{e}_y \otimes \vec{e}_x, \quad (2.24d)$$

and to rewrite equations (2.24b) as

$$h^{\leftrightarrow TT} = A_+(\psi) \vec{e}_+^{\leftrightarrow} + A_\times(\psi) \vec{e}_\times^{\leftrightarrow}. \quad (2.24e)$$

Another useful relation is

$$R_{\alpha'\beta'\gamma'\delta'} = \frac{1}{2} \left( \ddot{h}^{\leftrightarrow TT}_{\gamma'\delta'} k_{\beta'} k_{\gamma'} + \ddot{h}^{\leftrightarrow TT}_{\beta'\gamma'} k_{\alpha'} k_{\delta'} - \ddot{h}^{\leftrightarrow TT}_{\beta'\delta'} k_{\alpha'} k_{\gamma'} - \ddot{h}^{\leftrightarrow TT}_{\alpha'\gamma'} k_{\beta'} k_{\delta'} \right), \quad (2.24f)$$

where  $\dot{\phantom{x}} = d/d\psi$ .

\* \* \* \* \*

**Exercise 8.** Show that in the fiducial frame of this section, equation (2.19) is equivalent to  $R_{j0k0} = -(1/2)\dot{h}_{jk}^{TT} k_0 k_0$  where the dot means  $d/d\psi$ . Show further that in the fiducial frame the full Riemann tensor is given by equation (2.24f) without the primes. (Hint: use equations 2.9).

**Exercise 9.** Show that the Riemann tensor of (2.24f) with the primes and with  $h_{\alpha'\gamma'}^{TT}$  given by (2.24a,b) is obtained from that of Exercise 8 (no primes) by a standard Lorentz transformation. Convince yourself that this fully justifies the claimed behavior of  $h_{jk}^{TT}$  under a change of frames (eqs. 2.24a,b).

### 2.3.3 Relationship of $h_{jk}^{TT}$ to Bondi news function

Consider gravitational waves propagating radially outward from a source, and approximate the background as flat. Introduce spherical polar coordinates and denote the associated orthonormal basis vectors by,

$$\vec{e}_{\hat{r}} = \partial/\partial r, \quad \vec{e}_{\hat{\theta}} = r^{-1}\partial/\partial\theta, \quad \vec{e}_{\hat{\phi}} = (r \sin\theta)^{-1}\partial/\partial\phi. \quad (2.25a)$$

Let  $\vec{e}_{\hat{\theta}}$  be the fiducial direction (analog of  $\vec{e}_x$  above) used in defining the polarization base states, so that

$$\vec{e}_+^{\leftrightarrow} = \vec{e}_{\hat{\theta}} \otimes \vec{e}_{\hat{\theta}} - \vec{e}_{\hat{\phi}} \otimes \vec{e}_{\hat{\phi}}, \quad \vec{e}_\times^{\leftrightarrow} = \vec{e}_{\hat{\theta}} \otimes \vec{e}_{\hat{\phi}} + \vec{e}_{\hat{\phi}} \otimes \vec{e}_{\hat{\theta}}; \quad (2.25b)$$

$$h_{jk}^{TT} = A_+ \hat{e}_+^{\leftrightarrow} + A_\times \hat{e}_\times^{\leftrightarrow} . \quad (2.25c)$$

Because the wave fronts are spherical (though very nearly plane on length scales  $\lambda \ll r$ ),  $A_+$  and  $A_\times$  die out as  $1/r$  (Exercise 14 below)

$$A_+ = r^{-1} F_+(\psi; \theta, \varphi), \quad A_\times = r^{-1} F_\times(\psi; \theta, \varphi), \quad \psi = t - r. \quad (2.25d)$$

In gravitational-wave studies near "future timelike infinity"  $\mathcal{I}^+$ , mathematical physicists often use instead of  $h_{jk}^{TT}$  a different description of the waves due to Bondi, van der Burg, and Metzner (1962) and to Sachs (1962): The role of the gravitational-wave amplitude is played by the "Bondi News Function"

$$N \equiv \frac{1}{2} \frac{\partial}{\partial t} (F_+ + i F_\times) = \frac{1}{2} r \frac{\partial}{\partial t} (A_+ + i A_\times), \quad (2.26a)$$

where  $i \equiv \sqrt{-1}$ . This complex News function has the advantage of depending only on angles  $\theta$ ,  $\varphi$ , and retarded time  $\psi$  ( $1/r$  dependence factored out); but for this it pays the price of not being a scalar field. In the language of Geroch, Held, and Penrose, it has "boost weight 2", whereas  $A_+ + i A_\times$  has "boost weight 0". It is conventional in the Bondi-Sachs formalism to introduce the complex vector

$$\vec{m} = (1/\sqrt{2}) (\hat{e}_{\hat{\theta}} - i \hat{e}_{\hat{\varphi}}). \quad (2.26b)$$

In terms of  $N$  and  $\vec{m}$  the gravitational-wave field is

$$\frac{\partial}{\partial t} h_{jk}^{TT} = \text{Real} \left\{ \frac{4N}{r} \bar{m}_j \bar{m}_k \right\}. \quad (2.26c)$$

Several lecturers in this volume will use the Bondi-Sachs formalism (e.g., M. Walker, A. Ashtekar, and R. Isaacson).

## 2.4 Weak perturbations of curved spacetime in general relativity

### 2.4.1 Metric perturbations and Einstein field equations

Abandon, now, the approximation that the background spacetime is flat. As a foundation for discussing gravitational waves in curved spacetime, consider the general problem of linear perturbations of a curved background metric:

$$g_{\mu\nu} = g_{\mu\nu}^{(B)} + h_{\mu\nu}. \quad (2.27)$$

In analyzing the metric perturbations  $h_{\mu\nu}$ , I shall not make explicit the small dimensionless parameter that underlies the perturbation expansion. It might be  $\lambda/\mathcal{L}$  (gravitational wave expansion, §2.4.2 below); it might be the dimensionless amplitude of pulsation of a neutron star,  $\delta R/R$  (linear pulsation-theory expansion, Thorne and Campolattaro 1967); it might be the mass ratio  $m/M$  of a small body  $m$  falling into a Schwarzschild black hole  $M$  and generating gravitational waves as it falls (linear perturbations of Schwarzschild geometry; Davis et al. 1971). In the latter two cases, near the star and hole  $\lambda/\mathcal{L}$  is not  $\ll 1$ ; but nevertheless the linearized equations of this section are valid.

The perturbed Einstein field equations for  $h_{\mu\nu}$  are expressed most conveniently in terms of the "trace-reversed" metric perturbation

$$\bar{h}_{\mu\nu} \equiv h_{\mu\nu} - \frac{1}{2} h g_{\mu\nu}^{(B)}, \quad h \equiv h_{\mu\nu} g_{(B)}^{\mu\nu}. \quad (2.28)$$

A straightforward calculation (cf. §§35.13 and 35.14 of MTW) gives for the first-order perturbations of the field equations

$$\bar{h}_{\mu\nu|\alpha}^{\alpha} + g_{\mu\nu}^{(B)} \bar{h}^{\alpha\beta} |_{\beta\alpha} - 2\bar{h}_{\alpha(\mu}^{\alpha} |_{\nu)} + 2R_{\alpha\mu\beta\nu}^{(B)} \bar{h}^{\alpha\beta} - 2R_{\alpha(\mu}^{(B)} \bar{h}_{\nu)}^{\alpha} = -16\pi\delta T_{\mu\nu}. \quad (2.29)$$

Here a slash "|" denotes covariant derivative with respect to  $g_{\mu\nu}^{(B)}$ ; indices on  $\bar{h}_{\alpha\beta}$  are raised and lowered with  $g_{\mu\nu}^{(B)}$ ;  $R_{\alpha\beta\gamma\delta}^{(B)}$  and  $R_{\alpha\beta}^{(B)}$  are the Riemann and Ricci tensors of the background, and  $\delta T_{\mu\nu}$  is the first-order perturbation of the stress-energy tensor.

The first-order perturbed field equation (2.29) can be used to study a wide variety of phenomena, including wave generation (§3.5 below), wave propagation on a curved vacuum background (§2.4.2), absorption and dispersion of waves due to interaction with matter (§2.4.3), and scattering of waves off background curvature and the resulting production of wave tails (§2.4.2).

### 2.4.2 Wave propagation on a curved vacuum background

Consider gravitational waves of reduced wavelength  $\lambda$  propagating on a curved vacuum background with radius of curvature  $R$  and inhomogeneity scale  $\mathcal{L}$ . In keeping with the discussion in §1.2 assume  $\lambda \ll R$ , but for the moment do not assume  $\lambda \ll \mathcal{L}$ . Then "vacuum" implies  $\delta T_{\mu\nu} = 0$  in the field equations (2.29); and  $\lambda \ll R$  implies that the terms involving  $R_{\alpha\mu\beta\nu}^{(B)}$  and  $R_{\alpha\beta}^{(B)}$ , which are of size  $h/R^2$ , can be neglected compared to the first three terms, which are of size  $h/\lambda^2$ . Simplify the resulting field equations further by an infinitesimal coordinate change ("gauge change")

$$x_{\text{new}}^{\alpha} = x_{\text{old}}^{\alpha} + \xi^{\alpha}, \quad h_{\mu\nu}^{\text{new}} = h_{\mu\nu}^{\text{old}} - \xi_{\mu|\nu} - \xi_{\nu|\mu} \quad (2.30)$$

so designed as to make

$$\bar{h}_{\mu}^{\alpha} |_{\alpha} = 0 \quad (\text{"Lorentz gauge"}). \quad (2.31a)$$

(See, e.g., §35.14 of MTW for discussion of such gauge changes.) The first-order field equations (2.29) then become a simple source-free wave equation in curved spacetime:

$$\bar{h}_{\mu\nu|\alpha}^{\alpha} = 0. \quad (2.31b)$$

The Riemann curvature tensor associated with these waves

$$R_{\alpha\mu\beta\nu}^{(W)} = \frac{1}{2} (h_{\alpha\nu|\mu\beta} + h_{\mu\beta|\nu\alpha} - h_{\mu\nu|\alpha\beta} - h_{\alpha\beta|\mu\nu}) \quad (2.32)$$

will also satisfy the wave equation

$$R_{\alpha\mu\beta\nu|\sigma}^{(W)} = 0 \quad (2.33)$$

(covariant derivatives "|" commute because  $\lambda \ll R$ ). Note that although we require  $\lambda \ll \mathcal{L}$  in order to give a clear definition of "wave", we need not place any restriction on  $\lambda/\mathcal{L}$  in order to derive the wave equation (2.31b).

The Lorentz gauge condition (2.31a) is preserved by any gauge change (2.30) whose generating function  $\xi_{\alpha}$ , like  $\bar{h}_{\mu\nu}$ , satisfies the wave equation  $\xi_{\alpha|\mu}^{\mu} = 0$ . One of the four degrees of freedom in such a gauge change can be used to make  $\bar{h}_{\mu\nu}$  trace-free everywhere

$$\bar{h}_{\alpha}^{\alpha} = 0 \quad \text{so} \quad \bar{h}_{\mu\nu} = h_{\mu\nu} \quad (\text{"trace-free Lorentz gauge"}) \quad (2.34)$$

(MTW exercise 35.13); and the other three degrees of freedom can be used locally (in a local inertial frame of the background  $g_{\mu\nu}^{(B)}$ ) to guarantee that

$$h_{0\alpha} = 0, \quad h_{ij} = h_{ij}^{TT} \quad (\text{"local TT gauge"}), \quad (2.35)$$

where  $h_{ij}^{TT}$  is the gravitational-wave field defined, in the background LIF, by

$$R_{i0j0}^{(W)} \equiv -\frac{1}{2} h_{ij,00}^{TT}. \quad (2.36)$$

If the background is approximated as flat throughout the wave zone, then one can introduce a global inertial frame of  $g_{\mu\nu}^{(B)}$  throughout the wave zone and one can impose the TT gauge globally. However, if the background is curved, a global TT gauge cannot exist (MTW exercise 35.13).

One often knows  $h_{\alpha\beta}$  or  $\bar{h}_{\alpha\beta}$  in a Lorentz but non-TT gauge and wants to compute its "gauge-invariant part"  $h_{ij}^{TT}$  in some LIF of the background. Such a computation is performed most easily by a "TT projection", which is mathematically equivalent to a gauge transformation (MTW Box 35.1): One identifies the propagation direction  $n_j$  in the LIF as the direction in which the wave is varying rapidly (on length scale  $\lambda$ ). One then obtains  $h_{ij}^{TT}$  by discarding all parts of  $h_{ij}$  or  $\bar{h}_{ij}$  along  $n_j$  and by then removing the trace:

$$h_{ij}^{TT} = P_{ia} h_{ab} P_{bj} - \frac{1}{2} P_{ij} P_{ab} h_{ab} = (\text{same expression with } h_{ab} \rightarrow \bar{h}_{ab}), \quad (2.37)$$

where  $P_{ab} = \delta_{ab} + n_a n_b$ . WARNING: This projection process gives the correct answer only in an LIF of the background and only if  $h_{\mu\nu}$  is in a Lorentz gauge.

\* \* \* \* \*

Exercise 10. Show that the infinitesimal coordinate change (2.30) produces the claimed gauge change of  $h_{\mu\nu}$ . Show further that the Riemann tensor of the waves is correctly given by (2.32) in any gauge, and that this Riemann tensor is invariant under gauge changes (2.30).

Exercise 11. Show that a gauge change with  $\xi_{\alpha|\mu}{}^{\mu} = 0$  can be used to make a Lorentz-gauge  $h_{\mu\nu}$  trace-free globally (eq. 2.34) and TT locally (eq. 2.35). Show further that the TT projection process (2.37) produces the same result as this gauge transformation.

### 2.4.3 Absorption and dispersion of waves by matter

When electromagnetic waves propagate through matter (e.g., light through water, radio waves through the interplanetary medium), they are partially absorbed and partially scatter off charges; and the scattered and primary waves superpose in such a way as to change the propagation speed from that of light in vacuum ("Dispersion"). A typical model calculation of this absorption and dispersion involves electrons of charge  $e$ , mass  $m$ , and number density  $n$ , each bound to a "lattice point" by a 3-dimensional, isotropic, damped, harmonic-oscillator force:

$$\ddot{\underline{z}} + (1/\tau_*) \dot{\underline{z}} + \omega_0^2 \underline{z} = (e/m) \underline{E} = - (e/m) \dot{\underline{A}}, \quad (2.38a)$$

where  $\underline{A}$  is the vector potential in transverse Lorentz gauge and a dot denotes  $\partial/\partial t$ . These electrons produce a current density  $\underline{J} = ne(d\underline{z}/dt)$ , which enters into Maxwell's equations for wave propagation  $\square \underline{A} = -4\pi \underline{J}$  to give waves of the form  $\underline{E} = \underline{E}_0 \exp(-i\omega t + ik \cdot \underline{x})$  with the dispersion relation (for weak dispersion)

$$\frac{\omega}{k} = (\text{phase speed}) = 1 - \frac{2\pi n e^2 / m}{\omega_0^2 - \omega^2 - i\omega/\tau_*} \quad (2.38b)$$

This dispersion relation shows both absorption (imaginary part of  $\omega/k$ ) and dispersion (real part), and in real situations either or both can be very large.

When gravitational waves propagate through matter they should also suffer absorption and dispersion. However, in real astrophysical situations the absorption and dispersion will be totally negligible, as the following model calculation shows. (For previous model calculations similar to this one see Szekeres 1971.)

The best absorbers or scatterers of gravitational waves that man has devised are Weber-type resonant-bar gravitational-wave detectors (§§4.1.2 and 4.1.4). On larger scales, a spherical self-gravitating body such as the earth or a neutron star is also a reasonably good absorber and scatterer (good compared to other kinds of objects such as interstellar gas). Consider, then, an idealized "medium" made of many solid spheres (spheres to avoid anisotropy of response to gravity waves), each of which has quadrupole vibration frequency  $\omega_0$ , damping time (due to internal friction)  $\tau_*$ , mass  $m$  and radius  $R$ . For ease of calculation (and because we only need order of magnitude estimates) ignore the self gravity and mutual gravitational interactions of the spheres, and place the spheres at rest in a flat background spacetime with number per unit volume  $n$ . Let  $h_{jk}^{TT}$  be the gravitational-wave field and require  $\lambda > n^{-1/3} > R$ . The waves' geodesic deviation force drives each sphere into quadrupolar oscillations with quadrupole moment  $\mathcal{J}_{jk}$  satisfying the equation of motion (Exercise 22 in §4.1.4 below)

$$\ddot{\mathcal{J}}_{jk} + (1/\tau_*)\dot{\mathcal{J}}_{jk} + \omega_0^2 \mathcal{J}_{jk} = (1/5)mR^2 \ddot{h}_{jk}^{TT} \quad (2.39a)$$

(analog of the electromagnetic equation 2.38a). As a result of these oscillations each sphere reradiates. The wave equation for  $h_{jk}^{TT}$  with these reradiating sources (analog of  $\square A = -4\pi J$ ) is

$$\square h_{jk}^{TT} \equiv \nabla_{\alpha\beta} h_{jk, \alpha\beta}^{TT} = -8\pi n \ddot{\mathcal{J}}_{jk} \quad (2.39b)$$

(Exercise 12). By combining equations (2.39a,b) and assuming a wave of the form  $h_{jk} \propto \exp(-i\omega t + i\mathbf{k} \cdot \mathbf{x})$  we obtain the gravitational-wave dispersion relation

$$\frac{\omega}{k} = (\text{phase speed}) = 1 - \frac{(4\pi/5)n m R^2 \omega^2}{\omega_0^2 - \omega^2 - i\omega/\tau_*} \quad (2.39c)$$

To see that the absorption and dispersion are negligible, compare the length scale  $l = |(1 - \omega/k)\omega|^{-1}$  for substantial absorption or for a phase shift of  $\sim \pi/2$  with the radius of curvature of spacetime produced by the scatterers (i.e., the maximum size that the scattering region can have without curling itself up into a closed universe),  $R = (nm)^{-1/2}$ :

$$\frac{l}{R} = \left| \frac{\omega_0^2 - \omega^2 - i\omega/\tau_*}{(4\pi/5)\omega^2} \right| \frac{1}{\underbrace{(nR^3)^{1/2}}_{\lesssim 1} \underbrace{(m/R)^{1/2}}_{< 1/\sqrt{2}} \underbrace{(\omega R)}_{< 1}} \quad (2.40)$$

$\gtrsim 1$  off resonance  
 $\sim (1/Q)$  on resonance

Here  $Q = 1/\omega\tau_*$  is the quality factor of a scatterer,  $nR^3 \lesssim 1$  because the scatterers cannot be packed closer together than their own radii,  $m/R < 1/2$  because a scatterer cannot be smaller than a black hole of the same mass, and  $\omega R = R/\lambda < 1$

was required to permit a geodesic-deviation analysis (see above). In the most extreme of idealized universes  $l/R$  can be no smaller than unity off resonance (dispersion) and  $l/Q$  on resonance (absorption); and such extreme values can be achieved only for neutron stars or black holes ( $m/R \sim 1$ ) packed side by side ( $nR^3 \sim 1$ ) with  $R \sim \lambda$ . In the real universe,  $l/R$  will always be  $\gg 1$ ; i.e., absorption and dispersion will be negligible regardless of what material the waves encounter and regardless of how far they propagate through it.\*

For this reason, henceforth in discussing wave propagation through astrophysical matter (e.g., the interior of the Earth or Sun) I shall approximate  $\bar{h}_{\mu\nu}|_{\alpha} = -16\pi\delta T_{\mu\nu}$  by  $\bar{h}_{\mu\nu}|_{\alpha} = 0$ . The matter will influence wave propagation only through the background curvature it produces (covariant derivative "|"), not through any direct scattering or absorption ( $\delta T_{\mu\nu}$ ); see §2.6.1 below.

\* \* \* \* \*

Exercise 12. For non-self-gravitating matter in flat spacetime and in Lorentz coordinates, show that  $T^{\alpha\beta}_{;\beta} = 0$  implies  $T^{jk} = (1/2)(\rho x^j x^k)_{,00} +$  (perfect spatial divergence), where  $\rho$  is mass density. Average this over a lattice of oscillating spheres with number density  $n > \lambda^{-3}$  to get  $T^{jk} = (1/2)n\bar{i}^{jk}$ , where  $I_{jk} = \int \rho x^j x^k d^3x$  is the second moment of the mass distribution of each sphere. Passing gravitational waves excite the oscillations in accord with equation (2.39a) (result to be proved in Exercise 22). These oscillations involve no volume changes, so  $\bar{i}^{jk} = \bar{j}^{jk}$  = (trace-free part of  $\bar{i}^{jk}$ ); moreover, equation (2.39a) shows that  $\bar{j}^{jk}$  is transverse and traceless. Show that this permits TT gauge to be imposed in the field equations (2.29) in the presence of the oscillating, reradiating spheres (usually it can be imposed only outside all sources), and that the resulting field equations reduce to (2.39b). Then derive the gravitational-wave dispersion relation (2.39c) and the estimate (2.40) of the effects of dispersion and absorption.

#### 2.4.4 Scattering of waves off background curvature, and tails of waves

A self-gravitating body of mass  $m$  and size  $R$  will typically generate gravitational waves with reduced wavelength

$$\lambda \sim (R^3/m)^{1/2} \sim R_s = (\text{radius of curvature of spacetime near source}). \quad (2.41)$$

If the body has strong self gravity,  $m/R \sim 1$  (neutron star or black hole), then  $\lambda \sim R_s$  in the innermost parts of the wave zone; and the curvature coupling terms must be retained in the first-order Einstein equations (2.29). These terms cause the waves to scatter off the background curvature; and repetitively backscattered waves superimposing on each other produce a gravity-wave "tail" that lingers near the source long after the primary waves have departed, dying out as  $t^{-(2l+2)}$  for waves of multipole order  $l$ . See, e.g., Price (1972) for a more detailed discussion, and Cunningham, Price, and Moncrief (1978) for an explicit example.

I regard these backscatterings and tails as part of the wave generation problem and as irrelevant to the problem of wave propagation. In fact, I have defined the inner edge of the "local wave zone" to be so located that throughout it, and throughout the wave propagation problem,  $\lambda \ll R$  and backscatter and tails can be ignored (eq. 1.7 and associated discussion).

---

\* For description of a physically unrealistic but conceivable material in which dispersion is so strong that it actually reflects gravitational waves see Press (1979).



### 2.4.5 The stress-energy tensor for gravitational waves

Gravitational waves carry energy and momentum and can exchange them with matter, e.g., with a gravitational-wave detector. Isaacson (1968) (see also §35.15) has quantified this by examining nonlinear corrections to the wave-propagation equation (2.31b). In this section I shall sketch the main ideas of his analysis.

Consider a gravitational wave with  $\lambda \ll \mathcal{L} \lesssim \mathcal{R}$ , and expand the metric of the full spacetime in a perturbation series

$$g_{\mu\nu} = g_{\mu\nu}^{(B)} + h_{\mu\nu} + j_{\mu\nu} + \dots \quad (2.42a)$$

$1, \mathcal{L} \quad \mathcal{O}, \lambda \quad \mathcal{O}^2, \lambda$

Below each term I have written the characteristic magnitudes ( $1, \mathcal{O}, \mathcal{O}^2$ ) of the metric components, and the lengthscales ( $\mathcal{L}, \lambda$ ) on which they vary in the most "steady" of coordinate systems. Note that  $j_{\mu\nu}$  is a nonlinear correction to the propagating waves. By inserting this perturbation series into the standard expression (MTW eqs. 8.47-8.49) for the Einstein curvature tensor  $G_{\mu\nu}$  in terms of  $g_{\mu\nu}$  and its derivatives, and by grouping terms according to their magnitudes and their lengthscales of variation, one obtains

$$G_{\mu\nu} = G_{\mu\nu}^{(B)} + G_{\mu\nu}^{(1)}(h) + G_{\mu\nu}^{(2)}(h) + G_{\mu\nu}^{(1)}(j) + \dots \quad (2.42b)$$

$\leq 1/\mathcal{R}^2, \mathcal{L} \quad \mathcal{O}/\lambda^2, \lambda \quad \mathcal{O}^2/\lambda^2, \lambda \quad \mathcal{O}^2/\lambda^2, \lambda$

Here  $G_{\mu\nu}^{(B)}$  is the Einstein tensor of the background metric  $g_{\mu\nu}^{(B)}$ ;  $G_{\mu\nu}^{(1)}(h \text{ or } j)$  is the linearized correction to  $G_{\mu\nu}$  (MTW eq. 35.58a, trace-reversed); and  $G_{\mu\nu}^{(2)}(h)$  is the quadratic correction (MTW eq. 35.58b), trace-reversed).

Isaacson splits the Einstein equations into three parts: a part which varies on scales  $\mathcal{L}$  (obtained by averaging, " $\langle \rangle$ ", over a few wavelengths)

$$G_{\mu\nu}^{(B)} = 8\pi \left( T_{\mu\nu}^{(B)} + \langle T_{\mu\nu}^{(2)} \rangle + T_{\mu\nu}^{(W)} \right), \quad T_{\mu\nu}^{(W)} \equiv - (1/8\pi) \langle G_{\mu\nu}^{(2)}(h) \rangle; \quad (2.43a)$$

a part of magnitude  $\mathcal{O}/\lambda^2$  which varies on scales  $\lambda$  and averages to zero on larger scales

$$G_{\mu\nu}^{(1)}(h) = 8\pi T_{\mu\nu}^{(1)} \iff \bar{h}_{\mu\nu|\alpha}{}^\alpha = -16\pi T_{\mu\nu}^{(1)} \text{ in Lorentz gauge}; \quad (2.43b)$$

and a part of magnitude  $\mathcal{O}^2/\lambda^2$  which varies on scales  $\lambda$  and averages to zero on larger scales

$$G_{\mu\nu}^{(1)}(j) = - G_{\mu\nu}^{(2)}(h) + \langle G_{\mu\nu}^{(2)}(h) \rangle + 8\pi \left( T_{\mu\nu}^{(2)} - \langle T_{\mu\nu}^{(2)} \rangle \right). \quad (2.43c)$$

Here  $T_{\mu\nu}^{(B)}$  is the stress-energy tensor of the background;  $T_{\mu\nu}^{(1)}$  and  $T_{\mu\nu}^{(2)}$  are its first- and second-order perturbations;  $T_{\mu\nu}^{(W)} \equiv -(1/8\pi) \langle G_{\mu\nu}^{(2)}(h) \rangle$  is a stress-energy tensor associated with the gravitational waves; and the averaging  $\langle \rangle$  can be performed in the most naive of manners if the coordinates are sufficiently "steady", but must be performed carefully, by Brill-Hartle techniques (MTW exercise 35.14), if they are not. The "smoothed" field equations (2.43a), together with the contracted Bianchi identities  $G_{\mu\nu}^{(B)}|_{\nu}{}^\nu \equiv 0$ , imply a conservation law for energy and momentum in the presence of gravitational waves:

$$T_{(B)}^{\mu\nu}|_{\nu} + \langle T_{(2)}^{\mu\nu} \rangle|_{\nu} + T_{(W)}^{\mu\nu}|_{\nu} = 0. \quad (2.44)$$

(Here and throughout this section indices are raised and lowered with  $g_{\mu\nu}^{(B)}$ .)

To understand the physics of the field equations (2.43) and conservation law (2.44), let us reconsider the propagation of waves through a cloud of spherical oscillators (§2.4.3). Equation (2.43b) is the wave equation (2.39b) for  $h$ , which we used to calculate the absorption and dispersion of the waves. In this wave equation  $T_{\mu\nu}^{(1)}$  is the part of  $T_{\mu\nu}$  that is linear in the oscillators' amplitude of motion; in Exercise 12 its spatial part (after averaging over scales  $< \lambda$ ) was shown to be  $T_{jk}^{(1)} = \frac{1}{2} n \dot{j}_{jk}$ . Equation (2.43c) describes the generation of nonlinear corrections  $j_{\mu\nu}$  to the propagating waves. In Lorentz gauge it takes the explicit form

$$j_{\mu\nu}|_{\alpha} = \left( \begin{array}{l} \text{source terms quadratic in } h_{\alpha\beta} \text{ and in } \\ \text{the amplitude of oscillator motion} \end{array} \right). \quad (2.45)$$

In §2.6.2 we shall see that these nonlinear corrections, like absorption and dispersion, are negligible in realistic astrophysical circumstances. Equation (2.43a) describes the generation of smooth, background curvature by the stress-energy of the gravitational waves  $T_{\mu\nu}^{(W)}$  and of the matter. Note that the waves contribute an amount of order  $Q^2/\lambda^2$  to the background curvature  $1/R^2$ , and that therefore  $1/R^2 \gtrsim Q^2/\lambda^2$ ; i.e.,

$$Q \lesssim \lambda/R. \quad (2.46)$$

Since  $\lambda/R \ll 1$  for propagating waves, such waves must necessarily have dimensionless amplitudes  $Q \ll 1$ . If ever  $Q$  were to become of order unity, the wave would cease to be separable from the background curvature; the two would become united as a dynamically vibrating spacetime curvature to which the theory of propagating gravitational waves cannot be applied. Equation (2.44) describes the exchange of energy and momentum between matter and waves. In this conservation law  $T_{(B)}^{\mu\nu} = \rho u^{\mu} u^{\nu}$  is the stress-energy of the unperturbed spheres (number density  $n$ , mass  $m$ , 4-velocity  $u^{\mu}$ ) and by itself has vanishing divergence. The term  $\langle T_{(2)}^{\mu\nu} \rangle$  is the quadratic-order stress-energy associated with the spheres' oscillations, averaged spatially over a few wavelengths and temporally over a few periods of the waves. In an LIF of the oscillators the only nonzero components are the energy density  $\langle T_{(2)}^{00} \rangle$  which includes the kinetic energy and the potential energy of oscillation and the thermal energy produced when the oscillations are damped by internal friction [ $1/\tau_*$  term in oscillators' equation of motion (2.39a)], and a transverse stress of magnitude comparable to  $\langle T_{(2)}^{00} \rangle$ . Thus, for our idealized problem the conservation law (2.44) describes the absorption of gravitational-wave energy by the oscillators and the subsequent conversion of oscillation energy into heat.

The gravitational-wave stress-energy tensor  $T_{\mu\nu}^{(W)}$  "lives in" the background spacetime and is manipulated using background-spacetime mathematics [e.g., covariant derivative " $|$ " in the conservation law (2.44)]. Because of the averaging  $\langle \rangle$  in its definition,  $T_{\mu\nu}^{(W)}$  gives a well-defined localization of the waves' energy and momentum only on lengthscales somewhat larger than  $\lambda$  (no way to say whether the energy is in the "crest" of a wave or in its "trough"); no more precise localization of gravitational energy is possible in general relativity. Like  $R_{\alpha\beta\gamma\delta}^{(W)}$  and unlike  $h_{\alpha\beta}$ , the stress-energy tensor  $T_{\alpha\beta}^{(W)}$  is gauge invariant. Explicit calculations (Isaacson 1968; MTW §35.15) give

$$\begin{aligned} T_{\mu\nu}^{(W)} &= \frac{1}{32\pi} \langle \bar{h}_{\alpha\beta} |_{\mu} \bar{h}^{\alpha\beta} |_{\nu} - \frac{1}{2} \bar{h} |_{\mu} \bar{h} |_{\nu} - 2 \bar{h}^{\alpha\beta} |_{\beta} \bar{h}_{\alpha(\mu} |_{\nu)} \rangle \quad \text{in any gauge} \\ &= \frac{1}{32\pi} \langle \bar{h}_{\alpha\beta} |_{\mu} \bar{h}^{\alpha\beta} |_{\nu} \rangle \quad \text{in trace-free Lorentz gauge} \end{aligned} \quad (2.47)$$

(continued next page)

$$= \frac{1}{32\pi} \langle h_{jk,\mu}^{TT} h_{jk,\nu}^{TT} \rangle \text{ in LIF of any observer.}$$

## 2.5 Wave propagation in the geometric optics limit

### 2.5.1 Differential equations of geometric optics

Return now to the explicit problem of the propagation of gravitational waves from the local wave zone of a source out through the lumpy universe toward earth. Throughout the local wave zone, and almost everywhere in the universe, not only will  $\lambda$  be very small compared to the background radius of curvature  $\mathcal{R}$ , but also it will be small compared to the scale  $\mathcal{L}$  on which the background curvature varies

$$\lambda \ll \mathcal{L}. \quad (2.48)$$

Here, as in the above discussion of the waves' stress-energy, I shall assume that  $\lambda \ll \mathcal{L}$ ; later (§2.6.1) I shall relax that assumption. Here I shall also assume that  $\lambda \ll \mathcal{L}^{(W)} \equiv$  (radius of curvature of the wave fronts of the waves or any smaller scale length for transverse variation of the waves).

The assumptions  $\lambda \ll \mathcal{L}$  and  $\lambda \ll \mathcal{L}^{(W)}$  permit us to solve for the propagation using the techniques of geometric optics (e.g., MTW Exercise 35.15): Introduce trace-free Lorentz gauge everywhere, and ignore the effects of direct interaction between the propagating waves and matter (negligible absorption and dispersion). Then

$$h_{\alpha}^{\alpha} = 0, \quad h^{\mu\alpha} |_{\alpha} = 0, \quad h_{\mu\nu} |_{\alpha} = 0. \quad (2.49)$$

The solution of these gauge and propagation equations is a rapidly varying function of retarded time  $\psi$  and a slowly varying function of the other spacetime coordinates:

$$h_{\mu\nu} = h_{\mu\nu}(\psi, x^{\alpha}) \quad (2.50)$$

$\uparrow$  variation on scales  $\mathcal{L}^{(W)}, \mathcal{L}, \mathcal{R}$   
 $\uparrow$  variation on scale  $\lambda$ .

As in the discussion of waves in flat spacetime (§2.3.2), define the propagation vector

$$\vec{k} \equiv -\vec{\nabla}\psi. \quad (2.51a)$$

Then, aside from fractional corrections of order  $\lambda/\mathcal{L}^{(W)}$ ,  $\lambda/\mathcal{L}$ ,  $\lambda/\mathcal{R}$  the gauge and field equations (2.49) imply

$$k_{\alpha} k^{\alpha} = 0 \text{ and } k_{\beta} |_{\alpha} k^{\alpha} = 0 \iff \vec{k} \text{ is tangent to null geodesics ("rays"),} \quad (2.51b)$$

$$h_{\alpha}^{\alpha} = 0, \quad h_{\alpha\beta} k^{\beta} = 0 \iff h_{\alpha\beta} \text{ is trace free and orthogonal to } \vec{k}, \quad (2.51c)$$

$$h_{\mu\nu} |_{\alpha} k^{\alpha} = -\frac{1}{2} (\vec{\nabla} \cdot \vec{k}) h_{\mu\nu} \quad (\text{propagation equation for } h_{\mu\nu}). \quad (2.51d)$$

Had we been analyzing the propagation of electromagnetic waves rather than gravitational, our Lorentz gauge equations for the vector potential would have been

$$A^{\alpha} |_{\alpha} = 0, \quad A_{\mu} |_{\alpha} = 0 \quad (2.52a)$$

(MTW eq. 16.5' with curvature coupling term removed because  $\lambda \ll \mathcal{R}$ ) (cf. eq.

2.49); our geometric-optics ansatz would have been

$$A_{\mu} = A_{\mu}(\psi; x^{\alpha}) \quad (2.52b)$$

(cf. eq. 2.50); and in the geometric optics limit the gauge and wave equations (2.52a) would have reduced to

$$k_{\alpha} k^{\alpha} = 0, \quad k_{\beta|\alpha} k^{\alpha} = 0, \quad A_{\alpha} k^{\alpha} = 0, \quad A_{\mu|\alpha} k^{\alpha} = -\frac{1}{2}(\vec{\nabla} \cdot \vec{k}) A_{\mu} \quad (2.52c)$$

(cf. eqs. 2.51c,d).

\* \* \* \* \*

Exercise 13. Show that in the geometric optics limit  $\lambda \ll \mathcal{L} \lesssim \mathcal{R}$  and  $\lambda \ll \mathcal{L}^{(W)}$ , and with the geometric optics ansatz (2.50), the gravitational gauge and propagation equations (2.49) reduce to the geometric optics equations (2.51). Similarly show that for electromagnetic waves (2.52a) reduce to (2.52c).

### 2.5.2 Solution of geometric optics equations in local wave zone

In the local wave zone of the source introduce (flat-background) spherical coordinates  $(t, r, \theta, \varphi)$ . The waves propagate radially outward from the source along the null-geodesic rays

$$\psi = t-r, \quad \theta, \quad \varphi \text{ all constant}, \quad k^0 = k^r = 1. \quad (2.53a)$$

Throughout the local wave zone introduce transverse basis vectors  $\vec{e}_{\hat{\theta}} = r^{-1} \partial/\partial\theta$  and  $\vec{e}_{\hat{\varphi}} = (r \sin \theta)^{-1} \partial/\partial\varphi$  and polarization tensors

$$\vec{e}_{+}^{\hat{}} \equiv \vec{e}_{\hat{\theta}}^{\hat{}} \otimes \vec{e}_{\hat{\theta}}^{\hat{}} - \vec{e}_{\hat{\varphi}}^{\hat{}} \otimes \vec{e}_{\hat{\varphi}}^{\hat{}}, \quad \vec{e}_{\times}^{\hat{}} \equiv \vec{e}_{\hat{\theta}}^{\hat{}} \otimes \vec{e}_{\hat{\varphi}}^{\hat{}} + \vec{e}_{\hat{\varphi}}^{\hat{}} \otimes \vec{e}_{\hat{\theta}}^{\hat{}}. \quad (2.53b)$$

Then it turns out (Exercise 14) that in TT gauge the general solution to the gauge and propagation equations (2.51c,d) is

$$\overset{\leftrightarrow}{h}^{\text{TT}} = A_{+}(\psi; r, \theta, \varphi) \vec{e}_{+}^{\hat{}} + A_{\times}(\psi; r, \theta, \varphi) \vec{e}_{\times}^{\hat{}} \quad (2.53c)$$

$$A_{+} = r^{-1} F_{+}(\psi; \theta, \varphi), \quad A_{\times} = r^{-1} F_{\times}(\psi; \theta, \varphi);$$

and similarly for electromagnetic waves

$$\vec{A} = A_{\hat{\theta}}(\psi; r, \theta, \varphi) \vec{e}_{\hat{\theta}}^{\hat{}} + A_{\hat{\varphi}}(\psi; r, \theta, \varphi) \vec{e}_{\hat{\varphi}}^{\hat{}} \quad (2.54)$$

$$A_{\hat{\theta}} = r^{-1} F_{\hat{\theta}}(\psi; \theta, \varphi), \quad A_{\hat{\varphi}} = r^{-1} F_{\hat{\varphi}}(\psi; \theta, \varphi).$$

Stated in words: In polarization bases  $\vec{e}_{+}^{\hat{}}$ ,  $\vec{e}_{\times}^{\hat{}}$  and  $\vec{e}_{\hat{\theta}}^{\hat{}}$ ,  $\vec{e}_{\hat{\varphi}}^{\hat{}}$  which are parallel transported along the rays, the amplitude functions  $A_{+}$ ,  $A_{\times}$  of gravitational waves and  $A_{\hat{\theta}}$ ,  $A_{\hat{\varphi}}$  of electromagnetic waves die out as  $1/r$  but otherwise are constant along the rays.

The precise forms of  $F_{+}(\psi; \theta, \varphi) = r A_{+}$  and  $F_{\times}(\psi; \theta, \varphi) = r A_{\times}$  are to be determined by solution of the wave generation problem (§3 below). The local-wave-zone waves (2.53) are then to be used as "starting conditions" for propagation out through the universe.

Exercise 14. Show that equations (2.53) are the general solution of the gravitational geometric optics equations (2.51) specialized to TT gauge, for waves propagating radially outward through the local wave zone of a source. Similarly show that equations (2.54) are the solution of the electromagnetic equations (2.52c).

### 2.5.3 Solution of geometric optics equations in distant wave zone

Suppose that the wave generation problem has been solved to give  $h_{jk}^{TT}$  in the form (2.52) throughout the local wave zone. These waves can then be propagated throughout the rest of the universe (assuming  $\lambda \ll \mathcal{L}$  and  $\lambda \ll \mathcal{L}^{(W)}$ ) using the following constructive method [solution of geometric optics equations (2.51)]:

First extend the radial null rays (2.53a) of the local wave zone out through the universe by solving the geodesic equation. Continue to label each ray by  $\psi, \theta, \varphi$  and parametrize it by an affine parameter denoted  $r$  (and equal to the radial coordinate in the local wave zone):

$$\text{rays are } (\psi, \theta, \varphi) = \text{const}; \quad \vec{k} \equiv -\vec{\nabla}\psi = d/dr. \quad (2.55a)$$

Next, along each ray parallel propagate the fiducial basis vector  $\vec{e}_{\hat{\theta}}$

$$\vec{\nabla}_{\vec{k}} \vec{e}_{\hat{\theta}} = 0 \text{ everywhere,} \quad \vec{e}_{\hat{\theta}} = r^{-1} \partial/\partial\theta \text{ in local wave zone.} \quad (2.55b)$$

Together  $\vec{e}_{\hat{\theta}}$  and  $\vec{k}$  form a fiducial 2-flat  $\vec{k} \wedge \vec{e}_{\hat{\theta}}$  to be used below in defining the polarization of the waves. Next, propagate  $A_+$  and  $A_\times$  along each ray by solving the ordinary differential

$$(\partial A/\partial r)_{\psi, \theta, \varphi} = -\frac{1}{2} (\vec{\nabla} \cdot \vec{k}) A, \quad A = [\text{expression (2.53c) in local wave zone}]. \quad (2.55c)$$

The resulting  $A_+$ ,  $A_\times$ , and fiducial 2-flat  $\vec{k} \wedge \vec{e}_{\hat{\theta}}$  determine the gravitational-wave field in the manner of §2.3.2: At any event in the distant wave zone introduce an observer with 4-velocity  $\vec{u}$ ; introduce an orthonormal basis

$$\begin{aligned} \vec{e}_0 &\equiv \vec{u}, & \vec{e}_z &\equiv \left[ \begin{array}{l} \text{unit vector obtained by projecting } \vec{k} \\ \text{orthogonal to } \vec{u} \text{ and renormalizing} \end{array} \right], \\ \vec{e}_x &\equiv [\text{unit vector lying in } \vec{k} \wedge \vec{e}_{\hat{\theta}} \text{ and orthogonal to } \vec{u}]. \end{aligned} \quad (2.55d)$$

$$\vec{e}_y \equiv \left[ \begin{array}{l} \text{unit vector such that } \vec{e}_0, \vec{e}_x, \vec{e}_y, \vec{e}_z \text{ are a right-hand oriented,} \\ \text{orthonormal frame} \end{array} \right];$$

and introduce corresponding polarization tensors

$$\vec{e}_+ \equiv \vec{e}_x \otimes \vec{e}_x - \vec{e}_y \otimes \vec{e}_y, \quad \vec{e}_\times \equiv \vec{e}_x \otimes \vec{e}_y + \vec{e}_y \otimes \vec{e}_x. \quad (2.55e)$$

Then the gravitational-wave field in this LIF is

$$h^{TT} = A_+ \vec{e}_+ + A_\times \vec{e}_\times; \quad (2.55f)$$

and the Riemann tensor and stress-energy tensor associated with the waves are

$$R_{\alpha\beta\gamma\delta}^{(W)} = \frac{1}{2} (\dot{h}_{\alpha\delta}^{TT} k_\beta k_\gamma + \dot{h}_{\beta\gamma}^{TT} k_\alpha k_\delta - \dot{h}_{\beta\delta}^{TT} k_\alpha k_\gamma - \dot{h}_{\alpha\gamma}^{TT} k_\beta k_\delta),$$

$$T_{\alpha\beta}^{(W)} = \frac{1}{16\pi} \langle \dot{A}_+^2 + \dot{A}_\times^2 \rangle k_\alpha k_\beta, \quad \text{where } \dot{\phantom{x}} \equiv \partial/\partial\psi.$$
(2.56)

For electromagnetic waves the geometric optics equations (2.52c) have a similar solution. In a basis  $\vec{e}_{\hat{\theta}}$ ,  $\vec{e}_{\hat{\phi}}$  obtained by parallel transport (eqs. 2.55b) along the rays (eqs. 2.55a) the components of the vector potential,  $A_{\hat{\theta}}$  and  $A_{\hat{\phi}}$ , satisfy identically the same propagation equation (2.55c) as the gravitational-wave amplitude functions  $A_+$  and  $A_\times$ . Moreover, an observer with 4-velocity  $\vec{u}$  can always put the waves into purely spatial Lorentz gauge (no component of  $\vec{A}$  along  $\vec{u}$ ) by a gauge change, which produces

$$\vec{A}^S = A_{\hat{\theta}} \vec{e}_{\hat{x}} + A_{\hat{\phi}} \vec{e}_{\hat{y}} \quad (2.57)$$

(analog of eq. 2.55f) with  $\vec{e}_{\hat{x}}$ ,  $\vec{e}_{\hat{y}}$  given by equations (2.55d). The electromagnetic field tensor, and the stress-energy tensor of the waves averaged over several wavelengths (analog of eqs. 2.56) are

$$F_{\alpha\beta} = \dot{A}_\beta^S k_\alpha - \dot{A}_\alpha^S k_\beta,$$

$$\langle T_{\alpha\beta} \rangle = \frac{1}{4\pi} \langle A_{\hat{\theta}}^2 + A_{\hat{\phi}}^2 \rangle k_\alpha k_\beta.$$
(2.58)

\* \* \* \* \*

**Exercise 15.** Show that equations (2.55) constitute a solution of the gravitational geometric optics equations (2.51), transformed locally to TT gauge. Show further that this solution joins smoothly onto the local-wave-zone solution (2.53), and that the Riemann tensor and stress-energy tensor of these waves have the form (2.56). Similarly show that if  $A_{\hat{\theta}}$  and  $A_{\hat{\phi}}$  are propagated via (2.55c), then  $A_{\hat{\theta}} \vec{e}_{\hat{\theta}} + A_{\hat{\phi}} \vec{e}_{\hat{\phi}}$  is a solution of the electromagnetic equations (2.52c); (2.57) is this same solution in another gauge; and (2.58) are the field tensor and averaged stress-energy tensor of the waves.

#### 2.5.4 Example: Propagation through a Friedmann universe

As an example of the geometric optics solution for wave propagation consider, as the background spacetime, a closed Friedmann universe with metric

$$g_{\alpha\beta}^{(B)} dx^\alpha dx^\beta = a^2(\eta) [-d\eta^2 + d\chi^2 + \Sigma^2 (d\theta^2 + \sin^2\theta d\varphi^2)]$$
(2.59)

$$\Sigma = : \chi \text{ for } k = 0, \quad \sin \chi \text{ for } k = +1, \quad \sinh \chi \text{ for } k = -1.$$

Here  $k$  is the curvature parameter ( $k = 0$  for a spatially flat universe,  $k = +1$  for a closed universe,  $k = -1$  for an open universe; see, e.g., chapters 27-29 of MTW). Orient the coordinates so the source of the waves is at  $\chi = 0$ , and let the source be active (emit waves) at a coordinate time  $\eta \simeq \eta_e$  when the expansion factor of the universe is  $a = a_e$  ("e" for "emission"). The flat, spherical coordinates of the local wave zone, and the retarded time are

$$t = a_e(\eta - \eta_e), \quad r = a_e \chi, \quad \theta, \quad \varphi; \quad \psi = t - r = a_e(\eta - \chi - \eta_e); \quad (2.60)$$

and the waves in the local wave zone are described by equations (2.53b,c).

Throughout the wave zone (local and distant) the rays and propagation vector of equations (2.55a) are

$$\eta - \chi = \eta_e + \psi/a_e, \quad k^\eta = k^\chi = \left( \frac{\partial \eta}{\partial r} \right)_{\psi, \theta, \varphi} = \left( \frac{\partial \chi}{\partial r} \right)_{\psi, \theta, \varphi} = \frac{a_e}{a^2}; \quad (2.61a)$$

the parallel-propagated fiducial basis vector (eq. 2.55b) is

$$\vec{e}_{\hat{\theta}} = (1/a\Sigma) \partial/\partial\theta; \quad (2.61b)$$

and the transported gravity-wave and electromagnetic-wave amplitude functions (eq. 2.55c) are

$$A_J = \frac{F_J(\psi; \theta, \varphi)}{a\Sigma}; \quad J = + \text{ or } \times \text{ (gravity), } J = \hat{\theta} \text{ or } \hat{\varphi} \text{ (electromagnetism)}. \quad (2.61c)$$

If we approximate the earth as at rest in the Friedmann coordinate system at  $\chi_o, \theta_o, \varphi_o$  and we denote the present epoch by  $\eta \simeq \eta_o, a = a_o$ , then the basis vectors (2.53b) of the earth's LIF are

$$\vec{e}_o = \frac{1}{a_o} \frac{\partial}{\partial \eta}, \quad \vec{e}_x = \frac{1}{a_o \Sigma_o} \frac{\partial}{\partial \theta}, \quad \vec{e}_y = \frac{1}{a_o \Sigma_o \sin \theta_o} \frac{\partial}{\partial \varphi}, \quad \vec{e}_z = \frac{1}{a_o} \frac{\partial}{\partial \chi}; \quad (2.61d)$$

and the gravitational-wave field as measured at earth (eqs. 2.53b,c) is

$$\vec{h}^{\leftrightarrow TT} = \frac{1}{a_o \Sigma_o} \left[ F_+(\psi; \theta_o, \varphi_o) (\vec{e}_x \otimes \vec{e}_x - \vec{e}_y \otimes \vec{e}_y) + F_\times(\psi; \theta_o, \varphi_o) (\vec{e}_x \otimes \vec{e}_y + \vec{e}_y \otimes \vec{e}_x) \right]. \quad (2.61e)$$

The energy density in these waves as measured at earth (eq. 2.56) is

$$T_{00}^{(W)} = \frac{\langle \dot{F}_+^2 + \dot{F}_\times^2 \rangle}{4 \cdot 4\pi a_o^2 \Sigma_o^2} \left( \frac{a_e}{a_o} \right)^2, \quad \cdot = \partial/\partial\psi, \quad (2.62)$$

↑  
(surface area around source today)

where  $Z$  is the cosmological redshift of the source. Similarly, for electromagnetic waves

$$\vec{A}^S = (1/a_o \Sigma_o) [F_{\hat{\theta}}(\psi; \theta_o, \varphi_o) \vec{e}_x + F_{\hat{\varphi}}(\psi; \theta_o, \varphi_o) \vec{e}_y], \quad (2.63a)$$

$$\langle T_{00} \rangle = \frac{\langle \dot{F}_{\hat{\theta}}^2 + \dot{F}_{\hat{\varphi}}^2 \rangle}{4\pi a_o^2 \Sigma_o^2} \left( \frac{a_e}{a_o} \right)^2. \quad (2.63b)$$

Note that the factor  $1/a_o \Sigma_o$ , by which the amplitudes of the waves die out as they recede from the source, is given in terms of cosmological parameters by

$$\frac{1}{a_0 \Sigma_0} \equiv \frac{1}{R} = \frac{H_0 q_0^2 (1+Z)}{-q_0 + 1 + q_0 Z + (q_0 - 1)(2q_0 Z + 1)^{1/2}}$$

$$\approx \frac{H_0}{Z} [1 + \frac{1}{2} (1+q_0)Z + O(Z^2)] \quad \text{for } Z \ll 1 \quad (2.64)$$

$$\approx H_0 q_0 \quad \text{for } Z \gg 1 \text{ and } Z \gg 1/q_0$$

(MTW eqs. 29.28-29.33). Here  $H_0$  is the Hubble expansion rate;  $q_0$  is the deceleration parameter of the universe;  $Z$  is the cosmological redshift of the source; and I have assumed zero cosmological constant. For formulas with nonzero cosmological constant see MTW eqs. (29.32).

\* \* \* \* \*

Exercise 16. Show that for propagation through a Friedmann universe equations (2.55)-(2.58) become (2.59)-(2.63).

## 2.6 Deviations from geometric optics

I have already discussed in detail several ways that wave propagation can differ from geometric optics: absorption and dispersion by matter (§2.4.3; almost always negligible for gravitational waves), and scattering of waves off background curvature with resulting production of tails (§2.4.4; important primarily near source, but also if waves encounter a sufficiently compact body — e.g., a neutron star or black hole). In this section I shall describe two other nongeometric-optics effects: diffraction and nonlinear interactions of the wave with itself.

### 2.6.1 Diffraction

As gravitational and electromagnetic waves propagate through the universe, they occasionally encounter regions of enhanced spacetime curvature due to concentrations of matter (galaxies, stars, ...) which produce a breakdown in  $\lambda \ll \mathcal{L}$  and/or in  $\lambda \ll \mathcal{L}^{(W)}$  and a resulting breakdown in geometric-optics propagation. Such a breakdown is familiar from light propagation, where it is called "diffraction".

Consider, as an example, the propagation of waves through the neighborhood and interior of the sun (Fig. 4), and ignore absorption and dispersion by direct interaction with matter (justified for gravitational waves, §2.4.3; not justified for electromagnetic waves). As they pass near and through the sun, rays from a distant source are deflected and forced to cross each other; i.e., they are

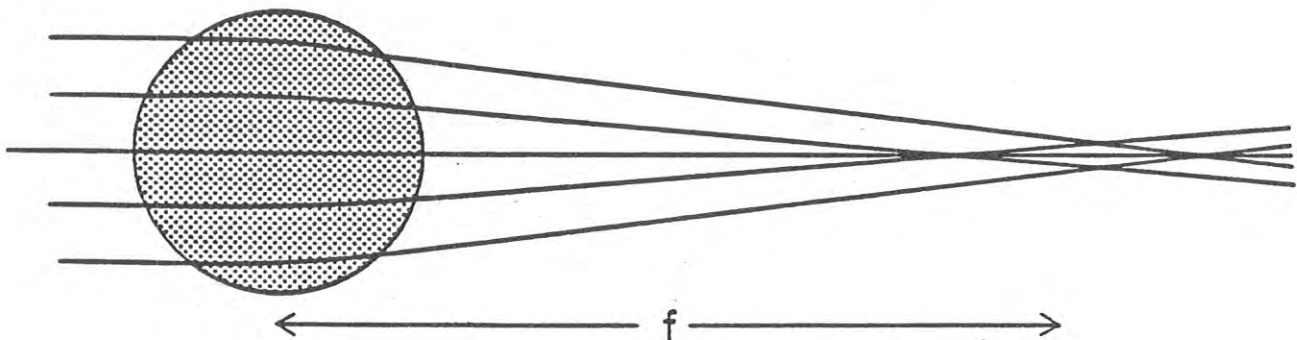


Fig. 4 The rays for geometric-optics wave propagation through the sun.



focussed gravitationally. The dominant source of deflection is the spacetime curvature of the solar core. It produces ray crossing ("caustics") along the optic axis at distances of order (and greater than) the "focal distance"

$$f \sim \frac{\mathcal{L}}{4M/\mathcal{L}} \simeq 20 \text{ AU} . \quad (2.65)$$

Here  $\mathcal{L} \sim 10^5$  km is the inhomogeneity scale of the solar core,  $M \sim 0.3 M_{\odot}$  is the mass of the solar core, and the value 20 AU comes from detailed calculations with a detailed solar model (Cyranski and Lubkin 1974).

Geometric optics would predict infinite amplification of the waves at the caustics. However, geometric optics breaks down there because it also predicts  $\mathcal{L}^{(W)} \rightarrow 0$ . To understand the actual behavior of the waves near the caustics, think of the waves which get focussed by the solar core as a single wave packet that has transverse dimension  $\Delta y \sim \mathcal{L}$  as it passes through the core. The uncertainty principle for waves ( $\Delta y \Delta k_y \gtrsim 1$ ) forces this wave packet to spread in a nongeometric optics manner with a spreading angle

$$\theta_s \sim \Delta k_y / k_x \sim \lambda / \mathcal{L} . \quad (2.66)$$

This spreading is superimposed on the geometric-optics focussing, and it spreads out the highly focussed waves near the caustics over a lateral scale  $y_s$

$$y_s \sim (\lambda / \mathcal{L}) f \sim (\lambda / 4M) \mathcal{L} . \quad (2.67)$$

If  $y_s \ll \mathcal{L}$  (i.e., if  $\lambda \ll 4M$ ) there is substantial focussing: the wave energy density increases near the caustics by a factor  $\sim (y_s / \mathcal{L})^2$  and the amplitude increases by  $\sim y_s / \mathcal{L} \sim \lambda / 4M$ . The details of this regime are described by the laws of "Fresnel diffraction". On the other hand, if  $y_s \gtrsim \mathcal{L}$  (i.e., if  $\lambda \gtrsim 4M$ ) there is negligible focussing; and the little focussing that does occur is described by the laws of "Fraunhofer diffraction". For full details see Bontz and Haugan (1981) and references therein.

For the case of the sun the dividing line between substantial focussing and little focussing is  $\lambda \sim$  (gravitational radius of sun), i.e., (frequency)  $\sim 10^4$  Hz. Since all strong sources of gravitational waves are expected to have  $\lambda \gtrsim$  (gravitational radius of source)  $\gtrsim$  (gravitational radius of Sun), i.e., (frequency)  $\lesssim 10^4$  Hz, they all lie in the "little focussing regime" - a conclusion that bodes ill for any efforts to send gravitational-wave detectors on spacecraft to the orbit of Uranus in search of amplified gravitational waves; cf. Sonnabend (1979).

Far beyond the focal region the geometric optics approximation becomes valid again, except for a smearing of lateral structure of the waves over an angular scale  $\sim \theta_s$ . For example, ray crossing may produce multiple images of a gravitational-wave source in this region; and those images can be computed by geometric optics methods aside from  $\theta_s$ -smearing.

### 2.6.2 Nonlinear effects in wave propagation

Once a gravitational wave has entered and passed through the local wave zone, its nonlinear interactions with itself are of no importance. To see this consider the idealized problem of a radially propagating, monochromatic wave in flat spacetime. At linear order, in spherical coordinates write the wave field as

$$\hat{h}_{\theta\theta} = -\hat{h}_{\varphi\varphi} = A_0(\theta, \varphi) \frac{\lambda}{r} \cos\left(\frac{t-r}{\lambda}\right), \quad (2.68)$$

where hats denote components in an orthonormal, spherical basis. Note that the

angular function  $A_0$  is the amplitude of the wave in the induction zone, where it is just barely starting to become a wave. For any realistic source  $A_0 \lesssim 1$ ; see eq. (3.55b) below.

As these waves propagate, their nonlinear interaction with themselves produces a correction  $j_{\mu\nu}$  to  $h_{\mu\nu}$ . Like  $h_{\mu\nu}$ ,  $j_{\mu\nu}$  has the outgoing-wave form

$$j_{\mu\nu} = J_{\mu\nu}(r, \theta, \phi) \cos[(t-r)/\lambda + \text{phase}]. \quad (2.69)$$

Equations (2.43c) and (2.45) describe the growth of this correction as it propagates. They have the form  $j_{\mu\nu}|_{\alpha} = (\text{source})$ , which for  $j_{\mu\nu}$  of the form (2.69) reduces to

$$\frac{1}{r\lambda} \frac{\partial}{\partial r} (r J_{\mu\nu}) = \alpha \left( \frac{A_0}{r} \right)^2 k_{\mu} k_{\nu} + O\left( \frac{A_0^2 \lambda}{r^3} \right), \quad (2.70)$$

where  $\alpha$  is a constant of order unity and  $k_{\hat{r}} = -k_{\hat{0}} = 1$  is the propagation vector.

The leading,  $1/r^2$  source term in (2.70) produces a rapidly growing correction

$$J_{\mu\nu} = \alpha A_0^2 \frac{\lambda}{r} \ln\left(\frac{r}{\lambda}\right) k_{\mu} k_{\nu}; \quad (2.71)$$

but this correction is purely longitudinal, i.e., it has no transverse-traceless part, i.e., it is purely a gauge change. The  $1/r^3$  source term in (2.70) produces corrections of negligible size:

$$J_{\mu\nu} \sim A_0^2 \lambda^2 / r^2 \ll A_0 \lambda / r \sim h_{\mu\nu}. \quad (2.72)$$

Thus, the effects of nonlinearities are negligible as claimed.

\* \* \* \* \*

Exercise 17. Use equations (35.58) of MTW to show that the wave equation (2.43c) for  $j_{\mu\nu}$  reduces to (2.70). Show that the solution has the form (2.71), (2.72).

### 3 THE GENERATION OF GRAVITATIONAL WAVES

Turn now from wave propagation to wave generation. Elsewhere (Thorne 1977) I have given a rather thorough review of the theory of gravitational wave generation, including a variety of computational techniques valid for a variety of types of sources. In these lectures I shall focus almost entirely on computational techniques that involve multipole-moment decompositions. My discussion in large measure will be an overview of a long treatise on "multipole expansions of gravitational radiation" which I published recently in *Reviews of Modern Physics* (Thorne 1980a; cited henceforth as "RMP").

#### 3.1 Foundations for multipole analyses

##### 3.1.1 Multipole moments of a stationary system in linearized general relativity

I shall motivate my discussion of multipole moments by considering a stationary (time-independent), weakly gravitating system surrounded by vacuum and described using the linearized approximation to general relativity (MTW chapters 18 and 19). In a Cartesian coordinate system and in Lorentz gauge the Einstein field equations and gauge conditions are

$$\begin{aligned} \nabla^2 \bar{h}^{00} &= -16\pi\rho, & \nabla^2 \bar{h}^{0j} &= -16\pi\rho v^j, & \nabla^2 \bar{h}^{jk} &= -16\pi T^{jk}, \\ \bar{h}^{0j},_{,j} &= 0, & \bar{h}^{ij},_{,j} &= 0. \end{aligned} \quad (3.1)$$

Here  $\nabla^2$  is the flat-space Laplacian,  $\bar{h}^{0\beta}$  is the trace-reversed metric perturbation,  $\rho = T^{00}$  is the source's mass density,  $v^j$  is its velocity field, and  $T^{jk}$  is its stress tensor. These equations can be solved for  $\bar{h}^{0\beta}$  using the usual flat-space Green's function  $-(1/4\pi)|\underline{x}-\underline{x}'|^{-1}$ ; and the resulting integrals can then be expanded in powers of  $1/r$ . By doing this and by then making gauge changes described in § VIII of RMP, one can bring the external gravitational field into the form

$$\bar{h}^{00} = \frac{4M}{r} + \frac{6}{r^3} \mathcal{J}_{jk} n_j n_k + \dots + \frac{4(2l-1)!!}{l! r^{l+1}} \underbrace{\mathcal{J}_{a_1 \dots a_l}}_{\mathcal{J}_{A_l}} \underbrace{n_{a_1} \dots n_{a_l}}_{N_{A_l}} + \dots, \quad (3.2a)$$

$$\bar{h}^{0j} = \frac{2}{r^2} \epsilon_{jka} \mathcal{S}_k n_a + \dots + \frac{4l(2l-1)!!}{(l+1)! r^{l+1}} \epsilon_{jka} \mathcal{S}_{kA_{l-1}} N_{A_{l-1}} + \dots, \quad (3.2b)$$

$$\bar{h}^{ij} = 0. \quad (3.2c)$$

Here  $r \equiv (\delta_{jk} x^j x^k)^{1/2}$  is radius,  $n_j \equiv x^j/r$  is the unit radial vector,  $\epsilon_{ijk}$  is the Levi-Civita tensor used to form cross products,  $(2l-1)!!$  is the product  $(2l-1) \cdot (2l-3) \dots 1$ , shorthand notations have been introduced for strings of indices  $a_1 \dots a_l \equiv A_l$  and for products of unit radial vectors  $n_{a_1} \dots n_{a_l} = N_{A_l}$ , and spatial indices are moved up and down with impunity because the spatial coordinates are Cartesian. The "multipole moments"  $M$ ,  $\mathcal{J}_{A_l}$ ,  $\mathcal{S}_{A_l}$  are given as integrals over the source by

$$M = (\text{mass}) = \int \rho d^3x, \quad (3.3a)$$

$$\mathcal{J}_{a_1 \dots a_l} = \left( \begin{array}{c} \text{mass } l\text{-pole} \\ \text{moment} \end{array} \right) = \left[ \int (\rho + T^{jj}) x^{a_1} \dots x^{a_l} d^3x \right]^{\text{STF}}, \quad (3.3b)$$

$$\mathcal{S}_{a_1 \dots a_l} = \left( \begin{array}{c} \text{current } l\text{-pole} \\ \text{moment} \end{array} \right) = \left[ \int (\epsilon_{a_l pq} x^p \rho v^q) x^{a_1} \dots x^{a_{l-1}} d^3x \right]^{\text{STF}}. \quad (3.3c)$$

Here "STF" means "symmetric, trace-free part", i.e., "symmetrize and remove all traces"; cf. equation (2.2) of RMP. Note that the mass moments, which produce Newtonian-type gravitational accelerations  $\underline{g} = (1/4)\nabla\bar{h}^{00}$ , are generated by  $\rho + T^{jj} = (\text{mass density} + \text{trace of stress tensor})$ . For a description of a possible future experiment to verify the role of  $T^{jj}$  see § IV.D of Braginsky, Caves, and Thorne (1977).

For any realistic, weakly gravitating astrophysical source  $T^{jj} \ll \rho$ , so  $\mathcal{J}_{a_1 \dots a_l} = \mathcal{J}_{A_l}$  is the STF part of the  $l$ 'th moment of the mass density; and  $\mathcal{S}_{A_l}$  is the STF part of the  $(l-1)$ 'th moment of the angular momentum density (though I call it the " $l$ 'th current moment"). Note that as in electromagnetism, so also here, the external gravitational field is fully characterized by just two families of moments: the "mass moments"  $\mathcal{J}_{A_l}$  are analogs of electric moments, the "current moments"  $\mathcal{S}_{A_l}$  are analogs of magnetic moments. In order of magnitude, for a source of mass  $M$ , size  $L$ , and characteristic internal velocity  $v$ ,

$$|\mathcal{S}_{A_l}| \lesssim ML^l, \quad |\mathcal{S}_{A_l}| \lesssim MvL^l. \quad (3.4)$$

It is remarkable that, by an appropriate adjustment of gauge,  $\bar{h}_{ij}$  can be made to vanish identically outside the source; and  $\bar{h}_{00}$  is then determined fully by the mass moments while  $\bar{h}_{0j}$  is determined fully by the current moments.

Note that the spatial coordinates of equations (3.2) have been "mass-centered" so the mass dipole moment  $\mathcal{S}_j$  vanishes. I always mass-center my coordinates, thereby avoiding the issue of arbitrariness in the moments associated with arbitrariness in the origin of coordinates. Note further that the current dipole moment  $\mathcal{S}_j$  is precisely the angular momentum of the source.

\* \* \* \* \*

Exercise 18. Write down the solution of equations (3.1) using the Green's function  $-(1/4\pi)|\underline{x}-\underline{x}'|^{-1}$ , expanded in powers of  $1/r$ . Then specialize the discussion of §VIII of RMP to the stationary case and use its gauge changes to bring  $\bar{h}^{0\alpha\beta}$  into the form (3.2), (3.3).

### 3.1.2 Relation of STF tensors to spherical harmonics

The "STF" expansions (3.2) for  $\bar{h}^{0\alpha\beta}$  are mathematically equivalent to the more familiar expansions in terms of spherical harmonics  $Y_{lm}(\theta, \varphi)$ . The precise relationship between STF expansions and  $Y_{lm}$  expansions is spelled out in §II of RMP. Here I shall describe only the flavor of that relationship.

Choose a specific value for the spherical-harmonic index  $l$ . Then there are  $2l+1$  linearly independent STF tensors of order  $l$  ("STF- $l$  tensors"); and there are  $2l+1$  linearly independent functions  $Y_{lm}(\theta, \varphi)$ . Moreover, the STF- $l$  tensors and the  $Y_{lm}(\theta, \varphi)$  generate the same irreducible representation of the rotation group. Any scalar function  $F(\theta, \varphi)$  can be expanded in two mathematically equivalent forms:

$$\begin{aligned} F(\theta, \varphi) &= \sum_{l, m} f_{lm} Y_{lm}(\theta, \varphi) \\ &= \sum_l \mathcal{F}_{A_l} N_{A_l}. \end{aligned} \quad (3.5)$$

In the first expansion the coefficients  $f_{lm}$  are constant scalars, and the angular dependence is contained in the harmonics  $Y_{lm}$ . In the second expansion the coefficients  $\mathcal{F}_{A_l}$  are constant STF- $l$  tensors, and the angular dependence is obtained by contracting the unit vectors  $N_{A_l} \equiv n_{a_1} \dots n_{a_l}$  into them.

STF expansions were widely used in the nineteenth century, before  $Y_{lm}(\theta, \varphi)$  came into vogue; see, e.g., Kelvin and Tate (1879); Hobson (1931). In recent years they have been restored to common use by relativity theorists (e.g., Pirani 1964, RMP, Thorne 1981) because they are rather powerful when the spherical harmonics being manipulated are tensorial rather than scalar. In part, this power stems from the fact that the indices of  $\mathcal{F}_{A_l}$  carry both angular dependence (implicitly) and tensorial component properties (explicitly), and carry them simultaneously. An example is the tensorial harmonic  $\epsilon_{pqj} \mathcal{S}_{kq} A_{l-2} n_p N_{A_{l-2}}$ . Harmonics of this form are second-rank tensors (two free indices  $j$  and  $k$ ); they have harmonic order  $l$  ( $l$  indices on  $\mathcal{S}$  implies these generate the same irreducible representation of the rotation group as do  $Y_{lm}$ ); and they have parity  $\pi = (-1)^{l+1}$  ("1" from  $\epsilon_{pqj}$ , "2" from  $\mathcal{S}$ ).

### 3.1.3 The Einstein equations in de Donder (harmonic) gauge

In performing multipole decompositions of fully relativistic gravitational

fields (the following sections) it is computationally powerful to work in de Donder (harmonic) gauge: Define the "gravitational field"  $\bar{h}^{\alpha\beta}$  in terms of the "metric density"  $g^{\alpha\beta}$  by

$$g^{\alpha\beta} \equiv (-g)^{\frac{1}{2}} g^{\alpha\beta} \equiv \eta^{\alpha\beta} - \bar{h}^{\alpha\beta}, \quad g \equiv \det \|g_{\mu\nu}\|, \quad (3.6)$$

where  $\eta^{\alpha\beta}$  is the Minkowski metric,  $\text{diag}(-1,1,1,1)$ ; and adjust the coordinates so as to impose the de Donder gauge conditions

$$g^{\alpha\beta}_{,\beta} = -\bar{h}^{\alpha\beta}_{,\beta} = 0. \quad (3.7)$$

Then the Einstein field equations take on the form (Landau and Lifshitz 1962, eq. 100.4; MTW eq. 20.21)

$$\underbrace{g^{\mu\nu} \bar{h}^{\alpha\beta}_{,\mu\nu}} = -16\pi(-g)(T^{\alpha\beta} + t_{LL}^{\alpha\beta}) - \bar{h}^{\alpha\mu}_{,\nu} \bar{h}^{\beta\nu}_{,\mu} \quad (3.8)$$

↑ characteristics: null rays of metric  $g_{\alpha\beta}$

or, equivalently

$$\underbrace{\eta^{\mu\nu} \bar{h}^{\alpha\beta}_{,\mu\nu}} = -16\pi(-g)(T^{\alpha\beta} + t_{LL}^{\alpha\beta}) - \bar{h}^{\alpha\mu}_{,\nu} \bar{h}^{\beta\nu}_{,\mu} + \bar{h}^{\alpha\beta}_{,\mu\nu} \bar{h}^{\mu\nu} \equiv W^{\alpha\beta}. \quad (3.8')$$

↑ characteristics: flat-spacetime rays

Here  $t_{LL}^{\alpha\beta}$  is the Landau-Lifshitz pseudotensor (Landau and Lifshitz 1962, eq. 100.7; MTW eq. 20.22) which, in de Donder gauge, can be written as

$$\begin{aligned} 16\pi(-g)t_{LL}^{\alpha\beta} = & \frac{1}{2} g^{\alpha\beta} g_{\lambda\mu} \bar{h}^{\lambda\nu}_{,\rho} \bar{h}^{\alpha\mu}_{,\nu} + g_{\lambda\mu} g^{\nu\rho} \bar{h}^{\alpha\lambda}_{,\nu} \bar{h}^{\beta\mu}_{,\rho} \\ & - (g^{\alpha\lambda} g_{\mu\nu} \bar{h}^{\beta\nu}_{,\rho} \bar{h}^{\mu\rho}_{,\lambda} + g^{\beta\lambda} g_{\mu\nu} \bar{h}^{\alpha\nu}_{,\rho} \bar{h}^{\mu\rho}_{,\lambda}) \\ & + \frac{1}{8} (2g^{\alpha\lambda} g^{\beta\mu} - g^{\alpha\beta} g^{\lambda\mu}) (2g_{\nu\rho} g_{\sigma\tau} - g_{\rho\sigma} g_{\nu\tau}) \bar{h}^{\nu\tau}_{,\lambda} \bar{h}^{\rho\sigma}_{,\mu} \end{aligned} \quad (3.9)$$

where  $g_{\alpha\beta} = (-g)^{-\frac{1}{2}} g^{\alpha\beta}$  is the inverse of  $g^{\alpha\beta}$ . The law of local conservation of energy and momentum  $T^{\alpha\beta}_{;\beta} = 0$  can be written in terms of partial derivations as

$$\left[ (-g)(T^{\alpha\beta} + t_{LL}^{\alpha\beta}) \right]_{,\beta} = 0 \quad (3.10)$$

(Landau and Lifshitz 1964, eq. 100.8; MTW eq. 20.23b).

The field equations (3.8) and (3.8') can be thought of as wave equations for  $\bar{h}^{\alpha\beta}$  with source terms that include "gravitational stress-energy" (nonlinear terms in  $\bar{h}^{\mu\nu}$ ). In the form (3.8) the wave operator is that of curved spacetime; its characteristics are the null rays of the curved spacetime metric  $g_{\alpha\beta}$ , and none of the source terms involve second derivatives of  $\bar{h}^{\mu\nu}$ . By contrast the form (3.8') involves a flat-spacetime wave operator; it is obtained from (3.8) by moving the second derivative term  $\bar{h}^{\alpha\beta}_{,\mu\nu} \bar{h}^{\mu\nu}$  out of the wave operator and into the source.

The form (3.8'), with its flat-spacetime wave operator  $\square \equiv \eta^{\mu\nu} \partial_\mu \partial_\nu$ , has great computational advantages over (3.8): It can be solved (formally) for  $\bar{h}^{\alpha\beta}$

using a flat-spacetime Green's function, whereas the (formal) solution of (3.8) requires a far more complicated curved-spacetime Green's function (cf. DeWitt and Brehme 1960); and its solution is naturally decomposed into spherical harmonics because spherical harmonics are eigenfunctions of the flat operator  $\square$  but not of the curve-spacetime wave operator (3.8).

On the other hand, the flat operator  $\square$  entails serious dangers: (i) It propagates gravitational waves with the wrong speed, thereby losing at linear order the "Coulomb" phase shift produced by the  $M/r$  field of the source, and then trying to correct for this loss at quadratic order with a term that diverges logarithmically in  $r$  far from the source. I avoid this danger by restricting my use of  $\square$  to the "wave generation problem", which is formulated entirely at radii  $r < r_0$ , and by using the correct curved-spacetime wave operator when studying "wave propagation" at radii  $r > r_0$  [cf. the paragraph preceding eq. (1.8)]. (ii) The flat-operator field equations (3.8') produce divergences, due to the second-derivative source terms  $\bar{h}^{\alpha\beta}_{,\mu\nu} \bar{h}^{\mu\nu}$ , in calculations of the gravitational interactions of (idealized) point particles; see, e.g., Crowley and Thorne (1977). I avoid this danger in these lectures and in RMP by not using point-particle idealizations.

I believe, and hope, that all of my calculations with the flat-operator field equations (3.8') have been so designed as to avoid these and other pitfalls.

### 3.1.4 Multipole moments of a fully relativistic, stationary system

The de Donder formulation (3.8') of the Einstein field equations can be used to extend the linearized multipole analysis of §3.1.1 to fully relativistic, stationary systems. Full details are given in §X of RMP. Here I shall sketch the methods and summarize the results.

The key idea of the analysis is to construct, in de Donder gauge, the general external gravitational field of a fully relativistic, stationary (time-independent) system surrounded by vacuum. The de Donder coordinates are chosen to be stationary and asymptotically flat - i.e., to satisfy, in addition to equations (3.6)-(3.10), also

$$\bar{h}^{\alpha\beta}_{,0} = 0; \quad \bar{h}^{\alpha\beta} \propto 1/r \text{ as } r \equiv (\delta_{ij} x^i x^j)^{1/2} \rightarrow \infty. \quad (3.11)$$

For such a system the gauge conditions (3.7) and vacuum field equations (3.8') are

$$\bar{h}^{\alpha j}_{,j} = 0; \quad \bar{h}^{\alpha\beta}_{,jj} = W^{\alpha\beta} = \left( \begin{array}{l} \text{expression of quadratic order and higher in} \\ \bar{h}^{\mu\nu} \text{ and its spatial derivatives, each term} \\ \text{containing precisely two spatial derivatives} \end{array} \right). \quad (3.12)$$

Here and throughout this section I use the notation of flat-space Cartesian coordinates in which the location of spatial indices, up or down, is of no importance. Equations (3.12) can be solved by a "nonlinearity expansion" in which terms of first order are linear in  $\bar{h}^{\alpha\beta}$  (or, equivalently, linear in the gravitation constant  $G = 1$ ), terms of second order are quadratic, etc. The first-order part of  $\bar{h}^{\alpha\beta}$ , denoted  ${}_1\bar{h}^{\alpha\beta}$ , satisfies the linearized equations  ${}_1\bar{h}^{\alpha j}_{,j} = 0$  and  ${}_1\bar{h}^{\alpha\beta}_{,jj} = 0$  and thus, with specialization of gauge and mass centering of coordinates, has the general linearized-theory form (3.2):

$${}_1\bar{h}^{00} = \frac{4M}{r} + \sum_{l=2}^{\infty} \frac{4(2l-1)!!}{l! r^{l+1}} \mathcal{J}_{A_l} N_{A_l}, \quad (3.13)$$

$${}_1\bar{h}^{0j} = \sum_{l=1}^{\infty} \frac{4l(2l-1)!!}{(l+1)! r^{l+1}} \epsilon_{jka_l} \mathcal{S}_{kA_{l-1}} N_{A_{l-1}}, \quad \bar{h}^{ij} = 0.$$

The quadratic-order part  ${}_2\bar{h}^{\alpha\beta}$  satisfies

$${}_2\bar{h}^{\alpha j}, j = 0, \quad {}_2\bar{h}^{\alpha\beta}, jj = \left( \begin{array}{l} \text{quadratic part of } W^{\alpha\beta} \\ \text{constructed from } {}_1\bar{h}^{\mu\nu} \end{array} \right). \quad (3.14)$$

It is straightforward, though tedious, to solve these equations for  ${}_2\bar{h}^{\alpha\beta}$  and for higher-order corrections – the kind of task ideally suited for symbolic-manipulation software on a computer; cf. Appendix of Gürsel (1982). The full details are not of interest here, but the spherical-harmonic structure of the solution is of interest. That structure is dictated by the following properties of spherical harmonics: (i) Taking gradients and inverting Laplacians does not change the spherical-harmonic order of a term; and (ii) the product of two harmonics of order  $l$  and  $l'$  contains pieces of orders  $l+l'$ ,  $l+l'-1$ , ...,  $|l-l'|$ . These properties plus the quadratic-order equations (3.14) and linear-order solutions (3.13) imply that the generic term in  ${}_2\bar{h}^{\alpha\beta}$  has the form

$${}_2\bar{h}^{\alpha\beta} \sim \frac{\mathcal{M}_{A_l}}{r^{l+1}} \cdot \frac{\mathcal{M}_{B_{l'}}}{r^{l'+1}} \sim \frac{S_{l+l'} + S_{l+l'-1} + \dots + S_{|l-l'|}}{r^{l+l'+2}}. \quad (3.15)$$

Here  $\mathcal{M}_{A_l} = (\mathcal{J}_{A_l} \text{ or } \mathcal{S}_{A_l})$ ,  $\mathcal{M}_{B_{l'}} = (\mathcal{J}_{B_{l'}} \text{ or } \mathcal{S}_{B_{l'}})$ , and  $S_l \equiv$  (something unspecified that has harmonic order  $l$  and is independent of  $r$ ). The key feature of this generic term is that the power  $l+l'+2$  of its radial dependence is larger by a factor 2 than the order of any of its harmonics. By an extension of this argument one sees that in  ${}_n\bar{h}^{\alpha\beta}$  the generic term of order  $1/r^k$  has harmonics of order  $k-n$  and smaller. Thus, the nonlinear parts of the solution add up to give

$${}_2\bar{h}^{\alpha\beta} + {}_3\bar{h}^{\alpha\beta} + \dots = \sum_{l=1}^{\infty} \frac{1}{r^{l+1}} (S_{l-1} + S_{l-2} + \dots + S_0). \quad (3.16)$$

By adding these to  ${}_1\bar{h}^{\alpha\beta}$  and then computing the corresponding metric from (3.6) one obtains

$$g_{00} = -1 + 2 \frac{M}{r} - 2 \frac{M^2}{r^2} + \sum_{l=2}^{\infty} \frac{1}{r^{l+1}} \left[ \frac{2(2l-1)!!}{l!} \mathcal{J}_{A_l} N_{A_l} + S_{l-1} + \dots + S_0 \right], \quad (3.17a)$$

$$g_{0j} = \sum_{l=1}^{\infty} \frac{1}{r^{l+1}} \left[ -\frac{4l(2l-1)!!}{(l+1)!} \epsilon_{jka_l} \mathcal{S}_{kA_{l-1}} N_{A_l} + S_{l-1} + \dots + S_0 \right], \quad (3.17b)$$

$$g_{ij} = \delta_{ij} \left( 1 + 2 \frac{M}{r} \right) + \frac{M^2}{r^2} (\delta_{ij} + n_i n_j) + \sum_{l=2}^{\infty} \frac{1}{r^{l+1}} \left[ \frac{2(2l-1)!!}{l!} \mathcal{J}_{A_l} N_{A_l} \delta_{ij} + S_{l-1} + \dots + S_0 \right]. \quad (3.17c)$$

Note the following features of this general, asymptotically flat, stationary, vacuum metric: (i) As in linearized theory, so also here, the metric is determined fully by two families of moments: the mass moments  $M, \mathcal{J}_{ij}, \mathcal{J}_{ijk}, \dots$ ; and the current moments  $\mathcal{S}_i, \mathcal{S}_{ij}, \mathcal{S}_{ijk}, \dots$ . (ii) The mass dipole moment vanishes because I have insisted that the coordinates be mass centered. (iii) The moments are constant STF tensors that reside in the asymptotically flat region of spacetime (i.e., rigorously speaking, at spacelike infinity). (iv) In de Donder coordinates

the mass  $l$ -pole moment  $\mathcal{J}_{A_l}$  can be "read off" the metric as the  $1/r^{l+1}$ ,  $l$ -harmonic-order part of  $g_{00}$ ; and  $\mathcal{S}_{A_l}$  the current  $l$ -pole moment  $\mathcal{S}_{A_l}$  can similarly be read off  $g_{0j}$ .

It would be very unpleasant if one had to transform a metric to de Donder coordinates in order to compute its multipole moments. Fortunately, there are other ways of computing them. If one only wants to know the moments of order  $l = 0, 1, 2, \dots, l_{\max}$ , it is adequate to find coordinates where the metric has the form

$$g_{\alpha\beta} = \eta_{\alpha\beta} + \sum_{l=0}^{l_{\max}-1} r^{-(l+1)} \left[ \mathcal{S}_l + \mathcal{S}_{l-1} + \dots + \mathcal{S}_0 \right] + o \left[ r^{-(l_{\max}+1)} \right], \quad (3.18)$$

with the  $1/r^2$  dipole of  $g_{00}$  vanishing. Such coordinates are called "Asymptotically Cartesian and Mass Centered to order  $l_{\max}-1$ " [ACMC -  $(l_{\max}-1)$ ]. In them one can read off the first  $l_{\max}$  moments (both mass and current) by the same prescription as in de Donder coordinates, and one will obtain the same answers as one would in de Donder coordinates (RMP §XI). Alternatively, one can compute the moments by elegant techniques at spacelike infinity, due to Geroch (1970) and Hansen (1974). As Gürsel (1982) has shown, the Geroch-Hansen prescription gives the same moments as the above, aside from normalization:

$$\mathcal{J}_{A_l} = \frac{1}{(2l-1)!!} \mathcal{M}_{A_l}, \quad \mathcal{S}_{A_l} = \frac{(l+1)}{2l(2l-1)!!} \mathcal{J}_{A_l}, \quad (3.19)$$

where  $\mathcal{M}_{A_l}$  and  $\mathcal{J}_{A_l}$  are the Geroch-Hansen moments.

### 3.2 Gravitational wave generation by slow-motion sources: $\lambda \gg L \gtrsim M$

#### 3.2.1 Metric in the weak-field near zone

Turn attention now from stationary systems to a system with slowly changing gravitational field:

$$\lambda \equiv \left( \begin{array}{c} \text{timescale} \\ \text{of changes} \end{array} \right) \gg L \equiv \left( \begin{array}{c} \text{size of} \\ \text{system} \end{array} \right) \gtrsim M \equiv \left( \begin{array}{c} \text{mass of} \\ \text{system} \end{array} \right). \quad (3.20)$$

Such a "slow-motion" system possesses a weak-field near zone (WFNZ)

$$(10M \text{ and } L) < r < \lambda/10 \quad (3.21)$$

(Fig. 2 and associated discussion). In that WFNZ and in de Donder gauge I have developed an algorithm for computing the general "gravitational field"  $\bar{h}^{\alpha\beta}$  and the spacetime metric  $g_{\alpha\beta}$ ; see §IX of RMP. That algorithm is based on a simultaneous "nonlinearity expansion" like that used above for stationary systems, and "slow-motion expansion" - i.e., expansion of the time evolution of the metric in powers of  $r/\lambda$ .

At lowest order in  $r/\lambda$ ,  $\bar{h}^{\alpha\beta}$  and  $g_{\alpha\beta}$  are identical to the general stationary solution (eqs. 3.13, 3.16, 3.17); except that now the multipole moments of order  $l \geq 2$  are slowly changing functions of time  $t$  rather than constants. [The  $l = 0$  and  $l = 1$  moments,  $M = (\text{mass})$  and  $\mathcal{S}_j = (\text{angular momentum})$  are forced, by the field equations, to be constant at lowest order in  $r/\lambda$ ; but they change due to radiation reaction at orders  $(r/\lambda)^5$  and higher.] The slow time changes of  $\mathcal{J}_{A_l}(t)$  and  $\mathcal{S}_{A_l}(t)$  produce, through the field equations (3.8') and gauge conditions (3.7) and through matching to outgoing waves at  $r \gtrsim \lambda$ , the "motional" corrections of order  $r/\lambda$ ,  $(r/\lambda)^2, \dots$  to  $\bar{h}^{\alpha\beta}$  and  $g_{\alpha\beta}$ .



### 3.2.2 Metric in the induction zone and local wave zone

In the inner parts  $r \ll \lambda$  of the WFNZ the motional corrections are very small but the nonlinear corrections may be large; and  $\bar{h}^{\alpha\beta}$ ,  $g_{\alpha\beta}$  are essentially those of a stationary system (eqs. 3.13, 3.16, 3.17) with slowly changing moments. In the outer parts  $r \gg L \geq M$  of the WFNZ the nonlinear corrections are very small but as  $r$  nears  $\lambda$  the motional corrections become large. This allows us to ignore nonlinearities when extending the  $\bar{h}^{\alpha\beta}$  of the outer part of the WFNZ into the induction zone and local wave zone. In other words, we can compute  $\bar{h}^{\alpha\beta}$  in the induction zone and local wave zone by constructing the general outgoing-wave solution of the linearized, time-dependent, vacuum field equations and gauge conditions

$$\eta^{\mu\nu} \bar{h}^{\alpha\beta}_{,\mu\nu} = 0, \quad \bar{h}^{\alpha\beta}_{,\beta} = 0; \quad (3.22)$$

and by matching that solution onto the  $O([r/\lambda]^0)$  solution (3.13), (3.16) in the WFNZ. The result is

$$\bar{h}^{00} = \frac{4M}{r} + \sum_{l=2}^{\infty} (-1)^l \frac{4}{l!} \left[ \frac{1}{r} \mathcal{J}_{A_l}(t-r) \right]_{,A_l} + \left( \begin{array}{c} \text{small nonlinear} \\ \text{terms} \end{array} \right), \quad (3.23a)$$

$$\begin{aligned} \bar{h}^{0j} = & \frac{2\epsilon_{j p q} \dot{S}_{p n q}}{r^2} + \sum_{l=2}^{\infty} (-1)^l \frac{4l}{(l+1)!} \left[ \frac{1}{r} \epsilon_{j p q} \dot{S}_{p A_{l-1}}(t-r) \right]_{,q A_{l-1}} \\ & - \sum_{l=2}^{\infty} (-1)^l \frac{4}{l!} \left[ \frac{1}{r} \dot{\mathcal{J}}_{A_{l-1}}(t-r) \right]_{,A_{l-1}} + \left( \begin{array}{c} \text{small nonlinear} \\ \text{terms} \end{array} \right), \end{aligned} \quad (3.23b)$$

$$\begin{aligned} \bar{h}^{jk} = & \sum_{l=2}^{\infty} \left\{ (-1)^l \frac{4}{l!} \left[ \frac{1}{r} \ddot{\mathcal{J}}_{j k A_{l-2}}(t-r) \right]_{,A_{l-2}} + (-1)^{l+1} \frac{8l}{(l+1)!} \times \right. \\ & \left. \times \left[ \frac{1}{r} \epsilon_{p q} (\dot{S}_{k p})_{,q A_{l-2}}(t-r) \right]_{,q A_{l-2}} \right\} + \left( \begin{array}{c} \text{small nonlinear terms} \end{array} \right). \end{aligned} \quad (3.23c)$$

Here dots denote  $\partial/\partial t$ , and as indicated the moments with  $l \geq 2$  are to be regarded as functions of  $t-r$ . The dominant nonlinear corrections to this solution are discussed in §IX of RMP; see also equation (3.25) below. The metric can be computed from (3.23) via equations (3.6), which reduce to

$$g_{\alpha\beta} = \eta_{\alpha\beta} + h_{\alpha\beta} + \text{nonlinearities}, \quad h_{\alpha\beta} = \bar{h}_{\alpha\beta} - \frac{1}{2} \bar{h} \eta_{\alpha\beta}, \quad (3.24)$$

where indices on  $\bar{h}^{\alpha\beta}$  are lowered (as usual) using  $\eta_{\mu\nu}$ .

The matching of the solution (3.23) onto that of the WFNZ can be done either by elementary techniques, which require care and thought, or by the sophisticated technique of "matched asymptotic expansions" (see the lecture by Kates in this volume; also those of Damour), which do the job with less danger of error.

\* \* \* \* \*

Exercise 19. Show that (3.23) without nonlinear terms is an exact solution of the linearized field equations and gauge conditions (3.22). Then, at radii  $r \ll \lambda$ , expand (3.23) in powers of  $r/\lambda$  and show that the leading term, of

$O([r/\lambda]^0)$ , is identical to the linear part (3.13) of the WFNZ field.

### 3.2.3 Gravitational-wave field in local wave zone

The gravitational-wave field  $h_{jk}^{TT}$  of the local wave zone can be computed from expression (3.23c) by letting the spatial derivatives all act on  $\mathcal{J}$  and  $\mathcal{S}$  (so as to keep only the  $1/r$  part of the field); and by then taking the TT part. The result is

$$h_{jk}^{TT} = \left\{ \sum_{l=2}^{\infty} \frac{1}{r} \frac{4}{l!} {}^{(l)}\mathcal{J}_{jkA_{l-2}}(t-r) N_{A_{l-2}} + \sum_{l=2}^{\infty} \frac{1}{r} \frac{8l}{(l+1)!} \epsilon_{pq(j} {}^{(l)}\mathcal{S}_{k)pA_{l-2}}(t-r) n_q N_{A_{l-2}} \right\}^{TT} \left\{ 1 + O\left(\frac{M}{\lambda} \frac{\lambda}{L}\right) \right\} \quad (3.25)$$

effects of nonlinearities  $\uparrow$ .

Here a prefix superscript  $(l)$  means "take  $l$  time derivatives"

$${}^{(l)}\mathcal{J} \equiv (\partial/\partial t)^l \mathcal{J}; \quad (3.26)$$

and I have indicated the magnitude of the cumulative effects of nonlinearities, integrated up from the inner part of the WFNZ into the local wave zone, which in effect cause the multipole moments of the radiation field to differ slightly from those one would measure in the inner part of the weak-field near zone; see §IX.H of RMP.

Note that the mass quadrupole part of the radiation field (3.25) has the familiar form first derived (in different notation) by Einstein (1918):

$$h_{jk}^{TT} = \frac{2}{r} \mathcal{J}_{jk}^{TT}(t-r). \quad (3.27)$$

For most slow-motion systems these mass quadrupole waves will dominate; but when quadrupole motions are suppressed by special symmetries (e.g., in torsional oscillations of neutron stars, §3.2.7 below), other moments may dominate. Note that, in the absence of suppression due to symmetries, the magnitudes of the various multipole components of the waves are

$$\left( h_{jk}^{TT} \right)_{\text{mass } l\text{-pole}} \sim \frac{M}{r} \left( \frac{L}{\lambda} \right)^l, \quad \left( h_{jk}^{TT} \right)_{\text{current } l\text{-pole}} \sim \frac{M}{r} v \left( \frac{L}{\lambda} \right)^l \quad (3.28)$$

(cf. eq. 3.4). Typically the internal velocity  $v$  will be of order  $L/\lambda$ , so

$$\begin{aligned} (\text{current quadrupole waves}) &\sim (\text{mass octupole waves}), \\ (\text{current } l\text{-pole waves}) &\sim (\text{mass } [l+1]\text{-pole waves}). \end{aligned} \quad (3.29)$$

This is the same pattern as one sees in electromagnetism, for which "electric" multipoles are the analogs of "mass" multipoles and "magnetic" multipoles are the analogs of "current" multipoles.

### 3.2.4 Slow-motion method of computing wave generation

Equations (3.17) and (3.25) are the foundation for the slow-motion method of computing gravitational-wave generation (RMP §XII): (i) Analyze the near-zone structure and evolution of any slow-motion ( $\lambda \gg L \gtrsim M$ ) system in any convenient coordinate system and by any approximation scheme that gives, with reasonable

fractional accuracy, the time evolution of the system's asymmetries. [One attractive approximation scheme is the "instantaneous gravity" method, in which one sets to zero all time derivatives of the metric (but not of the matter variables) when solving the near-zone Einstein field equations; see, e.g., Thorne (1983) and Schumaker and Thorne (1983).] (ii) From the near-zone analysis obtain an approximation to the system's external gravitational field which, at any moment, satisfies the time-independent, vacuum Einstein equations. (iii) Compute the dominant multipole moments of that quasistationary field (moments with largest values of  ${}^{(\ell)}\mathcal{J}_{A_\ell}$  or  ${}^{(\ell)}\mathcal{S}_{A_\ell}$ ) either by transforming to de Donder or APMC coordinates and comparing with equations (3.17), or by the methods of Geroch (1970) and Hansen (1974) plus equation (3.19). (iv) Insert those moments into equation (3.25) to obtain the radiation field in the local wave zone.

### 3.2.5 Example: Rigidly rotating neutron star

As an example, consider the gravitational waves produced by a slowly rotating neutron star (pulsar) idealized as a non-axisymmetric, fully relativistic body which rotates rigidly. Full details are given in Gürsel and Thorne (1983); the main ideas will be sketched here.

The star can rotate rigidly (distance between every pair of neighboring "material particles" forever fixed) only to first order in the angular velocity  $\Omega$ . At order  $(\Omega L)^2$  there is a Lorentz contraction of distances; and as the star's angular velocity precesses that Lorentz contraction changes. Thus, the Gürsel-Thorne analysis, which assumes rigid rotation and works to first order in  $\Omega$ , has fractional errors of order  $\Omega L$ .

Gürsel and Thorne show, by a de Donder-gauge analysis of the star's interior [step (i) of "slow-motion wave-generation method"] that to first order in  $\Omega$  the star's angular momentum  $\mathcal{S}_j$  and its angular velocity  $\Omega_j$  (which are both spatial vectors residing in the nearly flat, weak-field near zone) are proportional to each other

$$\mathcal{S}_j = I_{jk} \Omega_k; \quad (3.30a)$$

and that their ratio, the moment of inertia tensor, is symmetric and rotates with angular velocity  $\Omega_j$

$$I_{jk} = I_{kj}, \quad \dot{I}_{jk} = \epsilon_{jpk} \Omega_p I_{qk} + \epsilon_{kpq} \Omega_p I_{qj}. \quad (3.30b)$$

Of course, the angular momentum is conserved (aside from negligible radiation-reaction changes)

$$\dot{\mathcal{S}}_j = 0. \quad (3.30c)$$

Equations (3.30) are identical to the classical Euler equations which govern the precession of a rigidly rotating, nongravitating body (Goldstein 1980). Thus, any fully relativistic, slowly ( $\Omega L \ll 1$ ) and rigidly rotating body undergoes a free precession which is identical to that of a nongravitating body with the same moment of inertia  $I_{jk}$  and the same angular momentum  $\mathcal{S}_j$ . The only influence of relativistic gravity will be through its influence on the values of the components of the moment of inertia tensor  $I_{jk}$ ; cf. Hartle (1973). Gürsel and Thorne go on to show that the mass moments  $\mathcal{J}_{A_\ell}$ , which characterize  $g_{00}$  in the weak-field near zone, like  $I_{jk}$  rotate with angular velocity  $\Omega_j$ :

$$\dot{\mathcal{J}}_{jk} = \epsilon_{jpk} \Omega_p \mathcal{J}_{qk} + \epsilon_{kpq} \Omega_p \mathcal{J}_{jq}, \quad \text{and similarly for } \mathcal{J}_{A_\ell}. \quad (3.31)$$

The mass quadrupole  $\mathcal{J}_{jk}$  will be the dominant source of gravitational waves unless the star has very unexpected symmetries. The waves that it produces are described by the standard quadrupole-moment formula

$$h_{jk}^{TT} = (2/r) \ddot{\mathcal{J}}_{jk}^{TT}(t-r). \quad (3.32)$$

Because the precessional equations (3.30) are identical to those of Euler and the waves are given by the same standard quadrupole moment formula (3.32) as one often uses for weakly gravitating systems, one might expect the waves from a fully relativistic, rigidly and slowly rotating body to be the same as those from a weakly gravitating body with the same moment of inertia. However, I doubt that this is so, because I suspect that relativistic gravity destroys the classical relationship

$$\mathcal{J}_{jk} = I_{jk} - \frac{1}{3} I_{ii} \delta_{jk} \quad (3.33)$$

between the quadrupole moment and the moment of inertia.

Zimmermann and Szedenitz (1979) and Zimmermann (1980) have computed in detail the quadrupole waves from a rigidly and slowly rotating body under the assumption that the classical relationship (3.33) is preserved. They show that the spectrum of the waves is rather rich and contains much detailed information about the star's angular momentum vector and moment of inertia tensor. Future theoretical studies should probe the possible breakdown of the classical relation (3.33) and should quantify deviations from rigid-body rotation due to the finiteness of the shear modulus and bulk modulus of neutron-star matter.

### 3.2.6 Example: compact binary system

Consider a binary system with stars sufficiently compact that tidal distortions of each other can be ignored (this is frequently true), and with separation between stars that is large compared to gravitational radii. Then general relativistic "near-zone" analyses (e.g., Damour in this volume; or, for the case of two black holes, D'Eath 1975) show that the orbital motions are Keplerian, aside from post-Newtonian corrections of size (gravitational radii)/(separation of stars); and this is true no matter how strong the stars' internal gravity may be. Moreover, the quadrupole moment which one reads off the weak-field, near-zone metric in de Donder gauge (eq. 3.17; Damour in this volume) is the same and evolves the same as that which one would compute for the Kepler problem using Newtonian techniques; and thus the gravitational waves obtained by inserting that quadrupole moment into  $h_{jk}^{TT} = (2/r) \ddot{\mathcal{J}}_{jk}^{TT}$  are the same as one would compute for a nearly Newtonian system with the same masses and semimajor axis. For details of those waves see Peters and Mathews (1963).

### 3.2.7 Example: torsional oscillations of a neutron star

"Glitches" observed in the timing of pulsars are thought to be due to starquakes, i.e., due to ruptures in the crystalline crust of the neutron star. Such ruptures may trigger torsional oscillations of the star with a restoring force, due to the crystal's shear modulus, which is sufficiently small that the oscillations are slow ( $\lambda \gg L$ ). In such oscillations its mass-energy density  $T^{00}$  remains constant while the momentum density  $T^{0j}$  oscillates; and, as a result, the star's mass quadrupole moment  $\mathcal{J}_{jk}$  is constant but its current quadrupole moment  $\mathcal{S}_{jk}$  oscillates. The resulting gravitational waves are thus current quadrupole rather than mass quadrupole

$$h_{jk}^{TT} = \left[ \frac{8}{3r} \epsilon_{pq} (j \ddot{\mathcal{S}}_k)_p (t-r) n_q \right]^{TT}. \quad (3.34)$$

Schumaker and Thorne (1983) have analyzed such torsional oscillations in detail using perturbation theory and have derived, in the "instantaneous gravity approximation", an eigenequation that governs the oscillations and determines the current quadrupole moment  $S_{jk}(t)$  for insertion into the gravity-wave formula (3.34).

### 3.3 Multipole decomposition of arbitrary waves in the local wave zone

#### 3.3.1 The radiation field

The gravitational waves from any source — slow-motion or fast, weak-gravity or strong — can be decomposed into multipole components in the local wave zone. The multipole moments can be computed as surface integrals of the radiation field (RMP eq. 4.11):

$${}^{(l)}\mathcal{J}_{A_l} = \left[ \frac{l(l-1)(2l+1)!!}{2(l+1)(l+2)} \frac{r}{4\pi} \int h_{a_1 a_2 \dots a_l}^{\text{TT}} n_{a_3} \dots n_{a_l} d\Omega \right]^{\text{STF}}, \quad (3.35a)$$

$${}^{(l)}\mathcal{S}_{A_l} = \left[ \frac{(l-1)(2l+1)!!}{4(l+2)} \frac{r}{4\pi} \int \epsilon_{a_1 j k} n_j h_{k a_2}^{\text{TT}} n_{a_3} \dots n_{a_l} d\Omega \right]^{\text{STF}}; \quad (3.35b)$$

and the field can be reconstructed as a sum over the multipole moments — the same sum as we encountered in the theory of slow-motion sources (eq. 3.25)

$$h_{jk}^{\text{TT}} = \sum_{l=2}^{\infty} \left\{ \frac{1}{r} \frac{4}{l!} {}^{(l)}\mathcal{J}_{jkA_{l-2}} (t-r) N_{A_{l-2}} + \frac{1}{r} \frac{8l}{(l+1)!} \epsilon_{pq(j} {}^{(l)}\mathcal{S}_{k) p A_{l-2}} (t-r) n_q N_{A_{l-2}} \right\}^{\text{TT}}. \quad (3.36)$$

For slow-motion sources the lowest few moments will dominate; but for fast-motion sources the radiation may be highly directional and many moments may contribute. See, e.g., Kovács and Thorne (1978) for the example of "gravitational bremsstrahlung radiation", in which the radiation from one particle flying past another at a speed  $v \simeq 1$  is beamed forward into a cone of half angle  $\sim \gamma^{-1} = (1-v^2)^{1/2} \ll 1$ , and moments  $l = 2, 3, 4, \dots$ ;  $\gamma$  all contribute significantly to the waves. In such cases multipole expansions are not very useful.

#### 3.3.2 The energy, momentum, and angular momentum carried by the waves

In the local wave zone the gravitational waves, which have  $l \geq 2$ , coexist with the (nearly) time-independent  $l = 0$  (mass) and  $l = 1$  (angular momentum) parts of the source's gravitational field; in TT gauge and neglecting nonlinearities and induction terms the total spacetime metric is

$$g_{00} = \underbrace{-1 + 2M/r}_{l=0}, \quad g_{0j} = \underbrace{(-2/r^2) \epsilon_{jkl} S_k n_l}_{l=1}, \quad g_{jk} = \underbrace{(1 + 2M/r) \delta_{jk}}_{l=0} + \underbrace{h_{jk}^{\text{TT}}}_{l \geq 2}. \quad (3.37)$$

This metric is written in coordinates that coincide with the asymptotic rest frame of the source; in this frame the source's linear momentum  $P_j$  vanishes; i.e., the 4-momentum (a 4-vector residing in the asymptotically flat region) is  $\bar{P} = M\partial/\partial t$ .

The gravitational waves carry 4-momentum and angular momentum away from the

source, thereby causing changes in the asymptotic rest frame, in  $M$ , and in  $S_j$ . A detailed analysis of those changes is given in chapters 19 and 20 of MTW; here I shall sketch only one variant of the main ideas.

The foundation for the analysis is the quantity

$$H^{\mu\alpha\nu\beta} \equiv g^{\mu\nu} g^{\alpha\beta} - g^{\alpha\nu} g^{\mu\beta}, \quad (3.38)$$

where  $g^{\alpha\beta}$  is the metric density of equations (3.6) and Lorentz gauge is not being imposed. In the asymptotic rest frame of the source, where the metric is (3.37) plus nonlinearities and induction terms, the surface integral of  $H^{\mu\alpha\sigma j}$ ,<sub>, $\alpha$</sub>  plucks out the  $1/r$   $l=0$  and  $l=1$  parts of  $g_{\alpha\beta}$  (which have zero contribution from nonlinearities and induction terms); i.e., it gives the 4-momentum of the source:

$$P^\mu = \frac{1}{16\pi} \oint H^{\mu\alpha\sigma j}$$
,<sub>, $\alpha$</sub>   $d^2 S_j = \begin{cases} 0 & \text{for } P^j \\ M & \text{for } P^0, \end{cases} \quad (3.39)$

where  $d^2 S_j$  is the surface element computed as though spacetime were flat. The rate of change of the 4-momentum is computed, with the help of Einstein's vacuum field equations in the form  $H^{\mu\alpha\nu\beta}$ ,<sub>, $\alpha\beta$</sub>  =  $-H^{\mu\alpha\beta\nu}$ ,<sub>, $\alpha\beta$</sub>  =  $16\pi(-g)t_{LL}^{\alpha\beta}$  (MTW eq. 20.21):

$$\begin{aligned} \frac{dP^\mu}{dt} &= \frac{1}{16\pi} \oint H^{\mu\alpha\sigma j}$$
,<sub>, $\alpha$</sub>   $d^2 S_j = \frac{1}{16\pi} \oint \left[ H^{\mu\alpha\beta j}$ ,<sub>, $\alpha\beta$</sub>  -  $H^{\mu\alpha i j}$ ,<sub>, $\alpha i$</sub>  \right]  $d^2 S_j \\ &= -\oint (-g)t_{LL}^{\mu j} d^2 S_j - \frac{1}{16\pi} \underbrace{\int H^{\mu\alpha i j}$ ,<sub>, $\alpha i j$</sub>   $dx^1 dx^2 dx^3}_0. \end{aligned} \quad (3.40)$

The volume integral vanishes by symmetry; and the conversion from surface integral to volume integral requires the topology of the space slices to be Euclidean - which it always can be for astrophysically realistic systems, including those with black holes (see Fig. 5). By averaging equation (3.40) over  $\Delta t = (\text{several } \lambda)$  and noting that the average of the Landau-Lifshitz pseudotensor is equal to the Isaacson stress-energy tensor for the gravitational waves (MTW exercise 35.19), we obtain

$$\langle dM/dt \rangle = -\oint T_{(W)}^{0r} r^2 d\Omega, \quad \langle dP^j/dt \rangle = -\oint T_{(W)}^{jr} r^2 d\Omega. \quad (3.41)$$

When the waves are decomposed into multipoles (eq. 3.36) these integrals give (RMP eqs. 4.16' and 4.20'):

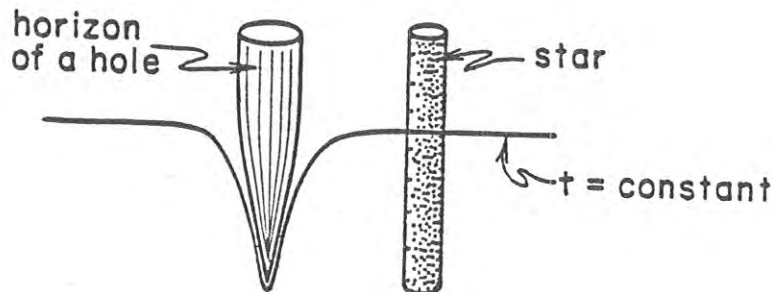


Fig. 5. Spacetime diagram showing how the slices of constant time can be chosen everywhere spacelike and have Euclidean topology even in the presence of a black hole.

$$\begin{aligned} \left\langle \frac{dM}{dt} \right\rangle = & - \sum_{l=2}^{\infty} \left\{ \frac{(l+1)(l+2)}{(l-1)l \cdot l! (2l+1)!!} \left\langle {}^{(l+1)}\mathcal{J}_{A_l} {}^{(l+1)}\mathcal{J}_{A_l} \right\rangle \right. \\ & \left. + \frac{4l(l+2)}{(l-1) \cdot (l+1)! (2l+1)!!} \left\langle {}^{(l+1)}\mathcal{S}_{A_l} {}^{(l+1)}\mathcal{S}_{A_l} \right\rangle \right\}, \end{aligned} \quad (3.42)$$

$$\begin{aligned} \left\langle \frac{dP_j}{dt} \right\rangle = & - \sum_{l=2}^{\infty} \left\{ \frac{2(l+2)(l+3)}{l(l+1)! (2l+3)!!} \left\langle {}^{(l+2)}\mathcal{J}_{jA_l} {}^{(l+1)}\mathcal{J}_{A_l} \right\rangle \right. \\ & + \frac{8(l+3)}{(l+1)! (2l+3)!!} \left\langle {}^{(l+2)}\mathcal{S}_{jA_l} {}^{(l+1)}\mathcal{S}_{A_l} \right\rangle \\ & \left. + \frac{8(l+2)}{(l-1)(l+1)! (2l+1)!!} \epsilon_{j pq} \left\langle {}^{(l+1)}\mathcal{J}_{pA_{l-1}} {}^{(l+1)}\mathcal{S}_{qA_{l-1}} \right\rangle \right\}. \end{aligned} \quad (3.43)$$

Note that for typical slow-motion sources, with moments of order (3.4) and  $v \sim L/\lambda$ , the mass loss is predominantly due to the mass quadrupole moment beating against itself

$$\left\langle \frac{dM}{dt} \right\rangle = -(1/5) \left\langle \ddot{\mathcal{J}}_{jk} \ddot{\mathcal{J}}_{jk} \right\rangle \sim M^2 L^4 / \lambda^6; \quad (3.44)$$

and the momentum change is due to the mass quadrupole beating against the mass octupole and against the current quadrupole:

$$\left\langle \frac{dP_j}{dt} \right\rangle = -\frac{2}{63} \left\langle \ddot{\mathcal{J}}_{ab} \ddot{\mathcal{J}}_{abj} \right\rangle - \frac{16}{45} \epsilon_{j pq} \left\langle \ddot{\mathcal{J}}_{pa} \ddot{\mathcal{S}}_{qa} \right\rangle \sim \frac{M^2 L^5}{\lambda^7}. \quad (3.45)$$

As the momentum of the source changes, its asymptotic rest frame changes. Since I have formulated my discussion of the external fields of slow-motion sources in mass-centered de Donder coordinates which coincide with the asymptotic rest frame, in applying my equations one must continually readjust the coordinates as time passes.

The intrinsic angular momentum of the source can be computed by a surface integral analogous to (3.39), which picks out the  $1/r^2$  dipole part of the metric (3.37):

$$\mathcal{S}_j = \frac{1}{16\pi} \oint \epsilon_{j pq} (x^p H^{q\alpha\alpha i}{}_{, \alpha} + H^{pi0q}) d^2 S_i. \quad (3.46)$$

By manipulations analogous to (3.40) one can show that

$$d\mathcal{S}_j/dt = -\oint \epsilon_{j pq} x^p (-g) t_{LL}^{qr} r^2 d\Omega. \quad (3.47)$$

By computing the Landau-Lifshitz pseudotensor (MTW eq. 20.22) for the local-wave-zone metric (3.37), inserting it into (3.47), and then averaging over  $\Delta t =$  (several  $\lambda$ ), we obtain (RMP eq. 4.22)

$$\left\langle \frac{d\mathcal{S}_j}{dt} \right\rangle = \frac{1}{16\pi} \oint \epsilon_{j pq} x^p \left\langle -(\dot{h}_{qa}^{\text{TT}} \dot{h}_{ab}^{\text{TT}})_{, b} + \frac{1}{2} \dot{h}_{ab, q}^{\text{TT}} \dot{h}_{ab}^{\text{TT}} \right\rangle r^2 d\Omega. \quad (3.48)$$

When the multipole expansion (3.36) is inserted this becomes (RMP eq. 4.23'):

$$\begin{aligned} \left\langle \frac{d\mathcal{S}_j}{dt} \right\rangle = & - \sum_{l=2}^{\infty} \left\{ \frac{(l+1)(l+2)}{(l-1)l!(2l+1)!!} \epsilon_{j pq} \left\langle \begin{matrix} (l) \\ \mathcal{J} \end{matrix} \right\rangle_{pA_{l-1}} \begin{matrix} (l+1) \\ \mathcal{J} \end{matrix} \right\rangle_{qA_{l-1}} \right. \\ & \left. + \frac{4l^2(l+2)}{(l-1)(l+1)!(2l+1)!!} \epsilon_{j pq} \left\langle \begin{matrix} (l) \\ \mathcal{S} \end{matrix} \right\rangle_{pA_{l-1}} \begin{matrix} (l+1) \\ \mathcal{S} \end{matrix} \right\rangle_{qA_{l-1}} \right\}. \end{aligned} \quad (3.49)$$

For typical slow-motion sources the dominant term is mass quadrupole beating against mass quadrupole:

$$\left\langle \frac{d\mathcal{S}_j}{dt} \right\rangle = \frac{2}{5} \epsilon_{j pq} \left\langle \begin{matrix} \ddot{\mathcal{J}} \\ \mathcal{J} \end{matrix} \right\rangle_{pa} \begin{matrix} \ddot{\mathcal{J}} \\ \mathcal{J} \end{matrix} \right\rangle_{qa} \sim \frac{M L^4}{\lambda^5}. \quad (3.50)$$

The above analysis encounters serious difficulties for a source which changes its asymptotic rest frame significantly in a few gravity-wave periods, i.e., for which  $|(dP_j/dt)\lambda| \sim M$ . Because the local wave zone, where one constructs the above surface integrals, must have a size  $\Delta r \gg \lambda$ , the momentum of such a source is not well defined there (it is changing too fast); and thus there is no clean prescription for constructing the source's asymptotic rest frame or for "mass centering" the coordinates in it. As a result, the instantaneous mass  $M$  and linear momentum  $P_j$  of the source (which depend on the choice of time  $t$ ) are somewhat ill defined; and the instantaneous angular momentum  $\mathcal{S}_j$  is even more ill defined because it is sensitive to the mass centering (factor of  $x^P$  in eqs. 3.47, 3.48). This difficulty is discussed, using the Bondi-Sachs formulation of gravitational waves at "future null infinity", in a lecture by Ashtekar in this volume.

Fortunately for theorists (unfortunately for experimenters) all realistic astrophysical sources are believed to radiate momentum only weakly

$$|dP_j/dt| \ll M/\lambda \quad (3.51)$$

(see the lectures by Eardley) and thus have asymptotic rest frames that are well enough defined for the above analysis to be well founded.

### 3.3.3 Order-of-magnitude formulas

For typical slow-motion sources the gravitational-wave amplitude at earth (eq. 3.27 propagated on out to earth through a nearly flat universe) will be

$$h_{jk}^{TT} \approx \frac{2}{r} \ddot{\mathcal{J}}_{jk}^{TT} \sim \frac{M}{r} \left( \frac{L}{\lambda} \right)^2 \sim \frac{G}{c^4} \frac{(\text{internal kinetic energy of source})}{r}$$

$\sim$  (Newtonian potential at earth produced by internal kinetic energy of source)

$$\sim 10^{-17} \times \frac{(\text{internal kinetic energy})}{(\text{total mass-energy of Sun})} \times \frac{(\text{distance to galactic center})}{(\text{distance to source})}. \quad (3.52)$$

In using this formula one must include only the internal kinetic energy associated with quadrupolar-type (nonspherical) motions. The total power carried by such sources is expressed most conveniently in terms of the "universal power unit"

$$\mathcal{L}_0 = c^5/G = 1 = 3.63 \times 10^{59} \text{ erg/sec} = 2.03 \times 10^5 M_\odot c^2/\text{sec} \quad (3.53)$$



and the source's internal power flow  $\mathcal{L}_{\text{int}} = (\text{internal kinetic energy})/\lambda$ :

$$\mathcal{L}_{\text{GW}} \approx \frac{1}{5} \langle \overset{\dots}{\mathcal{J}}_{jk} \overset{\dots}{\mathcal{J}}_{jk} \rangle \sim \left( \frac{ML^2}{\lambda^3} \right)^2 \sim \left( \frac{\mathcal{L}_{\text{int}}}{\mathcal{L}_0} \right)^2 \mathcal{L}_0. \quad (3.54)$$

Realistic astrophysical sources - even those with fast, large-amplitude motions and strong internal gravity - are not expected to deviate strongly from these order-of-magnitude formulas; see the lectures of Eardley. Moreover, all calculations to date suggest that no realistic source can radiate away a substantial fraction of its mass more quickly than the light travel time across its gravitational radius; i.e.,

$$\mathcal{L}_{\text{GW}} \lesssim M/\dot{M} = 1 = \mathcal{L}_0 \quad \text{for all sources} \quad (3.55a)$$

(a limit first suggested, so far as I know, by Dyson 1963); and, correspondingly, that the gravity-wave amplitude will always be smaller than

$$h_{jk}^{\text{TT}} \lesssim \lambda/r \quad \text{for all sources.} \quad (3.55b)$$

### 3.4 Radiation reaction in slow-motion sources

There are three approaches to the theory of gravitational radiation reaction in slow-motion sources, each of which is sufficiently rigorous to make me happy; but none of which is sufficiently rigorous to make the most mathematically careful of my colleagues happy (see, e.g., Ehlers, Rosenblum, Goldberg, and Havas 1976). I shall discuss each of these approaches in turn.

#### 3.4.1 Method of conservation laws

The method of conservation laws is based on equations (3.41) and (3.48), which express the rates of change of the source's mass  $M$ , momentum  $P_j$ , and angular momentum  $S_j$  in terms of integrals over its gravitational waves, and thence is based on expressions (3.42)-(3.45) and (3.49)-(3.50) for  $\dot{M}$  and  $\dot{P}_j$  in terms of multipole moments that are computable by "instantaneous-gravity", near-zone analyses. These formulas for  $\dot{M}$ ,  $\dot{P}_j$ , and  $\dot{S}_j$  ("conservation laws") rely, ultimately, on the vacuum Einstein equations (e.g., through the third equality of equation 3.40).

It is crucial for radiation-reaction theory that the  $M$ ,  $P_j$ , and  $S_j$  of these conservation laws are physically measurable (e.g., by Kepler's laws and the precession of gyroscopes) in the weak-field near zone or the local wave zone, and correspondingly that they are computable in terms of the physical near-zone properties of the gravitating system. For example, in the case of a compact binary system (e.g., the binary pulsar), near-zone analyses give

$$\begin{aligned} M &= m_1 + m_2 - \frac{m_1 m_2}{2a} + M_{\text{PN}} + M_{\text{PN}}^2 \\ \mathcal{S} &\equiv |\underline{\mathcal{S}}| = \left[ \frac{m_1^2 m_2^2}{m_1 + m_2} a(1-e^2) \right]^{1/2} + \mathcal{S}_{\text{PN}} + \mathcal{S}_{\text{PN}}^2. \end{aligned} \quad (3.56)$$

Here  $m_1$  and  $m_2$  are the masses of each of the stars as measured by Kepler's laws and as manifest in the stars' external metrics;  $a$  and  $e$  are the semimajor axis and eccentricity of the orbits at Newtonian order; and  $M_{\text{PN}}$ ,  $M_{\text{PN}}^2$ ,  $\mathcal{S}_{\text{PN}}$ ,  $\mathcal{S}_{\text{PN}}^2$  are post-

Newtonian and post-post Newtonian contributions. Moreover, for such a binary the conservation laws (3.44) and (3.50) reduce to

$$\begin{aligned} \left\langle \frac{dM}{dt} \right\rangle &= - \frac{32}{5} \frac{m_1^2 m_2^2 (m_1 + m_2)}{a^5 (1-e^2)^{7/2}} \left( 1 + \frac{73}{24} e^2 + \frac{37}{96} e^4 \right), \\ \left\langle \frac{dS}{dt} \right\rangle &= - \frac{32}{5} \frac{m_1^2 m_2^2 (m_1 + m_2)^{1/2}}{a^{7/2} (1-e^2)^2} \left( 1 + \frac{7}{8} e^2 \right) \end{aligned} \quad (3.57)$$

(Peters and Mathews 1963, Peters 1964).

Consider the evolution of such a binary over time scales  $\Delta t \gg M_{pN}/\langle dM/dt \rangle \simeq (10^3 \text{ years for the binary pulsar})$ . It is "physically obvious" (or one can show by a careful analysis such as that in Damour's lectures) that  $m_1$  and  $m_2$  are unaffected by the gravity-wave emission. Moreover, over these long time scales the changes of  $M_{pN}$ ,  $M_{p^2N}$ ,  $S_{pN}$ , and  $S_{p^2N}$  are negligible compared to the much larger  $M$  and  $S$  carried off in the radiation. Thus, the changes of  $M$  and  $S$  must be fully accounted for by changes of  $a$  and  $e$  — changes that are fully determined by equations (3.56) and (3.57). And from those changes one can compute the change of orbital period  $P = 2\pi[a^3/(m_1+m_2)]^{1/2}$ , the most directly measurable quantity.

For evolution of the binary pulsar on time scales  $P = 7.75 \text{ hours} \ll \Delta t \ll 1000 \text{ years}$  (corresponding to current measurements), the same argument gives the same result (which agrees with the measurements), if one makes a "highly plausible" assumption: that  $M_{pN} + M_{p^2N}$  and  $S_{pN} + S_{p^2N}$  are not sharply changing functions of the (nearly conserved) orbital parameters such as  $a$  and  $e$ , and thus cannot account for any significant piece of the changes in  $M$  and  $S$ . Of course, one can only feel fully comfortable about this conclusion after detailed  $pN$  and  $p^2N$  calculations have verified this assumption; see the lectures of Damour.

### 3.4.2 Radiation reaction potential

For systems which, unlike the binary pulsar, have weak internal gravity as well as slow motions, one can compute radiation reaction using Newtonian gravity augmented by Burke's (1969) radiation-reaction potential:

$$\begin{aligned} \underline{F}_{\text{grav}} &= - m \underline{\nabla} \phi; & \phi &= \phi_{\text{Newton}} + \phi_{\text{react}}; \\ \phi_{\text{react}} &= \frac{1}{5} (5)_{jk} \ddot{x}^j \ddot{x}^k. \end{aligned} \quad (3.58)$$

Here  $\underline{F}_{\text{grav}}$  is the gravitational force that acts on a material element of mass  $m$ .

Physically  $\phi_{\text{react}}$  results from matching the near-zone gravitational field onto outgoing gravitational waves. If the near-zone field were matched onto standing waves  $\phi_{\text{react}}$  would be zero; if it were matched onto ingoing waves  $\phi_{\text{react}}$  would change sign. Mathematically one derives the equation of motion (3.58) by constructing the outgoing-wave solution of the Einstein equations in any convenient gauge, matching it onto the near-zone solution, identifying the largest terms in the near-zone metric which are sensitive to outgoing waves versus ingoing waves, and discarding all terms except these sensitive ones and the terms of Newton. By an appropriate change of gauge one then obtains equations of motion of the form (3.58).

I have a confession to make: The derivation along these lines given in §36.11 of MTW is flawed. As Walker and Will (1980) point out, when one works in

de Donder gauge (as I did in writing §36.11), one obtains reaction terms of magnitude  $(3)\delta_{jk}$  in the near-zone metric when one matches onto outgoing waves. Although these terms are "pure gauge", i.e., have no direct physical consequences, they produce nonlinear corrections in the final gauge change, corrections which I mistakenly ignored in MTW but which are cancelled by a nonlinear iteration of the Einstein equations that I also mistakenly ignored. The reason for my sloppiness in writing MTW is that I had previously derived the radiation-reaction potential (3.58) working not in de Donder gauge but in "Regge-Wheeler gauge" (Thorne 1969); and in that gauge  $(3)\delta_{jk}$  terms never arise and a final gauge change and nonlinear iteration are not needed. Having been very careful in my Regge-Wheeler-type derivation, I was highly confident of the final result - and, buoyed by this confidence, I became careless when constructing the de Donder-gauge proof in MTW.

Historically, Peres (1960) gave the first correct analysis of gravitational radiation reaction by the technique of identifying the dominant terms sensitive to the outgoing-wave boundary condition. However, Peres did not write his answer in terms of a Newton-type radiation-reaction potential  $\Phi_{\text{react}}$ ; that was first done by Burke (1969).

### 3.4.3 $pN$ , $p^2N$ , and $p^{2.5}N$ iteration of the field equations

The method (3.58) of the radiation reaction potential discards all post-Newtonian and post-post-Newtonian effects in the evolution of the system - even though radiation reaction is a somewhat smaller, post $^{2.5}$ -Newtonian phenomenon over times of order  $\lambda$ . The justification is that radiation reaction, unlike  $pN$  and  $p^2N$  effects, produces secular changes of such quantities as the period of a binary system; and those secular changes can build up over long times  $\Delta t \gg \lambda$ , becoming ultimately much larger than post-Newtonian order. However, over shorter time-scales ( $\Delta t \lesssim 1000$  years in the case of the binary pulsar) the cumulative effects do not exceed post-Newtonian order; and thus for full confidence in one's results one should augment the Newtonian forces and  $p^{2.5}N$  radiation-reaction forces by a full  $pN$  and  $p^2N$  analysis of the system.

Damour, in his lectures in this volume, describes the history of attempts at such full analyses and presents a beautiful, full analysis of his own for the special case of binary systems with compact (white-dwarf, neutron-star, and black-hole) members.

### 3.5 Gravitational-wave generation by fast-motion sources: $\lambda \lesssim L$

Elsewhere (Thorne 1977) I have reviewed methods for computing gravitational waves from fast-motion sources. Here I shall give only a brief classification of the various methods and a few recent references where each method is used.

There are three ways to classify methods for computing wave generation: by strength of the source's internal gravity ("weak" if a Newtonian analysis gives  $|\phi| \ll 1$  everywhere; "strong" if  $|\phi| \gtrsim 1$  somewhere); by speed of the source's internal motions ("slow" if  $\lambda \gg L$ ; "fast" if  $\lambda \lesssim L$ ); and by the fractional amount that the source deviates from a nonradiating spacetime ("large deviations" or "small deviations"). Here is a list of frequently used methods of computing wave generation, classified in these three ways:

#### 1. Slow-Motion Method

- Arbitrary gravity, slow speed, arbitrary deviations.
- § 3.2 above.

#### 2. Post-Newtonian and Post-Post-Newtonian Wave-Generation Methods

- Moderate gravity, moderate speed, arbitrary deviations.
- Epstein and Wagoner (1975); Wagoner and Will (1976); RMP §§V.D,E.

### 3. Post-Linear ( $\equiv$ Post-Minkowski) Wave-Generation Method

- Weak gravity, arbitrary speed, arbitrary deviations.
- Kovács and Thorne (1978).

### 4. First-Order Perturbations of Nonradiating Solutions

- Arbitrary gravity, arbitrary speed, small deviations.
- Cunningham, Price, and Moncrief (1978); Schumaker and Thorne (1983); Detweiler (1980); lecture by Nakamura in this volume; eq. (2.29) above.

### 5. Numerical Relativity

- Arbitrary gravity, arbitrary speed, arbitrary deviations.
- Lectures by York, Piran, Nakamura, and Isaacson in this volume.

The strongest radiators of gravity waves will be those with strong gravity, fast motions, and large deviations (e.g., collisions between two black holes); and such systems can be analyzed quantitatively by only one technique: numerical relativity.

The results of wave-generation calculations for various astrophysical sources are reviewed in the lectures of Eardley in this volume.

## 4 THE DETECTION OF GRAVITATIONAL WAVES

Turn attention now from methods of analyzing the generation of gravitational waves to methods of analyzing their detection. If the size of the detector is small compared to a reduced wavelength,  $L \ll \lambda$ , it can be analyzed in the "proper reference frame" of the detector's center of mass (§4.1). If  $L \gtrsim \lambda$ , the proper reference frame is not a useful concept; and the detector is usually analyzed, instead, using "post-linear" ( $\equiv$  "post-Minkowski") techniques and some carefully chosen gauge (§4.2).

### 4.1 Detectors with size $L \ll \lambda$

#### 4.1.1 The proper reference frame of an accelerated, rotating laboratory

Most gravity-wave detectors reside in earth-bound laboratories whose walls and floor accelerate relative to local inertial frames ("acceleration of gravity") and rotate relative to local gyroscopes ("Foucault pendulum effect"). In such laboratories the mathematical analog of a LIF is a "proper reference frame" (PRF). A PRF is constructed by choosing a fiducial world line which is usually attached to the detector's center of mass and thus accelerates, by next constructing spatial slices of simultaneity,  $t = \text{const}$ , which are orthogonal to the fiducial world line and are as flat as the spacetime curvature permits; and by then constructing in each slice of simultaneity a spatial coordinate grid which is as Cartesian as the spacetime curvature permits and is attached to the laboratory walls and thus rotates. The origin of the spatial grid is on the fiducial world line, and the time coordinate  $t$  of the slices of simultaneity is equal to proper time along the fiducial world line. Such a PRF is a mathematical realization of the type of coordinate system that a very careful experimental physicist who knows little relativity theory would likely set up in his earth-bound laboratory.

One version of such a PRF is the rotating, accelerating analog of a Fermi normal coordinate system (eq. 2.15); its spacetime metric is (Ni and Zimmermann 1978)

$$\begin{aligned}
ds^2 = & -dt^2 \left[ 1 + \underbrace{2\mathbf{a} \cdot \mathbf{x} + (\mathbf{a} \cdot \mathbf{x})^2}_{\text{grav'l redshift}} - \underbrace{(\underline{\Omega} \times \mathbf{x})^2}_{\text{Lorentz time dilation}} + R_{0l0m} x^l x^m \right] \\
& + 2dt dx^i \left[ \underbrace{\epsilon_{ijk} \Omega^j x^k}_{\text{Sagnac effect}} - \frac{2}{3} R_{0lij} x^l x^m \right] + dx^i dx^j \left[ \delta_{ij} - \frac{1}{3} R_{iljm} x^l x^m \right] \\
& + O(r^3 dx^\alpha dx^\beta).
\end{aligned} \tag{4.1}$$

Here  $\mathbf{a}$  is the acceleration of the fiducial world line (minus the local "acceleration of gravity") and  $\underline{\Omega}$  is the angular velocity of the spatial grid, i.e., of the laboratory walls, relative to local gyroscopes. Other versions of a PRF have spatial grids and slices of simultaneity that are bent from those of (4.1) by amounts of the order of the bending enforced by the spacetime curvature:  $x^{j'} = x^j + O(r^3/R^2)$ ,  $t' = t + O(r^3/R^2)$  where  $R \sim (R_{\alpha\beta\gamma\delta})^{-1/2}$ ; cf. eq. (2.16). In them  $g_{00}$  will be the same as (4.1), but  $g_{0i}$  and  $g_{jk}$  may be different by amounts of  $O(r^2/R^2)$ .

In the PRF (4.1) a test particle acted on by an external force acquires a coordinate acceleration (obtained from the geodesic equation with a force term added)

$$\begin{aligned}
\frac{d^2 x^i}{dt^2} = & \underbrace{-a^i}_{\text{"acceleration of gravity"}} - 2(\underline{\Omega} \times \mathbf{v})^i - \underbrace{[\underline{\Omega} \times (\underline{\Omega} \times \mathbf{x})]^i}_{\text{centrifugal acceleration}} - \underbrace{(\dot{\underline{\Omega}} \times \mathbf{x})^i}_{\text{effect of changing } \underline{\Omega}} + \underbrace{f^i/m}_{\text{external force}} \\
& + \left[ \text{special relativistic corrections to these inertial effects,} \right. \\
& \quad \left. \text{equation (20) of Ni and Zimmermann (1978)} \right] \\
& - \underbrace{R_{0i0l} x^l}_{\text{geodesic deviation}} + \underbrace{2R_{ij0l} v^j x^l}_{\text{source of "spin-curvature coupling"}} + \frac{2}{3} R_{ijkl} v^j v^k x^l \\
& + 2v^i R_{0j0l} v^j x^l + \frac{2}{3} v^i R_{0jkl} v^j v^k x^l.
\end{aligned} \tag{4.2}$$

Here  $v^j$  is the coordinate velocity of the particle. The terms on the first line are far bigger than those on the last three lines; they are familiar from nonrelativistic mechanics in a uniform, Newtonian gravitational field.

#### 4.1.2 Examples of detectors

Figure 6 shows three types of gravitational-wave detectors with  $L \ll \lambda$  that are now under construction or look favorable for future construction.

"Weber-type resonant-bar detectors" have been under development for twenty years and are discussed in detail in the lectures of Blair, Braginsky, Hamilton, Michelson, and Pallotino. In such a detector the waves couple to and drive normal modes of oscillation of a mechanical system ("antenna"), usually a solid bar made

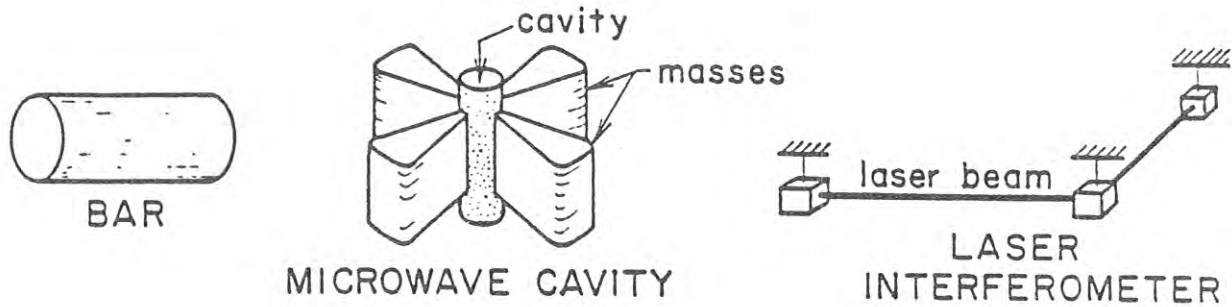


Fig. 6 Examples of gravitational-wave detectors with size  $L \ll \lambda$ .

of aluminum, and those oscillations are monitored by a transducer which is attached to the ends or sides of the bar.

In a "microwave-cavity detector" with  $L \ll \lambda$  the gravitational waves drive oscillatory deformations of the walls of a microwave cavity; and those wall motions pump microwave quanta from one normal mode of the cavity into another. To enhance the wall deformations, big masses may be attached to the walls at strategic locations. (See, e.g., Braginsky et al. (1974), Caves (1979), Pegoraro and Radicati (1980), Grishchuk and Polnarev (1981), and references therein.) Although the design sensitivities of such detectors are comparable to those of bars, no serious efforts are now under way to develop them.

"Laser interferometer detectors" have been under development for about a decade and are discussed in detail in the lectures of Drever and Brilliet. In such a detector three (or more) masses are suspended as pendula from overhead supports and swing back and forth in response to gravitational waves; and their relative motions are monitored by laser interferometry.

#### 4.1.3 Method of analyzing detectors

For me the conceptually clearest way to analyze these three detectors, and any other with  $L \ll \lambda$ , is using the PRF of the detector's center of mass. The gravitational waves enter such an analysis entirely through the Riemann curvature terms of the metric (4.1), which have sizes

$$g_{\alpha\beta}^{(W)} \sim R_{\alpha\beta\gamma\delta}^{(W)} L^2 \sim h_{jk}^{TT} (L/\lambda)^2 \ll h_{jk}^{TT} \quad \text{in PRF.} \quad (4.3)$$

By contrast, in TT gauge the waves would contribute  $g_{\alpha\beta}^{(W)} \sim h_{jk}^{TT}$  to the metric. An important consequence is this: In the PRF analysis the direct coupling of the gravitational waves to the detector's electromagnetic field can be ignored; and this is true whether the EM field is in a transducer on the bar, or in a microwave cavity, or in a laser beam. The direct coupling produces terms in Maxwell's equations for the vector potential with size  $\delta A/A \sim g_{\mu\nu}^{(W)} \sim h_{jk}^{TT} (L/\lambda)^2$ , which are smaller by  $(L/\lambda)^2$  than the "indirect" coupling effects

$$\left( \begin{array}{l} \text{gravity waves deform} \\ \text{or move masses} \end{array} \right) \rightarrow \frac{\delta L}{L} \sim h_{jk}^{TT} \rightarrow \left( \begin{array}{l} \text{changes of boundaries} \\ \text{for Maxwell equations} \end{array} \right) \rightarrow \frac{\delta A}{A} \gtrsim h_{jk}^{TT} \quad (4.4)$$

By contrast, in TT gauge the direct coupling is not negligible, and one must consider the direct interaction of the gravitational waves with both the electromagnetic field and the mechanical parts of the detector.

For all three detectors in Figure 6 and all other promising ones, the veloci-

ties of the mechanical parts of the system relative to the center of mass are  $|v^j| \ll 1$ . Consequently, in the mechanical equation of motion (4.2) all Riemann curvature terms except  $-R_{0i0l}x^l$  can be ignored. Because  $R_{0i0l}^{(W)} = -\frac{1}{2}\ddot{h}_{il}^{TT}$  (where a dot means  $\partial/\partial t$ ), the equation of motion for each mass element in the detector becomes

$$\ddot{x}^i = \frac{1}{2}\ddot{h}_{ij}^{TT} x^j + \left( \begin{array}{l} \text{all acceleration terms associated with} \\ \text{non-gravitational-wave effects} \end{array} \right). \quad (4.5)$$

In summary, if one knows how to analyze the detector in the absence of gravitational waves, one can take account of the waves by simply adding the driving acceleration  $\frac{1}{2}\ddot{h}_{jk}^{TT} x^j$  to the equation of motion of the detector's mass elements and by ignoring direct coupling of the waves to the detector's electromagnetic field.

This conclusion is valid even if the detector is large compared to inhomogeneities in the Newtonian gravity of the earth or solar system - e.g., if the detector is a normal mode of the earth itself. Then one cannot use the proper reference frame (4.1), so far as Newtonian-gravity effects are concerned; but one can still use (4.1) so far as gravitational-wave effects are concerned ( $g_{\alpha\beta}^{(W)} \sim \ddot{h}_{jk}^{TT} L^2$ ). In other words, one can graft the waves onto a Newtonian analysis by means of

$$g_{00}^{(W)} = -R_{0l0m}^{(W)} x^l x^m,$$

$$|g_{0i}^{(W)}| \sim |g_{ij}^{(W)}| \sim R_{\alpha\beta\gamma\delta}^{(W)} L^2 \left( \begin{array}{l} \text{details depend on specific variant of PRF} \\ \text{and are unimportant because } |v^j| \ll 1 \end{array} \right), \quad (4.6)$$

and by means of the resulting equation of motion (4.5).

The gravitational-wave driving acceleration  $\frac{1}{2}\ddot{h}_{jk}^{TT} x^j$  can be described by a quadrupole-shaped "line-of-force" diagram (Fig. 7; MTW Box 37.2).

#### 4.1.4 Resonant-bar detectors

Consider, as an example, the analysis of a Weber-type resonant-bar gravitational-wave detector (MTW Box 37.4). One begins by computing the normal-mode eigenfrequencies  $\omega_n$  and eigenfunctions  $y^{(n)}$  of the antenna ignoring the weak frictional and fluctuational coupling between modes and ignoring external forces (e.g., gravity waves). The resulting eigenfunctions, which are real (not complex) are normalized so that

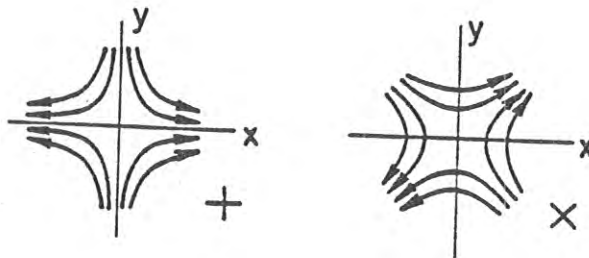


Fig. 7 "Lines of force" for the gravitational-wave acceleration (4.5) in the PRF of a detector. The two drawings correspond to waves with + polarization and with x polarization.

$$\int \rho \underline{u}^{(n)} \cdot \underline{u}^{(m)} d^3x = M \delta_{nm}; \quad \rho = \text{density}, \quad M = \text{antenna mass.} \quad (4.7)$$

One then expands the vibrational displacement of the bar's material in terms of normal modes

$$\delta \underline{x} = \sum_n X^{(n)} \underline{u}^{(n)}(\underline{x}) e^{-i\omega_n t}; \quad X^{(n)} \equiv \text{"complex amplitude of mode n"}. \quad (4.8)$$

Next one writes down the equation of motion for  $\delta \underline{x}$  in the presence of gravity waves [force per unit volume equal to  $\frac{1}{2} \rho h_{jk}^{TT} x^j$ ], internal friction, Nyquist forces [i.e., weak fluctuational couplings between normal modes], and coupling to the transducer. When one resolves that full equation of motion into normal modes one obtains

$$\dot{X}^{(n)} = -(2/\tau_n) X^{(n)} + \frac{i e}{M \omega_n} \int \underline{f} \cdot \underline{u}^{(n)} d^3x, \quad (4.9)$$

where  $\tau_n$  is the (very long) frictional damping time for mode  $n$  and  $\underline{f}$  is the force per unit volume in the antenna including gravity-wave force, Nyquist forces, and "back-action forces" of the transducer on the antenna. The gravity-wave force, when integrated over the normal mode,  $\underline{u}^{(n)}$ , gives

$$\int \underline{f}^{(W)} \cdot \underline{u}^{(n)} d^3x = \frac{1}{4} h_{jk}^{TT} \mathcal{Q}_{jk}^{(n)}, \quad (4.10a)$$

$$\begin{aligned} \mathcal{Q}_{jk}^{(n)} &= \int \rho (u_{(n)}^j x^k + u_{(n)}^k x^j - \frac{2}{3} \delta_{jk} u_{(n)} \cdot \underline{x}) d^3x \\ &= \left[ X^{(n)} e^{-i\omega_n t} \right]^{-1} \times \left( \text{contribution of mode } n \text{ to antenna's} \right. \\ &\quad \left. \text{quadrupole moment} \right). \end{aligned} \quad (4.10b)$$

Thus, the same quadrupole moment as would govern emission of gravitational waves by mode  $n$  also governs their reception; this is an aspect of the principle of de-tailed balance (MTW §37.7).

If the antenna is hit by a broad-band burst of gravitational waves with spectral energy flux  $\mathcal{F}_\nu$  (ergs  $\text{cm}^{-2} \text{Hz}^{-1}$ ) and polarization  $e_{jk}$  (normalized so  $e_{jk} e_{jk} = 2$ )

$$h_{jk}^{TT} = A(t) e_{jk}, \quad \mathcal{F}_\nu = \frac{\omega^2}{4} \left| \frac{1}{\sqrt{2\pi}} \int_{-\infty}^{+\infty} A(t) e^{i\omega t} dt \right|^2, \quad \omega = 2\pi\nu > 0, \quad (4.11)$$

then equations (4.9) and (4.10) give for the wave-induced change of complex amplitude  $\delta X^{(n)}$

$$\begin{aligned} \frac{1}{2} M \omega_n^2 |\delta X^{(n)}|^2 &= \left( \text{energy that would be absorbed by antenna mode } n \right. \\ &\quad \left. \text{if } X^{(n)} \text{ were zero when the wave burst hit} \right) \\ &= \mathcal{F}_\nu(\omega = \omega_n) \int \sigma_n d\nu. \end{aligned} \quad (4.12)$$

Here  $\int \sigma_n d\nu$  is the antenna cross section integrated over frequency



$$\int \sigma_n dv = \frac{\pi}{4} \frac{\omega_n^2}{M} \left( \mathcal{J}_{jk}^{(n)} e_{jk} \right)^2 \quad (4.13)$$

$\sim 10^{-21} \text{ cm}^2 \text{ Hz}$  for typical antennas with  $M \sim 1 \text{ ton}$ ,  $\omega_n/2\pi \sim 1 \text{ kHz}$ .

For further details and discussion see MTW, chapter 37; also the lectures by Blair, Braginsky, Hamilton, Michelson, and Pallotino in this volume.

\* \* \* \* \*

Exercise 20. Derive equation (4.9) by resolving the equation of motion for  $\delta x$  into normal modes. Show that the driving term due to gravity waves has the form (4.10) and show that  $\mathcal{J}_{jk}^{(n)}$  has the claimed relationship to the quadrupole moment.

Exercise 21. Show that (eq. 4.11) correctly represents the spectral energy flux of a gravity wave in the sense that  $\int \mathcal{F}_\nu dv$  is the energy per unit area that passes the detector. Show that the broad-band burst of gravity waves (4.11) produces the change (4.12) of the antenna's complex amplitude. Show that for typical antennas the frequency-integrated cross section is  $\sim 10^{-21} \text{ cm}^2 \text{ Hz}$  as claimed.

Exercise 22. Show that for a homogeneous, spherical antenna whose quadrupolar oscillations are being driven by gravity waves, the quadrupole moment  $\mathcal{J}_{jk}$  obeys the equation of motion (2.39a).

#### 4.2 Detectors with size $L \gtrsim \lambda$

Examples of gravitational-wave detectors with  $L \gtrsim \lambda$  include the Doppler tracking of spacecraft (lectures by Hellings in this volume), and microwave-cavity detectors in which the gravity waves pump microwave quanta from one normal mode to another via direct interaction with the electromagnetic field as well as via deformation of the walls or wave guides which confine the field (Braginsky et al. (1974), Caves (1979), Pegoraro and Radicati (1980), Grishchuk and Polnarev (1981) and references therein).

Because the Riemann tensor of the waves varies significantly over the volume of such a detector, the "proper reference frame" is not a useful tool in analyzing it. Instead, analyses are based on the linearized approximation to general relativity (MTW chapter 18), with the metric  $g_{\alpha\beta} = \eta_{\alpha\beta} + h_{\alpha\beta}$  including both Newtonian gravitational potentials  $\Phi$  and gravitational waves; and the waves are usually treated in TT gauge:

$$g_{00} = -1 - 2\Phi, \quad g_{0j} = 0, \quad g_{jk} = \delta_{jk}(1-2\Phi) + h_{jk}^{\text{TT}}.$$

The analysis is actually "post-linear" (or "post-Minkowski") in that the "equations of motion" for the matter (sun, planets, detector) are not taken to be  $T^{\alpha\beta}_{;\beta} = 0$ , but rather  $T^{\alpha\beta}_{;\beta} = 0$  with connection coefficients linear in  $h_{\mu\nu}$  and  $\Phi$ . See, e.g., §2 of Thorne (1977) for a careful discussion of the differences between linear theory and post-linear theory.

For an example of such an analysis see Hellings' treatment, in this volume, of the interaction of gravitational waves with NASA's doppler tracking system. As in that analysis, so in most analyses of detectors with  $L \gtrsim \lambda$ , direct interaction of the gravitational waves with the electromagnetic field is as important as interaction with the mechanical parts of the detector.

A mathematical trick that sometimes simplifies calculations of the interaction of gravity waves with electromagnetic fields is to write the curved-spacetime

Maxwell equations in a form identical to those for flat spacetime in a moving, anisotropic dielectric medium (e.g., Volkov, Izmet'ev, and Skrotskii 1970). Caves (unpublished) has combined this technique with gauge changes that attach the spatial coordinates onto the cavity walls even when the walls are wiggling, and has thereby produced an elegant and powerful formalism for analyzing microwave cavity detectors with  $L \gtrsim \lambda$ .

## 5 CONCLUSION

Most of my own research on gravitational-wave theory is motivated by the need to prepare for the day when gravitational waves are detected and astronomers confront the task of extracting astrophysical information from them. The task of preparing for that day is nontrivial. The ideas described in these lectures are a foundation for those preparations, but much further theoretical research is needed — especially the computation of gravitational wave forms  $h_{jk}^{\text{TT}}(t-r; \theta, \varphi)$  from fast-motion, strong-gravity sources such as black-hole collisions.

We theorists often pay great lip service to a second motivation for our research: to give guidance to experimenters who are designing and constructing gravitational-wave detectors; and experimenters often follow with avid interest and thumping hearts the fluctuations in theoretical predictions of the waves bathing the earth. However, we theorists are far more ignorant than most experimenters imagine. For those strong sources whose wave characteristics are fairly well known (e.g., collisions between black holes), the event rate is uncertain by many orders of magnitude; and for those whose event rates are fairly well known (e.g., supernovae), the wave strengths are uncertain by many orders. Our ignorance has a simple cause: The information carried by electromagnetic waves, which is the foundation of today's theories, is nearly "orthogonal" to the information carried by gravitational waves. As a corollary, when they are ultimately detected, gravitational waves will likely give us a revolutionary new view of the universe; but until they are detected, we theorists can offer little precious advice to our experimental colleagues, and our colleagues should turn a half-deaf ear to our most confident remarks about the characteristics of the waves for which they search.

## REFERENCES

- Aichelburg, P. C., Ecker, G., and Sexl, R. U. 1971, *Nuovo Cimento B*, 2, 63.
- Bontz, R. J. and Haugan, M. P. 1981, *Astrophys. Space Sci.*, 78, 204.
- Bondi, H., van der Burg, M. G. J., and Metzner, A. W. K. 1962, *Proc. Roy. Soc.*, A269, 21.
- Braginsky, V. B., Caves, C. M., and Thorne, K. S. 1977, *Phys. Rev. D*, 15, 2047.
- Braginsky, V. B., Grishchuk, L. P., Doroshkevich, A. G., Zel'dovich, Ya. B., Novikov, I. D., and Sazhin, M. V. 1974, *Sov. Phys.-JETP*, 38, 865.
- Burke, W. L. 1969, unpublished Ph.D. thesis, Caltech; see also *Phys. Rev. A*, 2, 1501 (1970).
- Caves, C. M. 1979, *Phys. Lett.*, 80B, 323.
- Caves, C. M. 1980, *Ann. Phys. (USA)*, 125, 35.
- Crowley, R. J. and Thorne, K. S. 1977, *Astrophys. J.*, 215, 624.
- Cunningham, C. T., Price, R. H., and Moncrief, V. 1978, *Astrophys. J.*, 224, 643.
- Cyrancki, J. F. and Lubkin, E. 1974, *Ann. Phys. (USA)*, 87, 205.
- Davis, M., Ruffini, R., Press, W. H., and Price, R. H. 1971, *Phys. Rev. Lett.*, 27, 1466.
- D'Eath, P. 1975, *Phys. Rev. D*, 12, 2183.
- Detweiler, S. 1980, *Astrophys. J.*, 239, 292.
- DeWitt, B. S. and Brehme, R. W. 1960, *Ann. Phys. (USA)*, 9, 220.
- Dicke, R. H. 1964, in Relativity, Groups, and Topology, ed. B. and C. DeWitt (Gordon & Breach, New York).
- Dyson, F. 1963, in Interstellar Communication, ed. A. G. W. Cameron (Benjamin, New York).
- ELLWW: See Eardley, Lee, Lightman, Wagoner, and Will (1973).
- Eardley, D. M., Lee, D. L., and Lightman, A. P. 1973, *Phys. Rev. D*, 8, 3308.
- Eardley, D. M., Lee, D. L., Lightman, A. P., Wagoner, R. V., and Will, C. M. 1973, *Phys. Rev. Lett.*, 30, 884; cited in text as ELLWW.
- Ehlers, J., Rosenblum, A., Goldberg, J. N., and Havas, P. 1976, *Astrophys. J. (Letters)*, 208, L77.
- Einstein, A. 1918, *Preuss. Akad. Wiss. Berlin, Sitzber.* 1918, 154.
- Epstein, R. and Wagoner, R. V. 1975, *Astrophys. J.*, 197, 717.
- Geroch, R. 1970, *J. Math. Phys.*, 11, 2580.
- Geroch, R., Held, A., and Penrose, R. 1973, *J. Math. Phys.*, 14, 874.

- Goldstein, H. 1980, Classical Mechanics, second edition (Addison Wesley, Reading, Mass.), §5-6.
- Grishchuk, L. P. and Polnarev, A. G. 1981, chapter 10 of General Relativity and Gravitation, Vol. 2, ed. A. Held (Plenum Press, N.Y.).
- Gürsel, Y. 1982, *J. Gen. Rel. Grav.*, submitted.
- Gürsel, Y. and Thorne, K. S. 1983, *Mon. Not. Roy. Astron. Soc.*, submitted.
- Hansen, R. O. 1974, *J. Math. Phys.*, 15, 46.
- Hartle, J. B. 1973, *Astrophys. Space Sci.*, 24, 385.
- Hartle, J. B. and Thorne, K. S. 1983, paper in preparation.
- Hobson, E. W. 1931, The Theory of Spherical and Ellipsoidal Harmonics (Cambridge U. Press, Cambridge), p. 119. Republished in 1955 by Chelsea Publishing Co., New York.
- Isaacson, R. A. 1968, *Phys. Rev.*, 166, 1263 and 1272.
- Kelvin, Lord (Sir William Thomson) and Tate, P. G. 1879, Treatise on Natural Philosophy, Appendix B of Chapter 1 of Volume 1 (Cambridge U. Press, Cambridge).
- Kovács, S. J. and Thorne, K. S. 1978, *Astrophys. J.*, 224, 62.
- MTW: see Misner, Thorne, and Wheeler (1973).
- Mashhoon, B. 1973, *Astrophys. J. (Letters)*, 181, 165.
- Misner, C. W., Thorne, K. S., and Wheeler, J. A. 1973, Gravitation (Freeman, San Francisco); cited in text as MTW.
- Ni, W.-T. and Zimmermann, M. 1978, *Phys. Rev. D*, 17, 1473.
- Pegoraro, F. and Radicati, L. A. 1980, *J. Phys. A*, 13, 2411.
- Peres, A. 1960, *Nuovo Cimento*, 15, 351.
- Peters, P. C. 1964, *Phys. Rev.*, 136, B1224.
- Peters, P. C. and Mathews, J. 1963, *Phys. Rev.*, 131, 435.
- Pirani, F. A. E. 1964, in Lectures on General Relativity, ed. A. Trautman, F. A. E. Pirani, and H. Bondi (Prentice Hall, Englewood Cliffs, N.J.).
- Press, W. H. 1979, *J. Gen. Rel. Grav.*, 11, 105.
- Price, R. H. 1972, *Phys. Rev. D*, 5, 2419.
- RMP: see Thorne (1980a).
- Rosen, N. 1973, *J. Gen. Rel. Grav.*, 4, 435; see also N. Rosen, *Ann. Phys. (USA)*, 84, 455 (1974).
- Sachs, R. K. 1962, *Proc. Roy. Soc.*, A270, 103.
- Schumaker, B. L. and Thorne, K. S. 1983, *Mon. Not. Roy. Astron. Soc.*, in press.

- Sonnabend, D. 1979, To the Solar Foci, JPL Publication 79-18 (Jet Propulsion Laboratory, Pasadena).
- Szekeres, P. 1971, Ann. Phys., 64, 599.
- Thorne, K. S. 1969, Astrophys. J., 158, 997.
- Thorne, K. S. 1977, in Topics in Theoretical and Experimental Gravitation Physics, ed. V. De Sabbata and J. Weber (Plenum Press, London).
- Thorne, K. S. 1980a, Rev. Mod. Phys., 52, 299; cited in text as RMP.
- Thorne, K. S. 1981, Mon. Not. Roy. Astron. Soc., 194, 439.
- Thorne, K. S. 1983, Astrophys. J., in preparation.
- Thorne, K. S. and Campolattaro, A. 1967, Astrophys. J., 149, 591.
- Turner, M. 1977, Astrophys. J., 216, 914.
- Volkov, A. M., Izmet'ev, A. A., and Skrotskii, G. V. 1970, Zh. Eksp. Teor. Fiz., 59, 1254 [Sov. Phys.-JETP, 32, 636 (1971)].
- Wagoner, R. V. and Will, C. M. 1976, Astrophys. J., 210, 764.
- Walker, M. and Will, C. M. 1980, Astrophys. J. (Letters), 242, L129.
- Will, C. M. 1982, Theory and Experimentation in Gravitational Physics (Cambridge University Press, New York).
- Zimmermann, M. 1980, Phys. Rev. D, 21, 891.
- Zimmermann, M. and Szedenits, E. 1979, Phys. Rev. D, 20, 351.